The Major Project on

ANALYSIS OF GEOGRID REINFORCED POND ASH EMBANKMENT USING FINITE ELEMENT METHOD

Submitted in Partial Fulfillment for the Award of the Degree of

MASTERS OF TECHNOLOGY

IN

CIVIL ENGINEERING

With Specialization in

GEOTECHNICAL ENGINEERING

By

Shilpi Gupta

(Roll No. 2K11/GTE/09)

Under The Guidance of

Prof. A.K. Gupta

Civil Engineering Department

Delhi Technological University, Delhi

Department of Civil Engineering

Delhi Technological University

Delhi - 110042

2013

DELHI TECHNOLOGICAL UNIVERSITY

CERTIFICATE

This is to certify that the major project report entitled "ANALYSIS OF GEOGRID REINFORCED POND ASH EMBANKMENT USING FINITE ELEMENT METHOD" is a bona fide record of work carried out by Shilpi Gupta (Roll No. 2K11/GTE/09) under my guidance and supervision, during the session 2013 in partial fulfillment of the requirement for the degree of Master of Technology (Geotechnical Engineering) from Delhi Technological University, Delhi.

The work embodied in this major project has not been submitted for the award of any other degree to the best of our knowledge.

Prof. A.K. Gupta

Department of Civil Engineering

Delhi Technological University

Delhi-110042

2013

DELHI TECHNOLOGICAL UNIVERSITY

ACKNOWLEDGEMENT

I would really like to thank my guide and motivator **Prof. A.K. Gupta**, Civil Engineering Department, Delhi Technological University for his valuable guidance and support in all the phases from conceptualization to experimental and final completion of the project.

I wish to convey my sincere gratitude to Prof. H.D. Sharma, Civil Engineering Department, Indian Institute of Technology, Delhi for permitting me to work on a FEM based software phase^2 (Rocscience), in IIT Delhi .

I would like to express my deepest sense of gratitude and indebtedness to my Maharaj ji and my parents for their encouragement and persistent support which has helped me to do better in all of my endeavors.

I would also like to thank all the faculties of Civil Engineering Department, Delhi Technological University.

I am deeply thankful towards all the lab assistants of my college who have helped me conduct the experiments.

I sincerely thank my friends Mr. Prateek Negi, Mr. Siddharth, Mr. Gaurav Tiwari whose moral support made this project possible.;

I thank all the people directly or indirectly involved in successful completion of this project.

SHILPI GUPTA
M. Tech (Geotechnical Engineering)
Roll No. 2K11/GTE/09
Department of Civil Engineering
Delhi Technological University
Delhi-110042

DECLARATION

I, hereby declare that the work being presented in this Project Report entitled **"Analysis of Geogrid Reinforced Pond Ash Embankment using Finite Element Method"** is the bonafide work carried out by me as a part of major project in partial fulfillment of the requirement for the award of the degree of Master of Technology in Geotechnical Engineering.

The matter presented in this report has not been submitted by me for the award of any other degree.

Shilpi Gupta
M. Tech (Geotechnical Engineering)
Roll No. 2K11/GTE/09
Department of Civil Engineering
Delhi Technological University
Delhi-110042

ABSTRACT

The disposal of enormous quantity of pond ash from thermal power plants has been a major environmental concern over a period of last few decades that encourages civil engineers worldwide to use pond ash extensively to protect the environment and save natural resources. An infrastructure project such as reclamation, highways, water reservoirs, railways etc, require earth material in very large quantity as there is a shortage of good soil in most urban areas. In such situations construction of pond ash embankments with steep slope is worth considering, as the pond ash is freely available material in vicinity of a thermal power plant.

In the present work an attempt has been made to use pond ash for construction of road embankment. This will not only solve the problems associated with the disposal of pond ash but will also help to conserve the precious top soil and land required for growing food as well as protecting environmental pollution. A parametric study has been carried out to investigate the effect of inclination of slope, vertical spacing of geogrid reinforcement on reinforced pond ash embankment, and effect of providing pond ash – lime mixed layer on top and side slopes of unreinforced pond ash embankment.

The Pond Ash sample was collected from the ash pond site of Rajghat thermal power station, Delhi, soil was collected from DTU campus, Delhi and the lime was procured from the open market in the form of quick lime. This lime was then mixed with pond ash, by weight (= 9%) (Gupta et al, 2013).Further, in the present work an experimental program was carried out to characterize the materials and strength tests were performed to study the behavior of pond ash mixed with lime; the results shows that in the presence of moisture, pond ash chemically reacts with lime at ordinary temperature and forms cementations material which is attributed to the increase in strength of pond ash. Numerical analysis was performed using the FEM based software PHASE^2 (Rocscience). Results divulge that use of full length of geogrid covering whole width of embankment increases the critical strength reduction factor (SRF) of embankment at steeper slope inclination. Also, the application of either geogrids layers or pond ash-lime mix layer, results in safer designs in comparison to unreinforced pond ash embankment.

In this research a substantial number of parameters were considered to study their effects on the stability of embankment which may prove useful from execution of actual prototypes.

CONTENTS

LIST OF FIGURES

FIGURES

LIST OF TABLES:

TABLES

CHAPTER- 1

INTRODUCTION

1.1 Embankment

Embankments are constructed when it is necessary to raise the grade line of a road or railway line. The grade line may be raised to keep sub grade above the high ground water table or to prevent damage of a pavement due to surface water and capillary water. Embankments should be constructed using a construction material which can provide adequate support to the formation and long-term stability. Large quantity of construction material is required to construct embankments. But there is scarcity of good quality soil for embankment construction. Industrial byproduct such as pond ash can provide a good alternative construction material for embankments. Their effective utilization can be result in lot of savings and eliminating environmental problems as disposal of pond ash from thermal power plants has been a major environmental concern over a period of last few decades.

The embankment slopes should be stable enough under adverse moisture and other conditions. Hence slopes should be designed providing minimum factor off safety of 1.5.

1.2 Introduction of Materials

1.2.1 Pond Ash

Fly ashes are a waste product from thermal power industry; more than 110 million tones of fly ashes are produced annually in India. When pulverized coal is burnt in the boiler of a thermal power station, a part of ash comes down at the bottom of the boiler and is known as bottom ash whereas, the major portion of the ash comes out along with the flue gases and is collected through electro static precipitation or filter bags or other means before allowing the exhaust gases through escape the chimney, this part is generally known as ESP ash. For deposition, the un-utilized ESP ash and bottom ash are taken to ash ponds. The ash deposited in the ash pond is known as pond ash.

Present majority of coal ashes generated is disposed of in ash ponds which are harmful for environment. Presently 20,000 hectares of land is occupied by pond ash. Thus this pond ash produced is being regarded as waste material with potential environmental implications.

Utilization of Pond Ash

- Construction of backfills/embankments
- Stabilization of sub-base and sub grade
- Construction of rigid /semi-rigid pavements

Advantages of using Pond Ash for road construction

1. Pond ash causes lesser settlements as it is lightweight material, therefore, It is preferable for embankment construction over weak sub grade such as alluvial clay or silt where excessive weight could cause failure.
2. Pond ash embankments can be compacted over a wide range of water content. Therefore, there is less variation in density with change in water content. Pond ash is easily to handle and compact because it is lightweight. It can be compacted using either static or vibratory rollers as there are no big lumps to broken down.
3. Pond Ash has high permeability so it ensures free and efficient drainage. Water gets drained out easily after rainfall ensures better workability than soil.
4. Pond ash has low compressibility which results in low subsequent settlement.
5. Good earth can be conserved, so it can help to protect the environment.
6. It has high value of California Bearing Ratio which results in more efficient design of road embankment.
7. Self hardening property imparts additional strength to the road embankments.
8. Pond ash is pozzolanic in nature. It chemically reacts with lime and cement and forms cementitious material.

.

Considering all the above advantages, it is extremely necessary to promote use of pond ash for construction of embankments.

Economy in use of Pond Ash

Use of Pond ash in embankments results in reduction in construction cost. Typical cost of borrow soil is about Rs.100 to 200 per cu-m. Pond ash is available free of cost at thermal power plant and hence it involves only transportation cost, laying and rolling cost. Hence, when pond ash is used as a construction material, the economy achieved is directly related to transportation cost of pond ash. If lead distance is less, construction cost can be very less. Similarly, the use of pond ash in embankment construction results in significant savings due to reduction in cost of cement and road aggregates. By using large quantity of pond ash for embankment construction, a large area of fertile agricultural land can be saved from ash deposition. Therefore the actual savings achieved will be much higher.

Environmental Impact of Pond Ash Use

Utilization of pond ash will not only reduces the cost of construction and disposal problem but will also help in utilizing precious land in a better way. When pond ash is used in concrete, pond ash chemically reacts with cement and minimizes leaching of heavy metals. Hence chances of pollution due to use of pond ash in road embankments are negligible.

Table 1.1: Typical geotechnical properties of pond ash/fly ash as recommended by IRC-SP: 58-2001

Parameter	**Range**
Sp. Gravity	1.90 - 2.55
Plasticity	NP
MDD (KN/mm^3)	9.0 – 16.0
OMC (%)	38.0 -18.0
Cohesion	Negligible
Angle of Internal Friction	30º- 40 º
Coefficient of Consolidation C_v (m^2 /sec)	1.75×10^{-5}- 2.01×10^{-3}
Compression Index	0.05-0.4
Permeability (m/sec)	8×10^{-8}- 7×10^{-6}
Particle Size Distribution (% of materials)	
Clay	1-10
Silt	8-85
Sand	7-90
Gravel	0-10
Coefficient of Uniformity	3.1-10.7

1.2.2 Lime

Lime is a white caustic alkaline substance, consists of calcium oxide. It is obtained by heating limestone. The word "lime" arises with its earliest consumption as building mortar and has a sense of “adhering or sticking”. It is commonly used as an additive to stabilize ash/soil. Types of commonly used lime are:

1) Hydrated high calcium lime ($Ca(OH)_2$)
2) Calcitic quicklime (CaO)
3) Monohydrated dolomitic lime [$Ca(OH)_2$.MgO]
4) Dolomitic quicklime

- Quicklime is acquireded according to the reaction: $CaCO_3$ + heat → CaO + CO_2.
- Quicklime can be hydrated (i.e. combined with water). Slaked lime or hydrated lime is produced according to the reaction: CaO + H_2O → $Ca(OH)_2$

High calcium lime, usually used for soil stabilization, should contain less than 5% of hydroxide or magnesium oxide. Lime can be used either alone or in combination with other materials to treat different soils.

In presence of moisture, Pond Ash reacts with lime at ordinary temperature and forms a compound possessing cementitious properties. After reactions between lime and pond ash, calcium silicate hydrates are produced which are responsible for the increase in strength.

1.2.3 Geogrid

Increasingly commercial, residential and transportation facilities have made it mandatory to utilize land efficiently. A part of usable land can be saved by constructing embankment at a steeper angle. To increase the stability of steeper slope, geosynthetic has been encountered to be the most efficient solution.
"Geosynthetics" are man-made materials made from various types of polymers used to increase cost effective geotechnical engineering, environmental and transportation projects.
The polymeric nature of the geosynthetics makes them suitable for employment in the ground where high durability is required.

Functions of Geosynthetics:

- Reinforcement (provide additional strength)
- Separation (prevent intermixing)
- Drainage (collect/convey)
- Protection (prevent puncture)
- Filtration (provide movement of fill material)
- Barrier (prevent transmission)

Categories: Geogrids, Geotextiles, Geonet, Geosynthetic clay liner and Geomembranes**.**

A **"Geogrid"** is commonly made from stiff or flexible polymers, such as polyester or polystyrene. They may be woven from yarns, heat-welded from strips of material or made by punching a regular pattern of holes in sheets of material, then stretched into a grid- like sheets with large apertures used primarily as reinforcement of weak soil and waste masses. Geogrids improves the strength of soil. Since Soils have no or little tensile strength. Because of that, placing geogrids in the soil mass horizontally in the direction of principle stress will improve the tensile property of soil. Geogrids are strong in tension as compared to soil. . This fact allows them to transfer loads to a larger area of soil. When load is applied to the reinforced soil, tensile forces will mobilize into the geogrid through friction, and therefore reduces the lateral deformation of soil.

1.3 Necessity of Study

- Large quantity of construction materials is required for embankment construction.
- Lack of availability of good quality soil for embankment construction
- Huge amount of waste material like pond ash is available.
- Disposal and environmental problems are arising due to pond ash.
- Need to steepen the slopes to use land efficiently.

In present study an attempt has been made to investigate the effect of various parameters such as slope inclination, vertical spacing on reinforced pond ash embankment and effect of providing pond ash lime mixed layer with varying thickness, on unreinforced pond ash embankment to provide most efficient and economical design. A parametric study has been carried using FEM based software PHASE^2 (Rocscience).

1.4 Objective of study

1. To predict the critical SRF values of unreinforced and reinforced pond ash embankment using finite element method (FEM) both in normal condition and flood condition.
2. To determine the effect of geogrid reinforcement on critical SRF values of pond ash embankment both in normal condition and flood condition
3. To determine the effect of providing pond ash mixed with lime layer of varying thickness over top and on side slope of unreinforced pond ash embankment both in normal condition and flood condition.
4. To predict the critical SRF values of unreinforced pond ash mixed with lime embankment both in normal condition and flood condition.
5. To predict the settlement of unreinforced pond ash embankment and pond ash mixed with lime embankment.

CHAPTER -2

LITERATURE SURVEY

2.1 General

An enormous quantity of coal ash is produced as a by-product of combustion of coal in thermal power stations. This enormous quantity encourages using pond ash/ fly ash in bulk. Among the various uses of pond ash/fly ash, its bulk utilization is possible only in geotechnical engineering applications. Pond ash/fly ash by itself has little cememtitious property but in the presence of water it reacts chemically with lime and forms cementatious compounds which results in increase of strength of pond ash/fly ash. Therefore, pond ash can be successfully used in geotechnical applications.

Pozzolanic reaction between pond ash and lime involves a reaction between quick or hydrated lime and silica and alumina of the pond ash to form cementitious material. Pozzolanic reaction is as follows **(Beeghly and Schrock, 2009)**:

- **Silicates:**

$$SiO_2 + Ca(OH)_2 + H_2O \longrightarrow CaO\text{-}SiO_2\text{-}H_2O \text{ (calcium silicate hydrate)}$$

- **Aluminates:**

$$Al_2O_3 + Ca(OH)_2 + H_2O \longrightarrow CaO\text{-}Al_2O_3\text{-}H_2O \text{ (calcium aluminate hydrate)}$$

- **Ferro Aluminates:**

$$Fe_2O_3 + Al_2O_3 + Ca(OH)_2 \longrightarrow CaO\text{-}Al_2O_3\text{-}Fe_2O_3\text{-}H_2O \text{ (calcium ferroaluminate hydrate)}$$

Reviews of Literature:

Pandian (2004): The author has presented a review on characterization of the fly ash with reference to geotechnical applications. The study has revealed that the detailed investigations carried out on fly ash elsewhere as well as at the Indian Institute of Science show that fly ash has good potential for use in geotechnical applications. It has low specific gravity, ease of compaction, , good frictional properties, insensitiveness to changes in moisture content, freely draining nature, etc. which shows that it can be gainfully employed in the construction of embankments, as a sub-base material, as a backfill material etc.. It can be also used in reinforced concrete construction since the alkaline nature will not corrode steel. The specific gravity is lower leading to lower unit weights resulting in lower earth pressures.

Mohanty (2012): The author has been carried out a study to evaluate geotechnical property of lime stabilized fly ash sample. The following conclusions were drawn:

1. Fly ash consists of grains mostly of fine sand to silt size with uniform gradation of Particles.
2. Specific gravity of particles is lower than that of the conventional earth materials.
3. Fly ash sample responds very poorly to the compaction energy. Maximum dry density increases and optimum moisture content decreases with addition of lime.
4. Increase in curing period of lime treated fly ash specimen show improvement in the UCS value of fly ash.
5. With increase in compaction energy followed by curing period shows a significant increase in strength due to closer packing of particles.
6. The angle of internal friction and unit cohesion vary from 24.84 to 27.34 degree and 10.7 to 13.4 kPa with the change in compaction energy.
7. The unsoaked CBR value is more than soaked CBR value.
8. Permeability of the lime treated fly ash specimens, reduces with increase in lime content due to the pozzolanic reaction between fly ash and lime which results in blocking of the flow paths thus reducing the value of coefficient of permeability.

2.2 Slope Stability Analysis

Slope stability analysis is performed to evaluate the safe design and the equilibrium conditions of a human-made or natural slopes such as embankments, road cuts, open-pit mining, excavations, landfills etc. The term slope stability may be defined as the resistance offered by the inclined surface to failure by collapsing or sliding.

Aim of Slope Stability Analysis:

- Investigation of optimal slopes with regard to safety
- Finding endangered areas
- Reliability and economics
- Investigation of the slope sensitivity to different triggering mechanisms
- To investigate the mechanisms of potential failure
- Evaluation of possible remedial measures such as barriers and stabilization

Successful design of the slope necessitates geological information and site characteristics, e.g. slope geometry, groundwater conditions, properties of soil/rock mass, alternation of materials by faulting, movements and tension in joints, joint or discontinuity systems, earthquake activity etc.

The most common methods of slope stability analysis are:

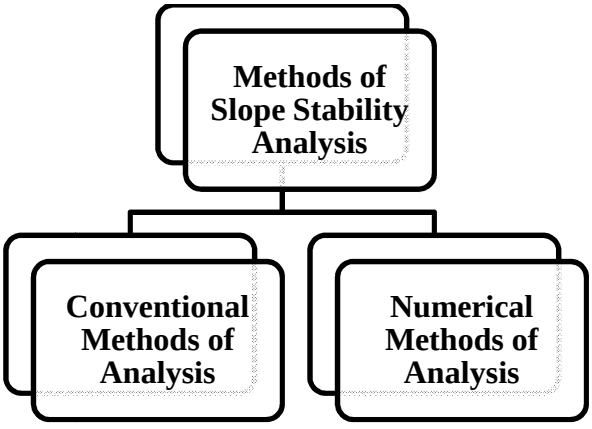

Fig. 2.1: Methods of Slope Stability

The correct choice of analysis technique depends on both site conditions and the potential mode of failure.

2.2.1 Conventional Methods of Analysis

Common conventional methods of slope stability analysis are :

- Limit equilibrium method
- Stereographic and kinematic method
- Rock fall simulators

Limit Equilibrium Method

Limit equilibrium methods are the most popular conventional method of the slope stability analysis. Limit equilibrium methods are used to investigate the equilibrium of the soil mass tending to slide down under the influence of gravity. Rotational or transitional movement is considered on assumed potential slip surface below soil or rock mass. Limit equilibrium methods are based on Mohr-Coulomb criteria in which all the forces (moments or stresses) resisting instability of the mass are compared with those that causing instability (disturbing forces). In these methods two-dimensional sections are analyzed assuming plain strain conditions. These methods it is assumed that the shear strengths of the materials along the potential failure surface are governed by linear or non-linear relationships between shear strength and the normal stress on the failure surface. Limit equilibrium analysis provides a factor of safety, delineated as a ratio of shear resistance (available) to the shear resistance (required) for equilibrium. The slope is considered unstable if the value of factor of safety is less than 1.0.

There are many different limit equilibrium methods such as:

- Ordinary method of slices (Swedish circle method/Fellenius), 1927
- Bishop simplified method, 1955
- Janbu simplified method, 1968
- Janbu general procedure to slices, 1968
- Spencer method, 1967
- Sarma method, 1973

Sarma and Spencer are called as rigorous methods because they satisfy all three conditions of equilibrium: force equilibrium in horizontal and vertical direction and moment equilibrium condition. These methods can provide more accurate results than non-rigorous methods. Bishop simplified method are non-rigorous methods satisfying only some of the equilibrium conditions.
Results (factor of safety) of particular methods can vary because methods differ in assumptions and satisfied equilibrium conditions.

Functional slope design considers calculation with the critical slip surface where is the lowest value of factor of safety. Failure surface can be located with the help of computer programs using search optimization techniques. There is wide variety of slope stability software is available which are based on limit equilibrium concept.

Reviews of Literature:

Vashi et al. (2012): The authors have carried out a parametric study is to investigate the applicability of limit equilibrium method for analyzing reinforced embankment on soft soil using the GEO5 – slope stability software version 12. On the basis on the study the following conclusions are drawn:

1. The use of full length of geotextile covering whole width of embankment can increase factor of safety (F.S) at steeper slope inclination.
2. Due to geotextile reinforcement, slope inclination and vertical spacing of geotextile decreases which resulting safer designs.
3. As compared to PP geotextile reinforced embankment, PET geotextile reinforced embankment gives economical and safe design, when the creep phenomenon is considered as a governing factor.
4. Factor of safety tended to increase linearly with increase in reinforcement strength and decreasing vertical spacing Sv of reinforcement & embankment slope β.
5. For all the cases it is found that because of the flooded condition there is a decrease in the slope stability which might lead to instability as it does not have minimum level of safety against failure.

Zornberg et al. (1998): The authors have used limit equilibrium method to evaluate failure of geotextile reinforced slope models tested in a centrifuge. They have performed a parametric study to describe the effect geotextile tensile strength, reinforcement overlapping layers, orientation of reinforcement forces, non-uniformity of unit weight in the centrifuge models, lateral friction of the models against centrifuge box. The following conclusions are given below:

1. Orientation of the reinforcement forces should be considered horizontal in the analysis of reinforced soil slopes.
2. Important contribution was provided by the overlapping reinforcement layers to the stability of the reinforced slope models.
3. On the basis of centrifuge test, they have suggested that geotextile improves the soil properties by the restricting the lateral deformations.

Shiwakoti et al (1998): In order to study the behavior of geosynthetic-reinforced slopes, the authors have carried out an analysis using limit equilibrium analysis with log spiral and two-

part wedge failure mechanisms. The authors have conducted a Parametric study to investigate the effects of varying the soil strength, porewater pressure, vertical spacing of geosynthetic, geosynthetic strength, soil-geosynthetic interaction coefficients, surcharge load, backslope and facing slope. The following conclusions were drawn:

1. Due to higher pore water pressures, the unstable zone is larger because of deeper potential failure surfaces. In this condition, to provide greater reactive forces to stabilize the unstable zone, additional reinforcement length and strength of reinforcement is necessary.
2. The extent of the mobilized reactive force greatly changes with depth. Therefore, from a technical and economic point of view, the selection of a geosynthetic with an appropriate ultimate strength is essential. For more cost-effective design a greater number of medium strength geosynthetic layers should be used instead of using a few strong reinforcement layers.
3. To reduce the required base length and avoid failure of the base geosynthetic layer, a geosynthetic with a rough surface is desirable. Alternatively, soil layers with greater friction angles can be laid at the base.
4. The required total reinforcement length and destabilizing force increases significantly, with an increase in the surcharge load intensity.
5. As wall face slope increases, it causes mobilization of greater tensile forces, as well as an increase in number of reinforcement layers subjected to compound failure.
6. The overall required reinforcement length, as well as mobilized reinforcement reactive force increases significantly due to inclusion of a backslope, particularly when the value of φ' is small.

Limitation of Limit Equilibrium Method:

Limit equilibrium is most commonly used and simple solution method, but if the slope fails by complex mechanisms (e.g. internal deformation and brittle fracture, liquefaction of weaker soil layers, progressive creep, etc.), it can become inadequate. In these cases more appropriate numerical methods of slope stability analysis should be utilized.

2.2.2 Numerical Methods of Analysis

Full scale reinforced test embankments are difficult and expensive to construct and monitor. Therefore an alternate method such as numerical methods or simulation is necessary. Numerical modelling techniques provide an approximate solution to problems which otherwise cannot be solved by conventional methods, e.g. complex geometry, material anisotropy, non-linear behavior, in situ stresses. Numerical analysis allows for material deformation, failure, modelling of pore pressures, creep deformation, dynamic loading, assessing effects of parameter variations etc. However, numerical modelling is restricted by some limitations. For example, input parameters are not usually measured and availability of these data is generally poor. To use numerical analysis, user should be aware of boundary effects, meshing errors, hardware memory and time restrictions.

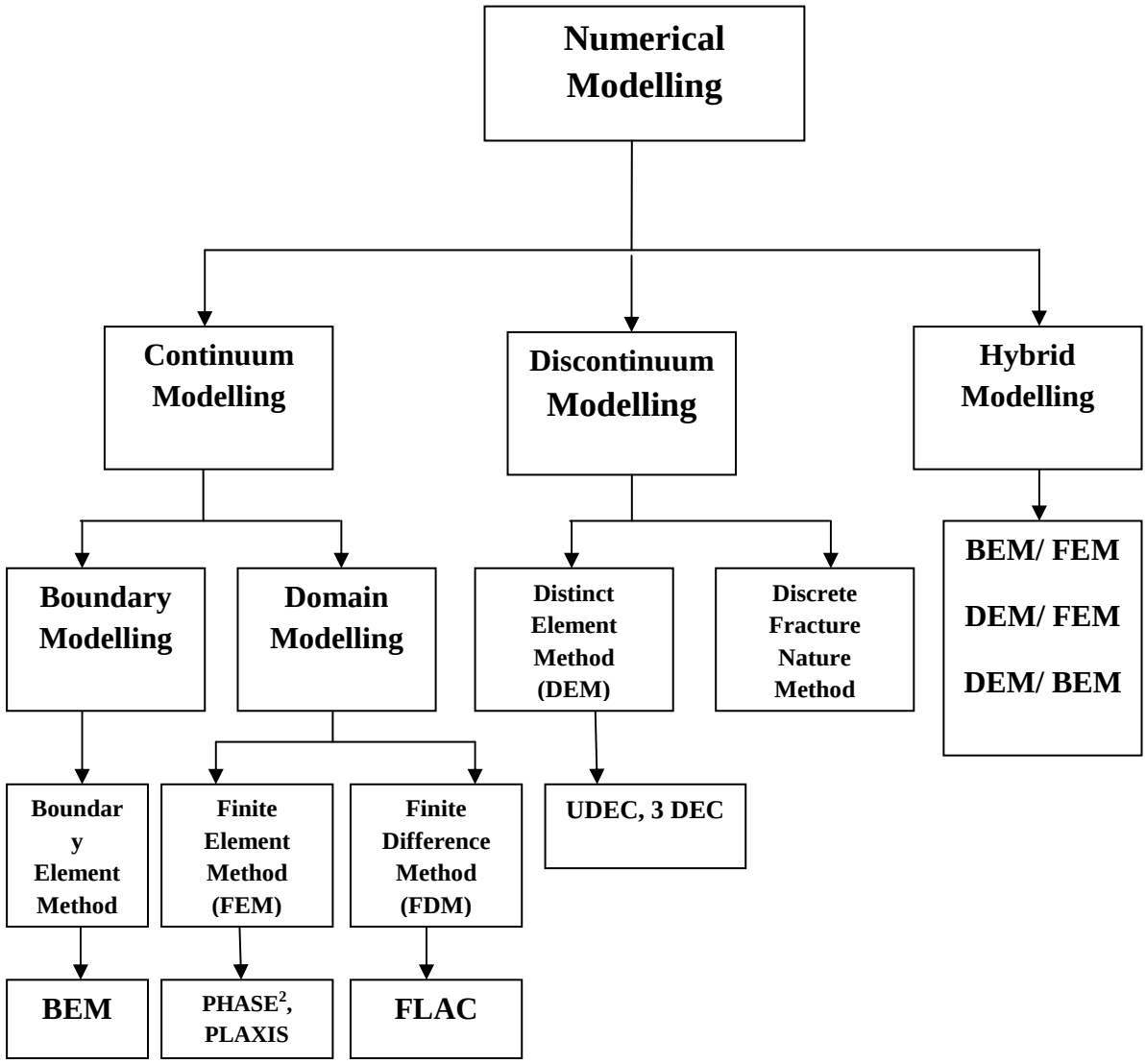

Fig. 2.2: Numerical Methods of Slope Stability Analysis

Modelling of the continuum is suitable for the analysis of soil slopes, massive intact rock or rock mass with small discontinuity spacing. Continuum approach includes the finite-difference and finite element methods that discretize the whole mass to finite number of elements with the help of generated mesh. In finite-difference method (FDM) differential equilibrium equations (i.e. strain-displacement and stress-strain relations) are solved. Finite element method (FEM) uses the approximations to the connectivity of elements, stresses between elements and continuity of displacements. Several constitutive models are usually available, e.g. elasticity, strain-softening, elasto-plasticity, elasto-viscoplasticity etc.

Finite Element method:

Finite element method (FEM) is a numerical technique which involves:

- Dividing the domain of the problem into the number of sub domains of standard shapes (triangular, tetrahedral and quadrilateral) with fix number of nodes at vertices and / or on the sides.
- Sub domains interact with each other and they are assigned a constant rate of strain. These strains are expressed in terms of nodal displacements.
- Sub domains are represented by a set of element equations. These elements equations are categorized according to the topological relation between nodes and elements.
- Then all sets of element equations are assembled in to global system of algebraic equation.
- The solution techniques are known for global system of equations, and can be calculated from the initial values of the original problem to obtain a numerical answer.

A mesh generation technique is used for dividing a complex problem into small elements. The subdivision of a whole domain into simpler parts has several advantages:

1. Inclusion of dissimilar material properties
2. Accurate representation of complex geometry
3. Easy representation of the total solution

In finite element method, Mohr-Coulomb criteria is generally used to evaluate the shear strength along the sliding surface. According to this criteria factor of safety against failure can be defined as the ratio of available shear strength of the soil (i.e. maximum shear stress which a soil can resist without failure) to the mobilized shear stress. Factor of safety, by Mohr-Coulomb criteria, usually expressed as:

$$F = \tau / \tau_f \qquad (2.1)$$

$$F = (c + \sigma_n \tan\Phi) / \tau_f \quad (2.2)$$

Where, F = Factor of safety

τ = Shear strength (available)

τ_f = Shear stress (mobilized)

c = Cohesion and

Φ = Angle of internal friction

In terms of the moment, FOS can be defined as the ratio of resisting moment, developed by soil shear forces to the driving moment, developed due to the driving shear forces originated by weight of the failed soil mass. It can be expressed as:

$$F= M_R / M_D \quad (2.3)$$

Where, M_R = Resisting Moment (MR)

M_D = Driving Moment (MD)

With the addition of geosynthetics, the factor of safety is increased due to the additional resisting moment provided by the tension developed in the geosynthetics.

$$F_R = (M_R + R\Sigma T) / M_D \quad (2.4)$$

Where, R = Radius of the slip circle and

T = Tension developed in the geosynthetic layers installed in the slope.

Advantages of the Finite Element method (Griffiths and lane, 1999):

The advantages of a finite element method of slope stability analysis over limit equilibrium method can be summarized as follows:

1. No assumption needs to be made in advance about the shape or location of failure surface. Failure occurs “naturally” through the zones within the soil mass in which the soil shear strength is unable to resist the applied shear stresses.
2. Since there is no concept of slices in the finite element method there is no need for assumptions about slice side forces. The finite element method maintains global equilibrium until “failure” is reached.
3. If realistic soil compressibility data is available, the finite element method will give information about deformations at working stress levels.
4. The finite element method is able to monitor failure up to and including overall shear failure.
5. It is also capable to analyze complex slope geometries which are not possible to analyze by LEM. Analysis.

Reviews of Literature:

Griffiths and lane (1997): The authors have described advantage of using finite element method over limit equilibrium method for slope stability. On the basis on study, it can be concluded that the main advantage of finite element analysis over the conventional method is that complete interaction of the embankment foundation system can be simulated. In the case of limit equilibrium method, the maximum tensile force developed in the reinforcement due to the embankment loading need to be determined beforehand. This raises the question of how to assign the magnitude of the stabilizing force used to represent the geotextile. In this regard, finite element analysis can be used to determine the magnitude of the stabilizing force and limit equilibrium analysis can then be carried out to determine the overall safety factor. Another disadvantage of limit equilibrium method is that the mode of failure probably encounter has to be pre determine.

Hammah et al. (2004): The authors have considered the rock slopes for which strength is modeled with the Generalized Hook-Brown failure criterion. The results suggest shear strength reduction (SSR) for technique analysis of rock slopes with the Mohr-Coulomb criterion. SSR uses FEM method to calculate FOS of slope. On the basis of analysis, it have can be concluded that this technique is capable of predicting stresses and deformations of support elements, such as piles, anchors and geotextiles, at failure.

Chai et al. (2002): The authors have been carried out both field and laboratory tests, as well as numerical analysis to study the effect of geotextile reinforcements on embankment. The field data together with FEM analyses revealed the following:

1. Geotextile reinforcement can increase the FOS value of the embankment on soft deposits. The magnitude of the effect is a function of the mobilized tensile force in the reinforcement and the geometry of the embankment.
2. Base reinforcement will only have a beneficial effect on subsoil deformation when the unreinforced case approaches failure.
3. The restraining effect of reinforcement can reduce the deviator stress of the soil elements directly under the reinforcement. This effect increases with an increase in embankment loading.
4. The lateral displacement and excess pore pressure development in the subsoil are sensitive indicators of embankment stability.

Kamal, et al. (2005): The authors have conducted a parametric study to investigate the influence of geotextile reinforcement on embankment using finite element method. They have drawn the following conclusions:

1. Maximum pore pressure occurs beneath the centre of the embankment.

2. The mode of embankment failure occurred in the form of circular shape with base heave occurring near the toe of the embankment.
3. Increasing the reinforcement stiffness does not contribute much to the reduction in vertical displacement compared to horizontal displacement.
4. Maximum vertical displacement does not occur beneath the centre of the embankment.
5. There is a limit to the reinforcement stiffness, which can be mobilized.

Siavoshnia et al. (2010): The authors have carried out a parametric study to investigate the applicability of finite element method for analyzing reinforced embankment on soft soil. They have determined the effect of number of geotextile layers, slope inclination, geotextile modulus and geotextile effective length on the behavior of reinforced silty sand embankment on soft clay. The study reveals the following:

1. Using one layer of geotextile between the embankment base and the under laying soft layer decrease vertical and horizontal displacement.
2. The best place for installing geotextile layer is between the embankment base and under laying soft layer.
3. We can use a geotextile with high stiffness when it is required to construct a high embankment or an embankment with steeper slope on soft soil.

Zornberg and Arriaga (2003): In order to estimate the factor of safety for stability of geosynthetic reinforced slopes using limit equilibrium method, a linear distribution of reinforcement peak tension with height has often been assumed, with zero tension at the crest and maximum peak tension at the toe of the structure. Although this assumption may be appropriate for the design of vertical geosynthetic reinforced walls. The authors have carried out a study to justifying this distribution for the design of geosynthetic reinforced slopes. They have performed a combination of centrifuge testing and digital image analysis to obtain the strain distribution within geosynthetic reinforced slopes under pre-failure conditions. Specifically, digital image analysis techniques are used to determine the displacement distribution along reinforcement layers in reduced-scale models subjected to increasing g levels. On the basis of test results they have drawn the following conclusions:

1. The location of the reinforcement maximum peak strain does not occur near the toe of the structure as assumed by conventional design methods, but was located approximately at mid-height of the reinforced slopes.
2. Also, the location of the reinforcement maximum peak strain does not occur near the toe of the structure.
3. The reinforcement maximum peak strain was located approximately at the point along the potential failure surface where overburden pressures are highest, i.e., below the crest of the slope.
4. Location and magnitude and of the maximum peak strain was obtained similar for the different geosynthetic reinforced models, even though the models had different

reinforcement layout, different backfill soil densities, and different reinforcement tensile strength.

5. The estimated factors of safety indicate that the maximum peak strain values in the reinforcements for geosynthetic-reinforced slopes built with different configurations.

CHAPTER – 3
LABORATORY INVESTIGATIONS

3.1 Introduction

In the present study, laboratory investigations have been conducted to evaluate index as well as engineering properties of Pond ash and Soil. The geotechnical behavior of Pond ash+ lime (91:09, by weight), as per the laboratory results by Gupta et al. (2013), was also investigated. The following experiments were performed:

1) Scanning Electron Microscopy (SEM)
2) Energy Dispersive Spectroscopy (EDS)
3) Specific Gravity test using Density Bottle
4) Grain Size Analysis
    a) Sieve Analysis
    b) Hydrometer test
5) Atterberg Limits
    a) Liquid Limit
    b) Plastic Limit
6) Standard Proctor Test
7) Permeability Test
8) Unconfined Compression Test
9) UU Triaxial test
10) Brazilian Test

3.2 Scanning Electron Microscopy

A scanning electron microscope (SEM) is a type of electron microscope that helps to provide the information about morphology of sample. It produces images of a sample by focusing a beam of electrons on sample and scanning it. These electrons interact with electrons in the sample, and produce various signals. These signals contain the information about the morphology of sample. By detecting the signals, produced due to interaction of electrons, information about sample's surface topography and composition can be obtained. Characteristic X-rays, which are emitted when the electron beam remove an inner shell electron from the sample, are used to predict the composition and elements in the sample. Due to the shifting of electrons, energy get released. (Liu, F. et al. 2010).

The SEM instrument is made up of two main components, (i) the electronic console and (ii) the electron column. SEM can attain resolution better than 1 nanometer. Samples can be observed in low vacuum, high vacuum and in Environmental. SEM samples can also be observed in wet condition. A scanning electron microscope (SEM) has been shown in Fig. 3.1. SEM micrographs of pond ash, soil, and lime and pond ash - lime mixture are shown from Fig. 3.2 to 3.5.

Fig. 3.1: Scanning Electron Microscope

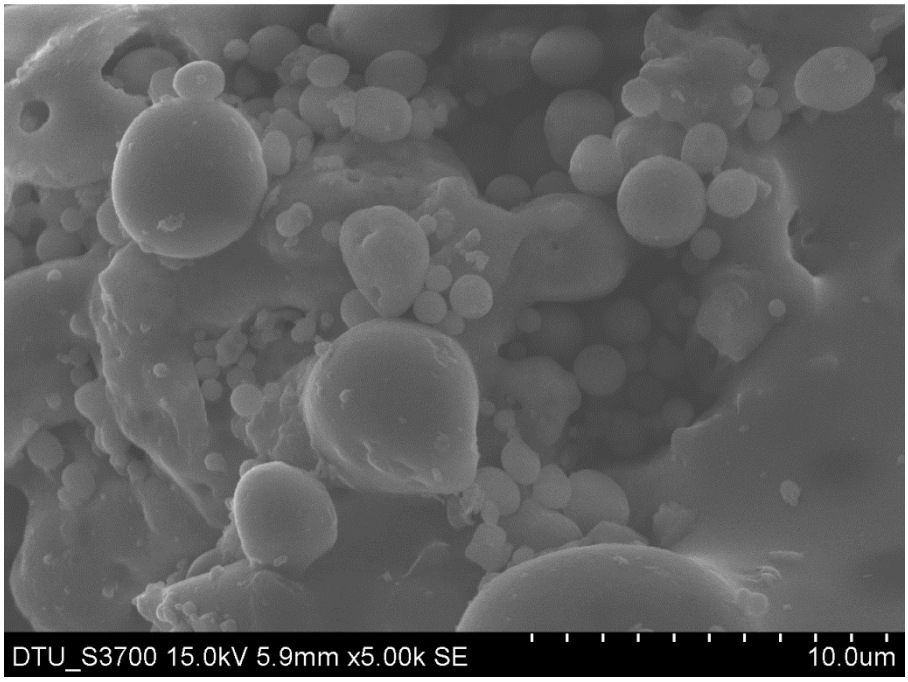

Fig. 3.2: Pond Ash at 10 μm scale

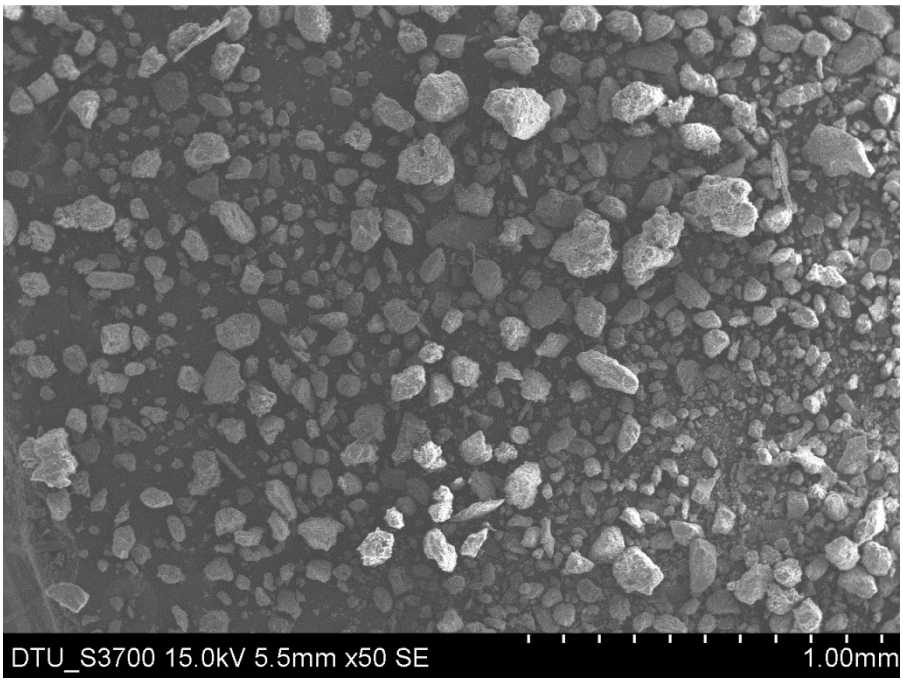

Fig. 3.3: Soil at 1 mm scale

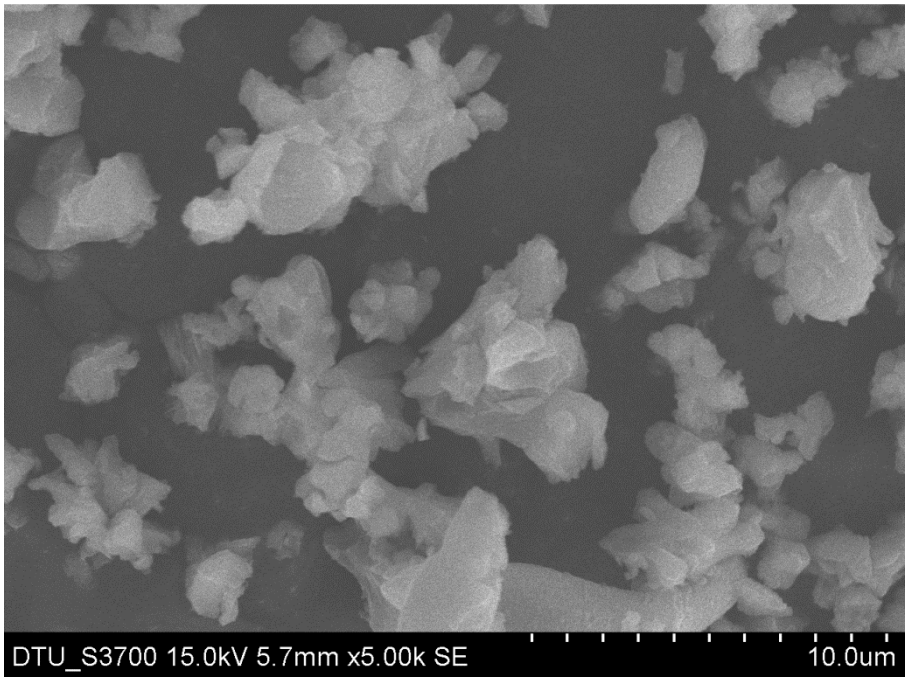

Fig. 3.4: Lime at 10 μm scale

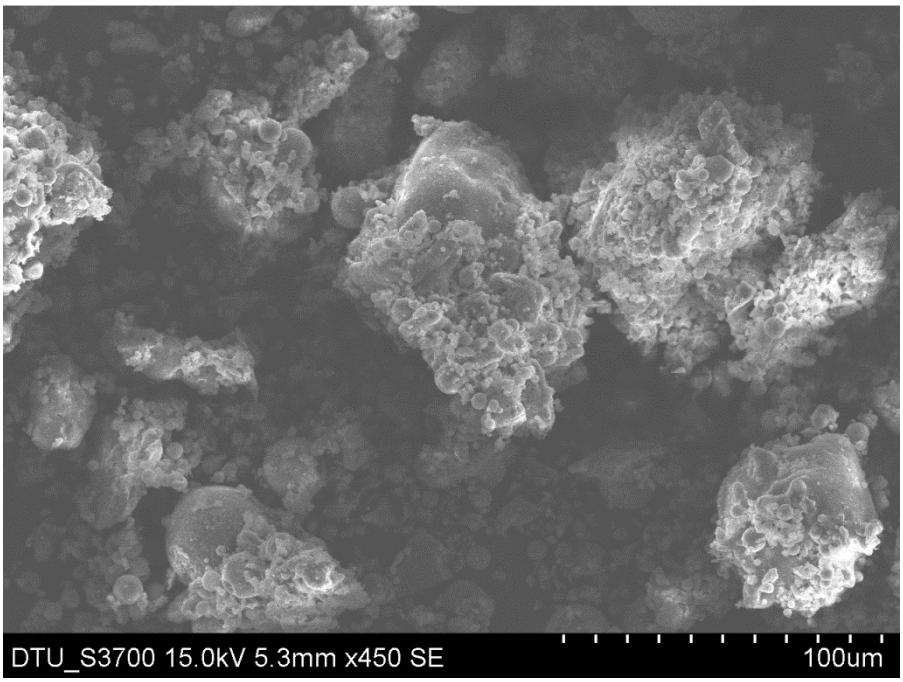

Fig. 3.5: Pond Ash+ Lime at 100 μm scale (after 28 days curing)

3.3 Energy Dispersive Spectroscopy (EDS)

An Energy dispersive spectroscopy (EDS) is an analytical technique used for chemical characterization of a sample. Scanning electron microscope (SEM) instrument, shown in Fig. 3.1 is used for energy dispersive spectroscopy, if an energy-dispersive spectrometer (or X-ray spectrometer) is added as shown in Fig. 3.6. As in SEM, in energy dispersive spectroscopy (EDS) also, a beam of electrons is focused on the sample. Then, the number and energy of the characteristic X-rays emitted from the sample is measured by an energy-dispersive spectrometer. The energy of the X-rays are characteristic of the atomic structure of the element from which they were emitted and of the difference in energy between the two shells, which allows the elemental composition (chemical composition) of the sample to be measured. EDS spectrum of pond ash, soil, and lime are shown from Fig. 3.7 to 3.9. Chemical compositions of these samples are shown in Table 3.1 to 3.3.

Fig. 3.6: Energy-Dispersive Spectrometer in SEM

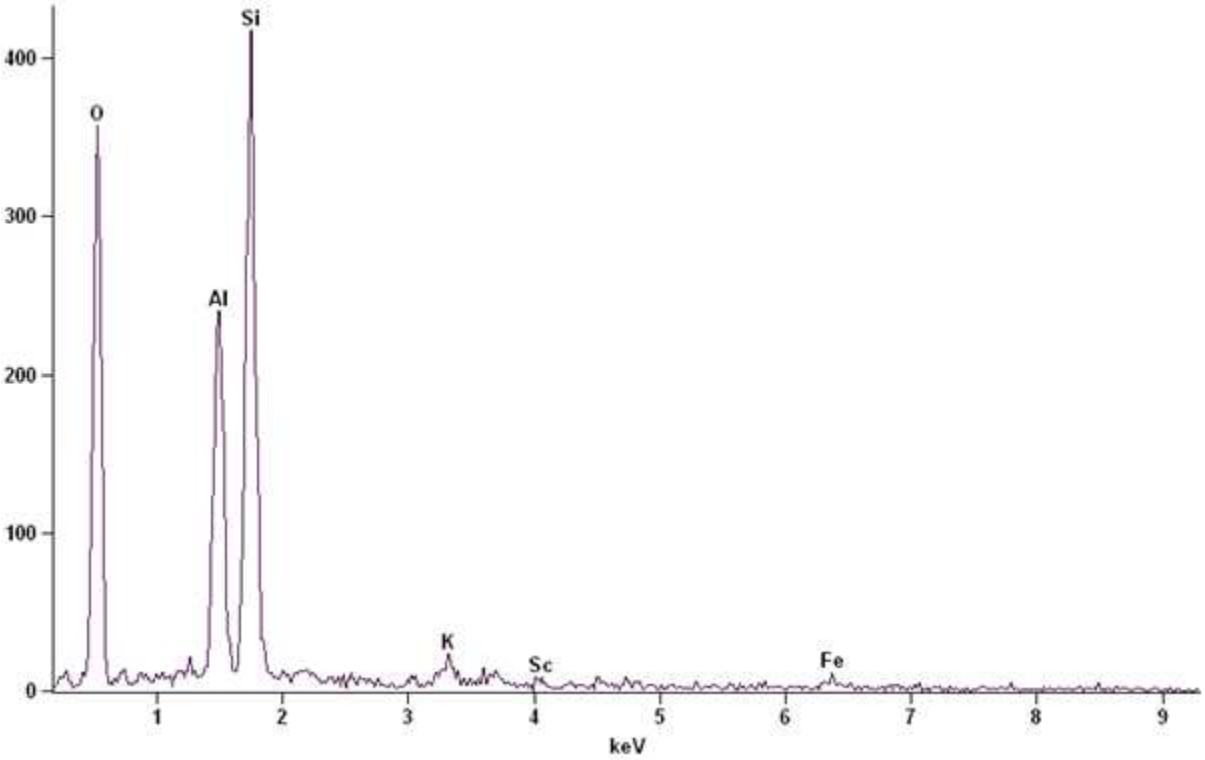

Fig. 3.7: EDS Spectrum of Pond Ash particles

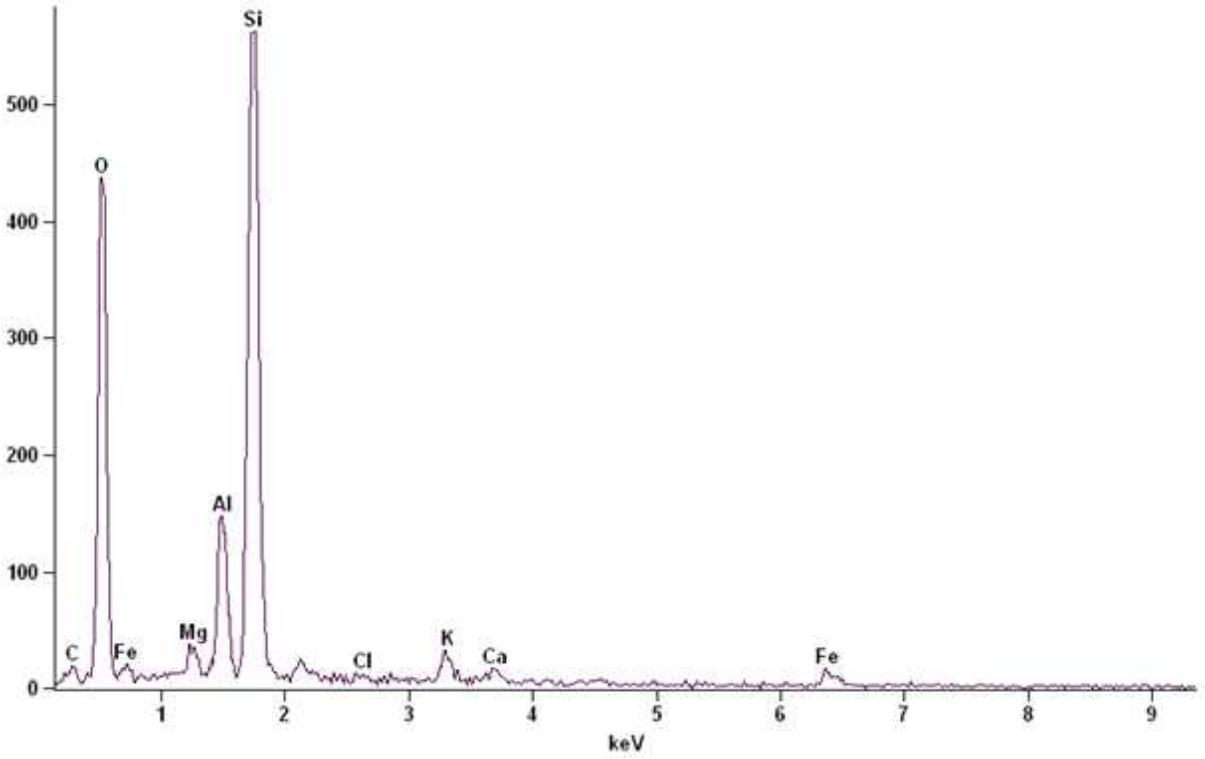

Fig. 3.8: EDS Spectrum of Soil particles

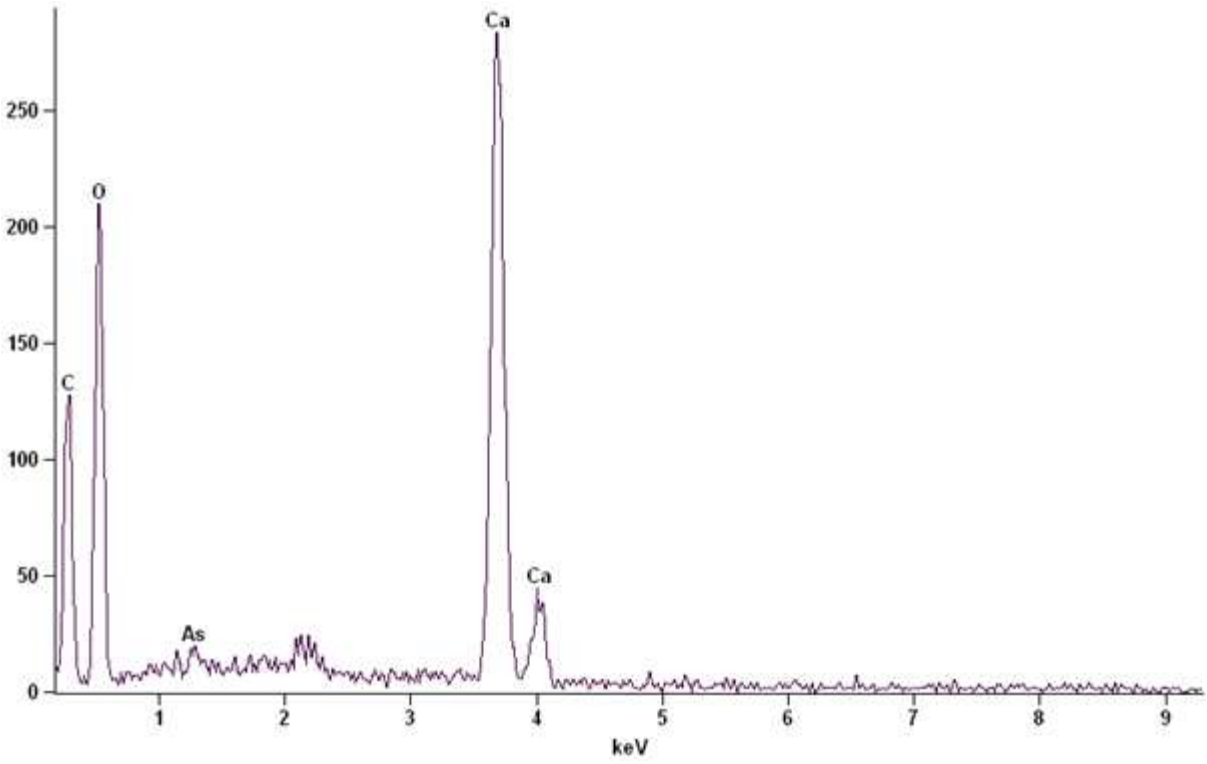

Fig. 3.9: EDS Spectrum of Lime

Table 3.1: Chemical Composition of Pond Ash

Element	Atom (%)
O	59.29
Si	24.64
Al	12.88
K	1.74
Fe	1.24
Sc	0.20

Table 3.2: Chemical Composition of Soil

Element	Atom (%)
O	56.79
Si	27.30
Al	5.48
C	4.43
Fe	2.26
K	1.65
Mg	0.97
Ca	0.85
Cl	0.28

Table 3.3: Chemical Composition of Lime

Element	Atom (%)
O	61.82
Ca	25.97
C	12.02
As	0.20

3.4 Specific Gravity Test IS: 2720 (Part 3)- 1980

Specific gravity is the ratio of the mass of unit volume of soil at a stated temperature to the mass of the same volume of distilled water at a stated temperature, generally taken at 4 degree centigrade.

To calculate the specific gravity of material following formula is used:

$$G = \frac{(M_2 - M_1)}{(M_2 - M_1) - (M_3 - M_4)} \quad (3.4.1)$$

In the present study, specific gravity of pond ash soil and lime is determined using a density bottle, shown in Fig 3.10. As lime quickly reacts with water, specific gravity of lime is determined with kerosene in place of distilled water.

The Specific gravity of pond ash, soil and lime were found to be **2.12, 2.53** and **2.57** respectively.

Fig. 3.10: Density Bottle

3.5 Grain Size Analysis IS: 2720 (Part 4)- 1985

The grain size analysis of a soil sample provides the information about the percentage of various sizes of particles. The grain size analysis (or mechanical analysis) is performed in two steps (i) Sieve Analysis and (ii) Hydrometer Test

3.5.1 Sieve Analysis

Sieve Analysis is carried out by placing sieves of various sizes in order of their mesh openings, on over other. The weight of soil retained in each sieve is used to find the percentage finer "by weight" and obtain the grain size distribution curve. It can be either done manually or by mechanical sieve shaker as shown in Fig. 3.11.

Fig. 3.11: Sieves with Mechanical shaker used for sieve analysis

3.5.2 Hydrometer Test

To determine the percentage of particles having particle size less than 75μ sieve, hydrometer test is used. The percentage of silt and clay in the soil sample is measured in this test by using a hydrometer, shown in Fig. 3.12.

Fig. 3.12: Hydrometer

The Grain size distribution curve for pond ash and soil are shown in Fig. 3.13 and 3.14

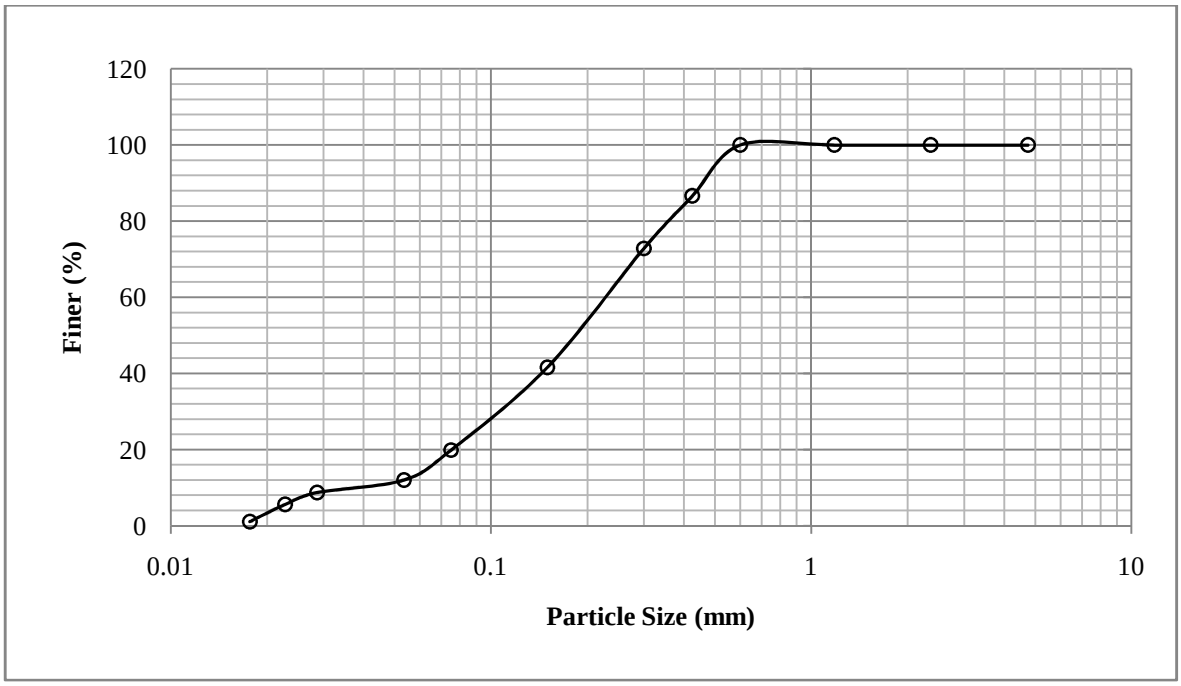

Fig. 3.13: Grain Size Distribution of Pond Ash

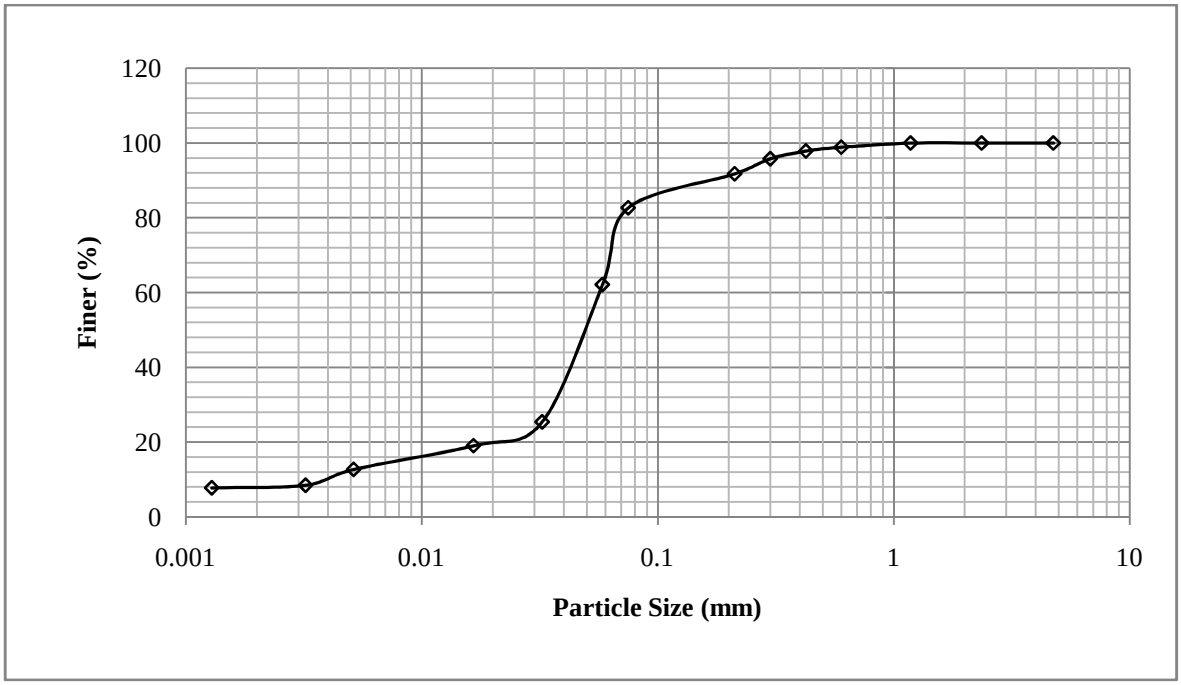

Fig. 3.14: Grain Size Distribution of Soil

3.6 Atterberg Limits IS: 2720 (Part 5)- 1985

The Atterberg's limits or consistency limits of a soil are the water content at which the soil changes from one state to other state. The Atterberg's limits, most useful for geotechnical engineering purposes are: Liquid limit, plastic limit and shrinkage limit.

3.6.1 Liquid Limit

Liquid Limit of a soil is the minimum water content, at which the soil is in liquid state but has a small strength against flowing. The liquid limit soil sample is determined using Casagrade liquid limit apparatus, shown in Fig. 3.15. The Flow curve of soil is shown in Fig. 3.16. Liquid limit of pond ash was tried to be determined with this percussion cup method but was found very difficult to make a groove in pond ash.

Fig. 3.15: Casagrade Apparatus

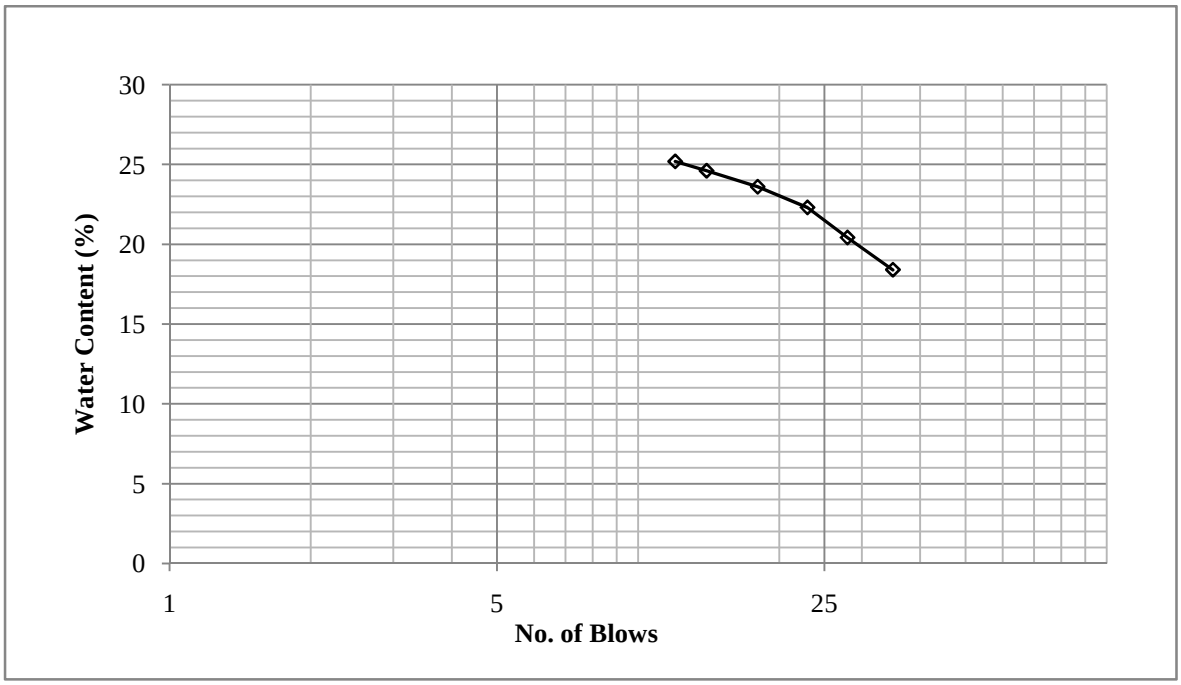

Fig. 3.15: Flow Curve of Soil

Liquid Limit, w_L = 21.44 %

3.6.2 Plastic Limit

Plastic limit of a soil is the minimum water content, at which soil will just start to crumble water rolled into a thread approximately 3mm in diameter. The soil shows the properties of a semi solid, just after the plastic limit.

A thread for pond ash was tried to be made but tit crumbled very early due to its non-plastic behavior nature. The Plastic limit (w_P) of soil is found to be **18.12 %**

The Plasticity index of a soil sample is determined as:

$$I_P = w_L - w_P \quad (3.6.1)$$

Where, I_P = Plasticity Index
w_L = Liquid Limit
w_P = Plastic Limit

The Plasticity index of a soil is = 3.32

3.7 Standard Proctor Test IS: 2720 (Part 7)-1980

Compaction is the process in which soil particles are rearranged in a dense state by impact of loading and air is expelled from the voids. The dry density of soil changes with the change in water content. Initially density of soil increase with increase in water content since this water helps in bringing the soil particles closer. If we add the water after a certain stage, there is a decrease in dry density of soil, since the excess of water replace the soil particles. The water content, at which the dry density of soil is maximum, is termed as optimum moisture content.

The bulk density and the corresponding dry density for soil are determined as:

$$\Upsilon = M/V \quad (3.7.1)$$

$$\Upsilon_d = \Upsilon/(1+w) \quad (3.7.2)$$

Where,

Υ = Bulk density of soil, Υ_d = Dry density of soil, w= Water content (%), M= Mass of wet compacted mould, V= Volume of the mould

Equipments used in Proctor Test:

Fig. 3.16: Mould with Collar

Fig. 3.17: Hammer

The Compaction curves for pond ash, soil and pond and lime mixture are shown in Fig. 3.18 to 3.20

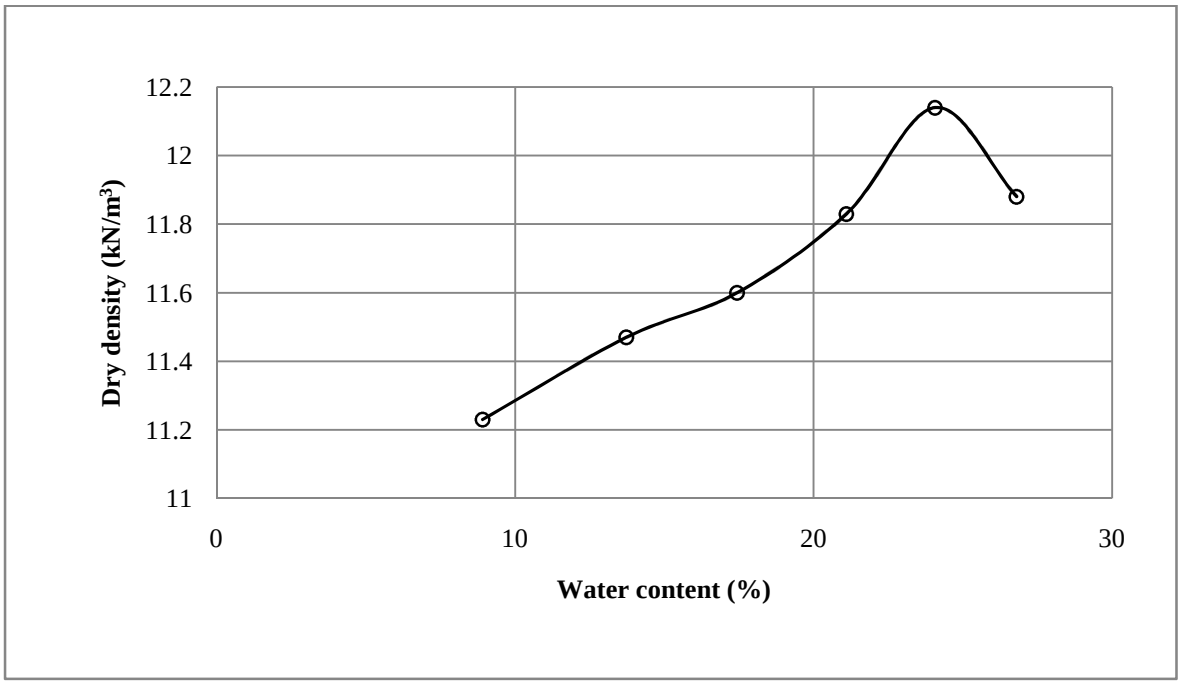

Fig. 3.18: Plot between Moisture Content and Dry Density for Pond Ash

Optimum Moisture Content, OMC = 24.07 %
Maximum Dry Density, MDD = 12.14 kN/m^3

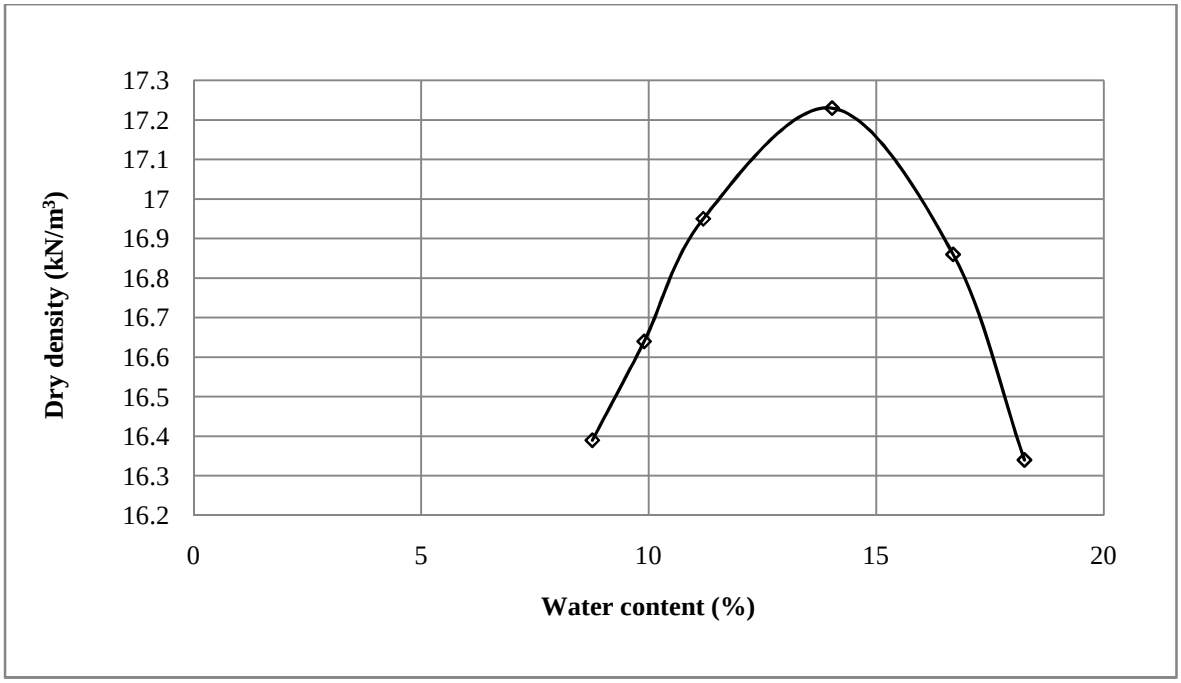

Fig. 3.19: Plot between Moisture Content and Dry Density for Soil

Optimum Moisture Content, OMC = 14.03. %
Maximum Dry Density, MDD = 17.23 kN/m^3

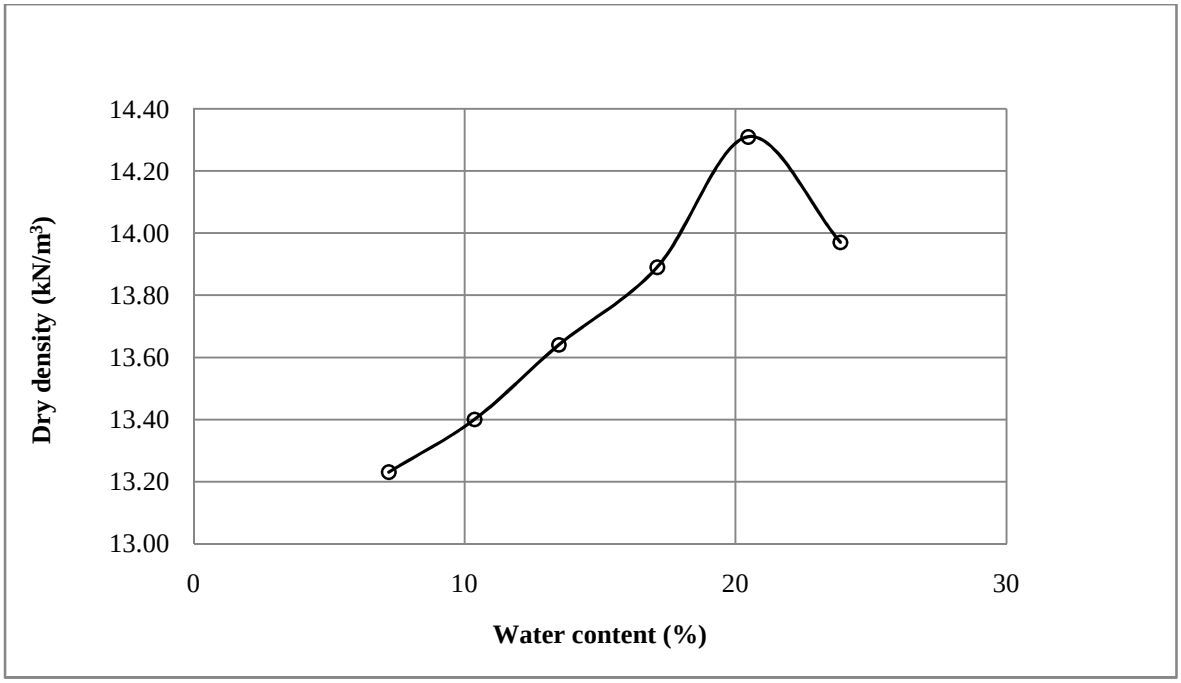

Fig. 3.20: Plot between Moisture Content and Dry Density for Pond Ash + Lime

Optimum Moisture Content, OMC = 20.47 %
Maximum Dry Density, MDD = 14.31 kN/m^3

3.8 Permeability Test IS: 2720 (Part-17)-1986

Permeability (or hydraulic conductivity) is the property of a soil which allows the seepage of water through the voids. This property is very essential for the calculation of seepage through soil structure. The Permeability test apparatus is shown in Fig. 3.21.

In the present study, falling head permeability test is performed for pond ash, soil and pond ash- lime mixture. The Coefficient of permeability of a sample is given as:

$$k = 2.3\frac{aL}{At}\log_{10}\frac{h_1}{h_2} \quad (3.8.1)$$

Where, k = Coefficient of Permeability
a = Area of stand pipe
A = Cross- sectional area of soil sample
L = Length of sample
t = Time interval
h_1 = Initial head
h_2 = Final head

The Coefficient of permeability of pond ash, soil and pond ash-lime mixture was found to be 7.00×10^{-6} m/s, 1.53×10^{-7} m/s and 3.27×10^{-6} m/s respectively.

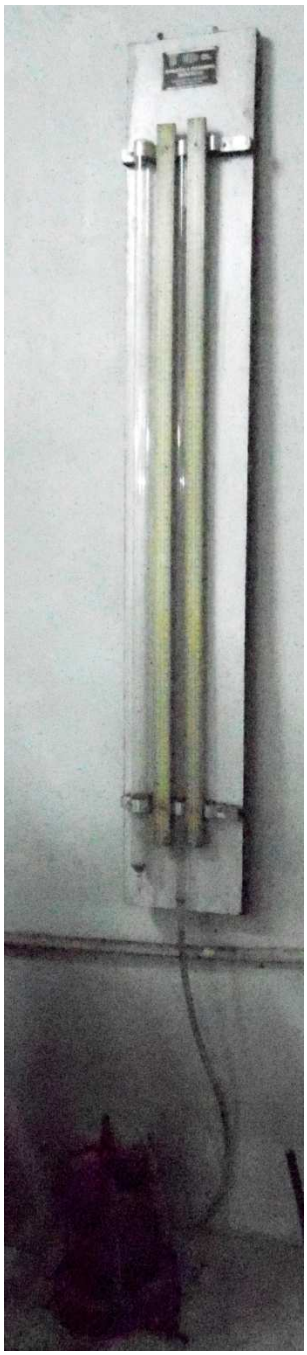

Fig. 3.21: Permeability Test Apparatus

3.9 Unconfined Compression Test IS: 2720 (Part-10)-1991

Unconfined compressive strength of soil can be determined by using Unconfined compression test apparatus as shown in Fig.3.22. To determine the unconfined compressive strength of soil, samples were prepared as shown in Fig. 3.23. The Unconfined compression test is done on pond ash and soil sample at OMC, immediately after the preparation of sample. The Pond ash mixed with lime samples are cured for 28 days, and then UCS test was performed on those samples. The stress v/s strain curve for pond ash, soil and pond-lime mixture are shown in Fig. 3.25 to 3.27.

Fig. 3.22: Unconfined Compression Test Apparatus

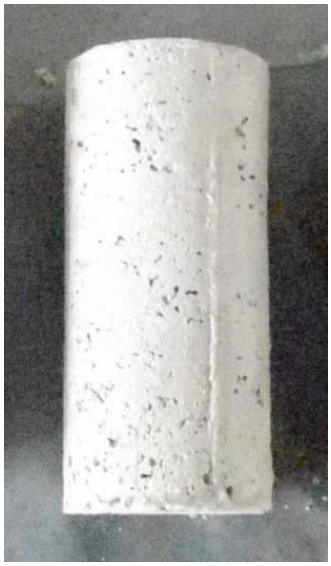

Fig. 3.23: Samples prepared for UCS test

Fig. 3.24: Failure pattern of sample obtained in UCS test

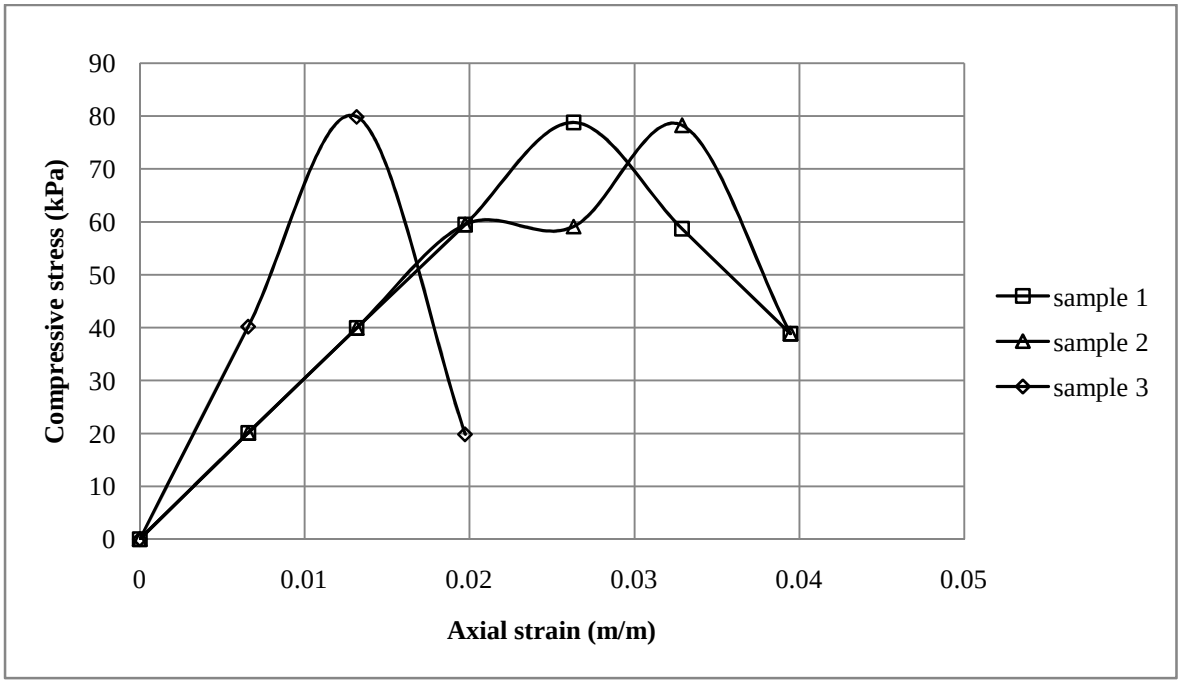

Fig. 3.25: Compressive Stress v/s Axial Strain curve for Pond Ash

Unconfined compressive strength = 78.99 kPa

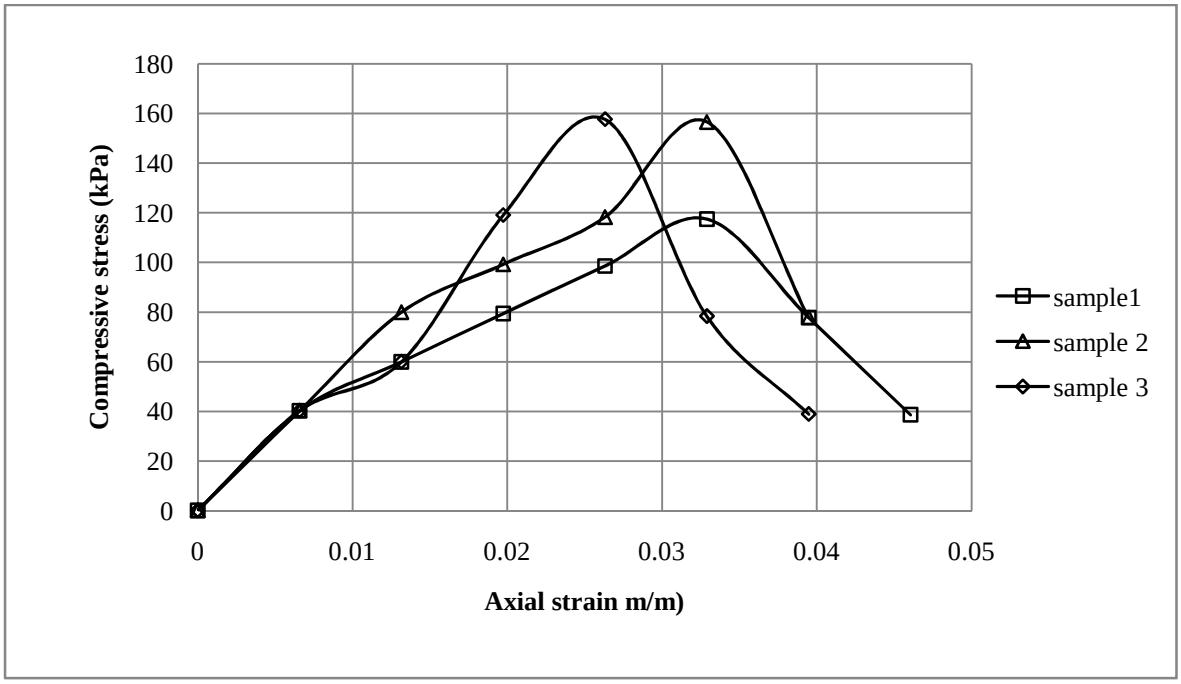

Fig. 3.26: Compressive Stress v/s Axial Strain curve for Soil

Unconfined compressive strength = 143.87 kPa

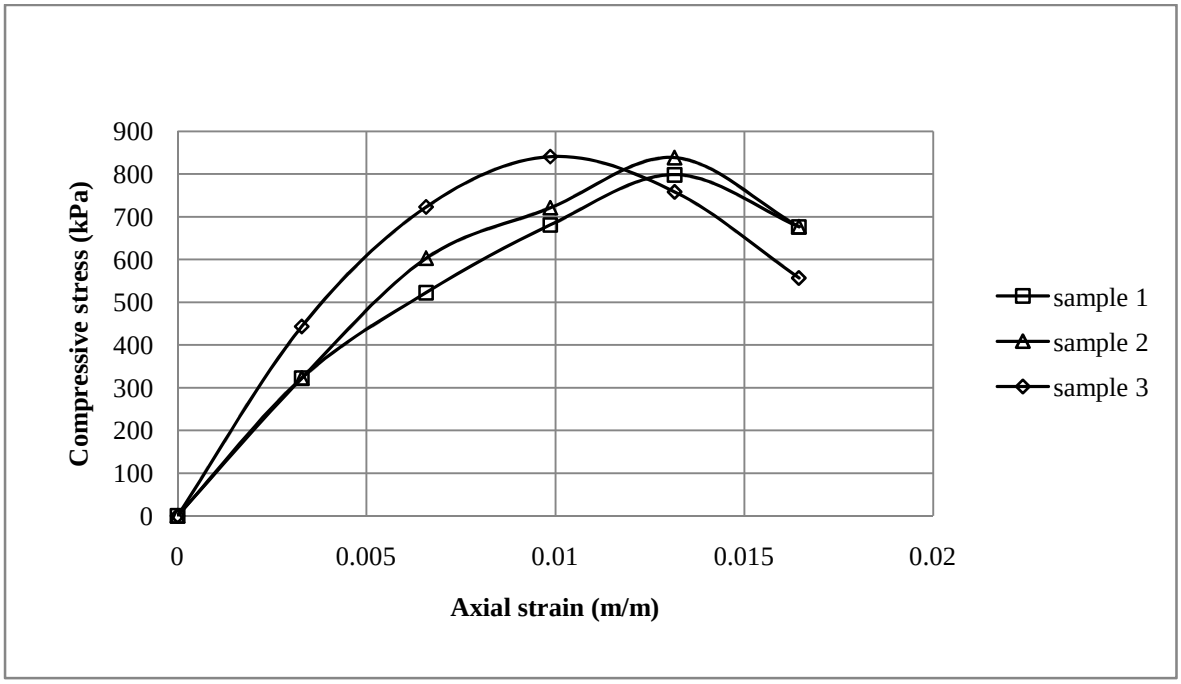

Fig. 3.27: Compressive Stress v/s Axial Strain curve for Pond Ash + lime (after 28 days curing)

Unconfined compressive strength = 826.33 kPa

3.10 UU Triaxial Test IS 2720: (Part-11)-1993

UU triaxial test is used to find the shear strength of soil. It can be used to obtain the shear strength parameters of both fine and coarse grained soils. In this test drainage is not permitted and consolidation is not necessary, so this test is very quick, and also referred as Q-test.
The test is different from the UCS test in a way that the confinement from the surrounding soil inside the ground can be simulated by applying water. Since, UCS is unconfined, so the test is representative of soils in construction sites where the rate of construction is very fast and the pore waters do not have enough time to dissipate.

Some useful terms in triaxial testing:
Total stress: $\sigma = \gamma.H$
Pore water pressure: $u = \gamma_w.H$
Effective stress: $\sigma' = \sigma - u$
Confining pressure: σ_3
Deviatoric stress: σ_d
Axial stress: $\sigma_1 = \sigma_d + \sigma_3$

As drainage is not allowed, u increases right after the application of σ_3' as well as after the application of σd.
As $U_c = B.\ \sigma_3$ and $U_d = A\ .\ \sigma_d$
Total $u = B.\ \sigma_3 + A\ .\ \sigma_d$
$u = B.\ \sigma_3 + A\ .\ (\sigma_1 - \sigma_3)$

The test has been carried out with the triaxial teat apparatus shown in Fig. 3.28. To perform this test samples has been prepared with pond ash, soil and pond ash-lime mixture at MDD and OMC. Pond ash and soil samples were tested at OMC, immediately after the preparation of samples. The Pond ash mixed with lime samples, shown in Fig.3.29, were cured for 28 days, and then UU triaxial test was performed on those samples. The deviator stress v/s axial strain plots and mean stress v/s shear stress plots for pond ash, soil and pond-lime mixture are shown in Fig. 3.31 to 3.36.

Fig. 3.28: Triaxial Test Apparatus

Fig. 3.29: Samples Prepared

Fig. 3.30: Failure pattern of sample

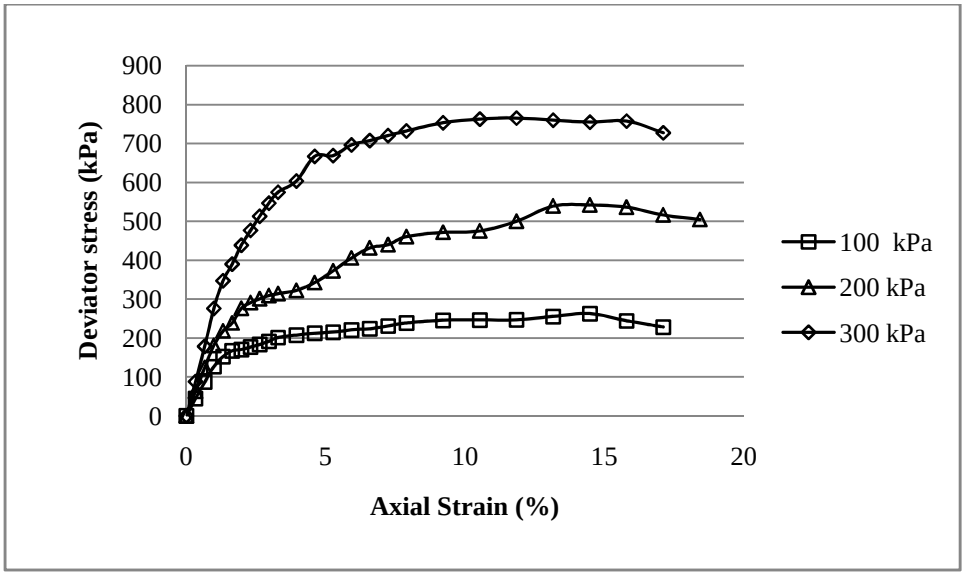

Fig. 3.31: Plot between Deviator stress v/s Axial stain for Pond Ash

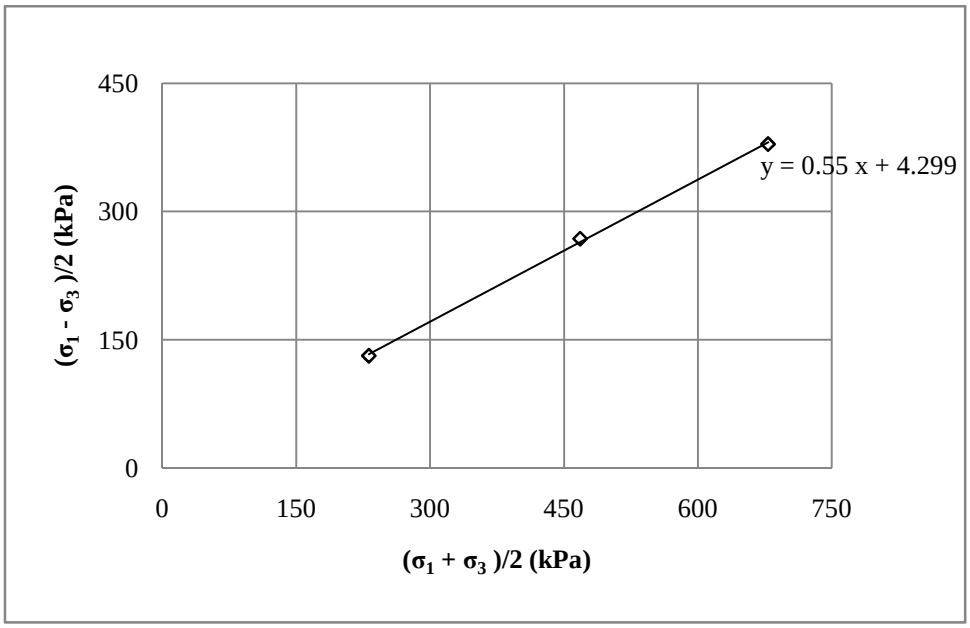

Fig. 3.32: Plot between Mean stress v/s Shear stress for Pond Ash

Cohesion, c = 5.15 kPa
Angle of internal friction, ϕ = 33.40 deg.

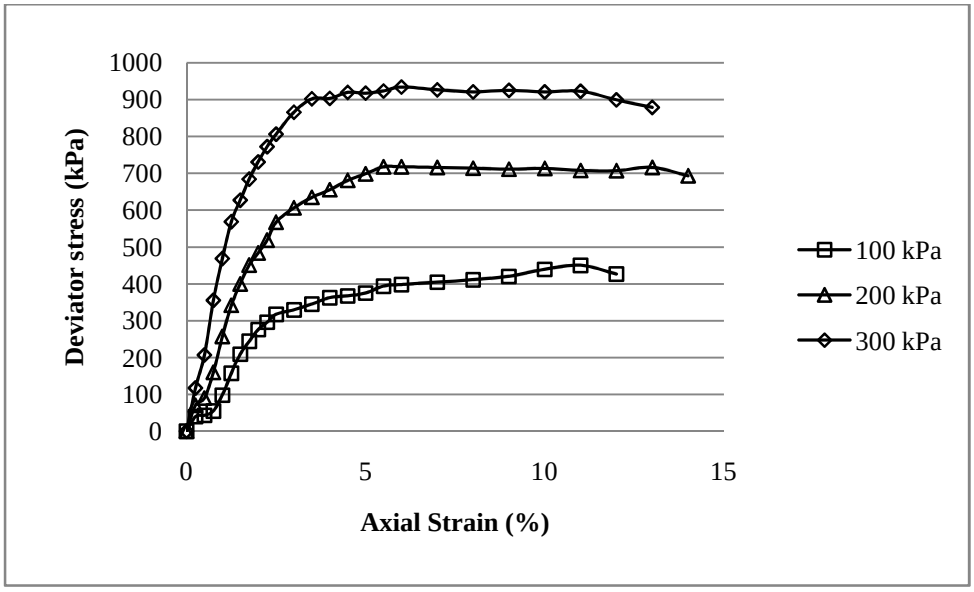

Fig. 3.33: Plot between Deviator stress v/s Axial stain for Soil

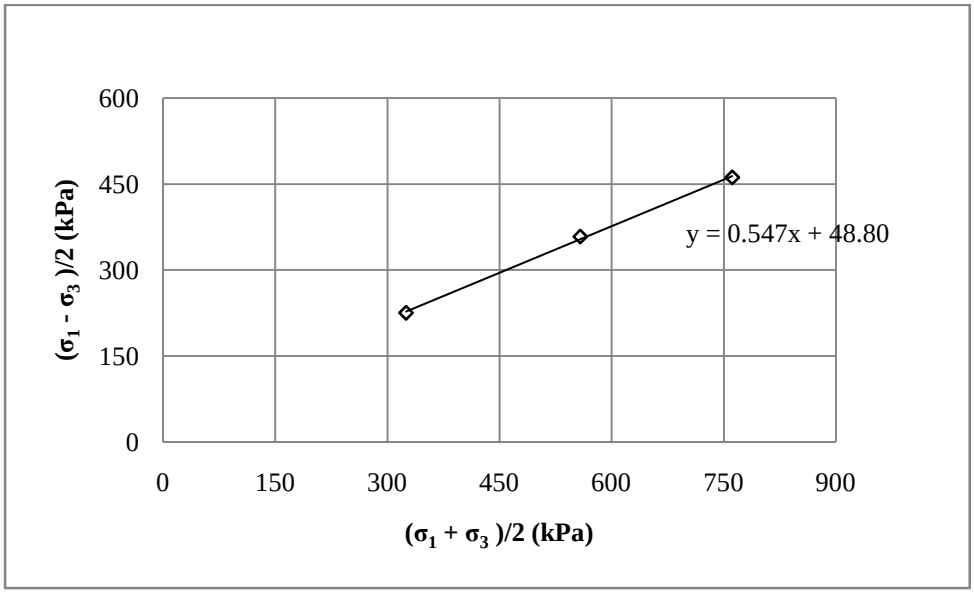

Fig. 3.34: Plot between Mean stress v/s Shear stress for Soil

Cohesion, c = 58.32 kPa
Angle of internal friction, ϕ = 33.20 deg.

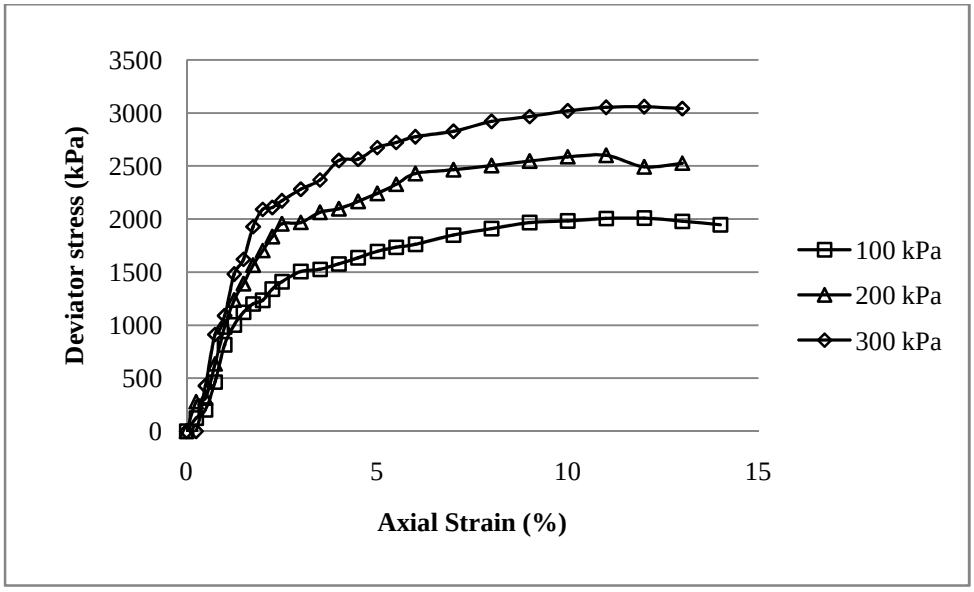

Fig. 3.35: Plot between Deviator stress v/s Axial stain for Pond Ash + Lime (after 28 days curing)

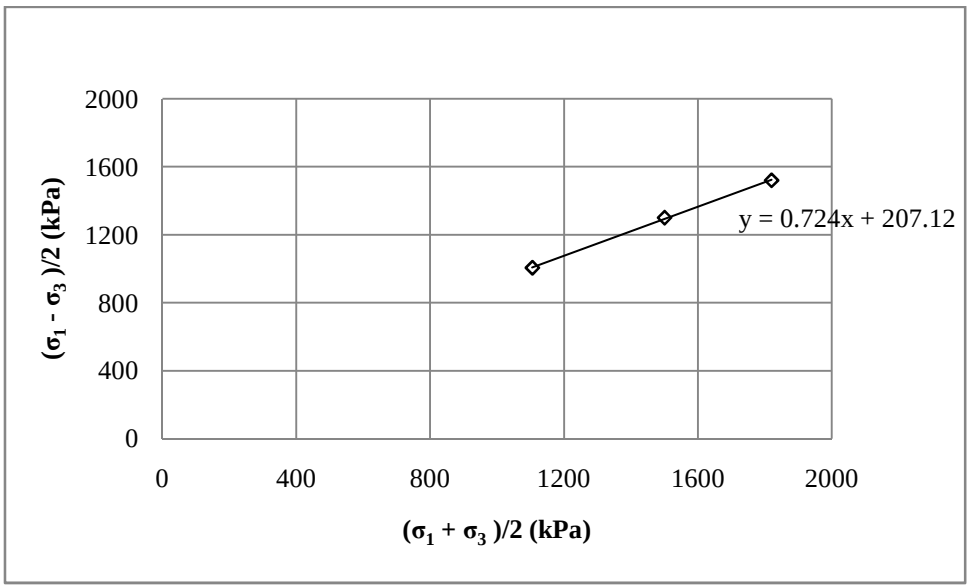

Fig. 3.36: Plot between Mean stress v/s Shear stress for Pond Ash + Lime (after 28 days curing)

Cohesion, c = 300.35 kPa
Angle of internal friction, ϕ = 46.40 deg.

3.11 Brazilian Test

The Tensile strength of a sample can be determined with the help of Brazilian test. The Brazilian test apparatus, shown in Fig.3.37 is useful only for hard samples, but soft samples cannot be tested with this apparatus. The soil and pond ash-lime mixed samples were prepared with length-to-diameter ratios (L/D) of 2, shown in Fig.3.38. The soil samples were placed in a compression loading machine (shown in Fig. 3.22) with the load platens situated diametrically across the specimen and Pond ash mixed with lime samples were cured for 28 days and were tested with Brazilian apparatus. The tensile stress v/s lateral strain curves for soil samples were shown in Fig.3.40. The maximum load to fracture the sample was recorded and tensile strength of samples was calculated as:

$$\sigma_T = 2P/ (\Pi LD) \qquad (3.11.1)$$

Where, σ_T = Tensile strength of sample

P = Maximum failure load

L = Length of the sample

D = Diameter of the sample

Fig. 3.37: Brazilian Test Apparatus

Fig. 3.38: Samples prepared for test

Fig. 3.39: Failure patterns of sample

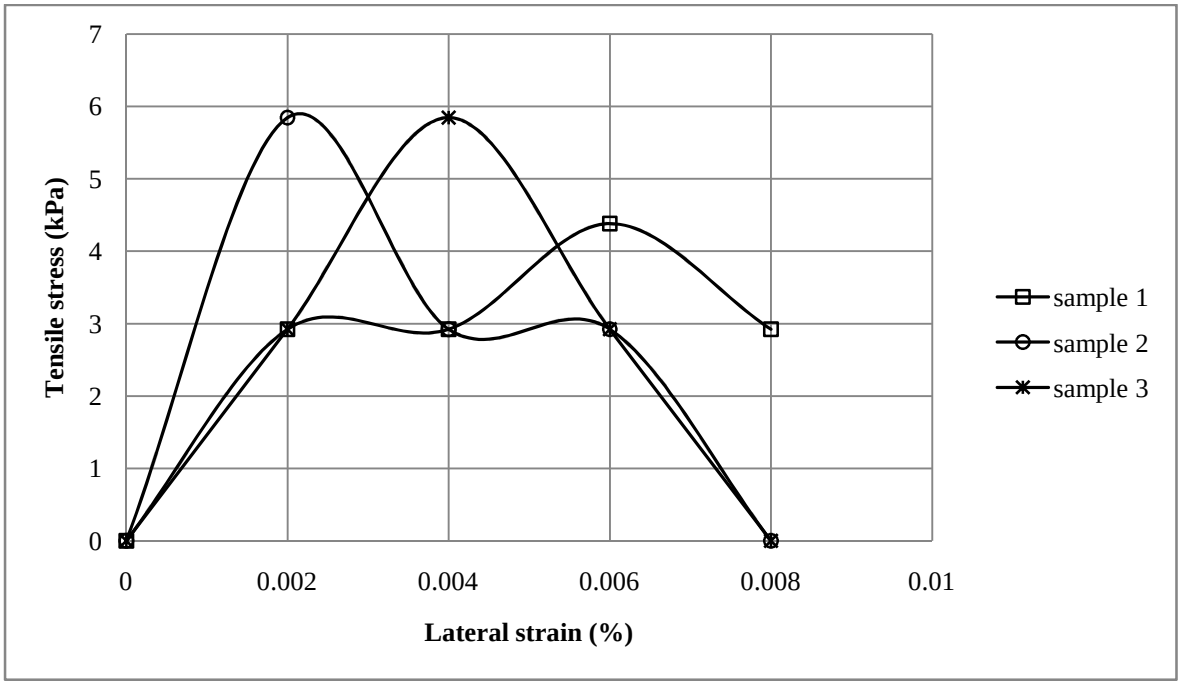

Fig. 3.40: Tensile Stress v/s Lateral Strain curve for Soil

The Tensile Strength of soil and pond ash + lime sample was found to be 5.36 kPa and 137.93 kPa respectively.

CHAPTER- 4

MODEL DETAILS FOR ANALYSIS

4.1 Model Geometry

For Slope Stability Analysis using a computer software program, the first step is to model the embankment geometry in the software interface. The geometry characteristics of an embankment are modeled which includes embankment crest width, height, slope angle and thickness of foundation soil layer. Reinforcement characteristics are also modeled such as its location, tensile strength, stiffness and vertical spacing. The second step is to provide the information about geotechnical characteristics of the embankment soil and the under laying soil.

In the present study, a theoretical model of a highway embankment is considered with horizontal crest width of 20 m for four lane highway, each of 7.5 m wide carriageway with 2 m wide median at center and walkways of 1.5 m on either side of the highway as per IRC: 6-2000. A vertical clearance of 6 m is considered for flyover openings as per IRC: 6-2000. Based on commonly adopted industry practice, nominal height of embankment is considered as 9 m. The thickness of embankment foundation soil layer is considered to be 5 m. A nominal surcharge load of 50 kPa has been considered for modeling the traffic load as commonly adopted in practice (IRC: 6-2000).

In the present study, an embankment model is considered having slope angles varied from 1H:1.5V, 1H:2.0V, 1H:2.5V, 1H:3.0V and1H:4.0V (56, 64, 68, 72 and 76 deg.) The embankment was reinforced by layers of geogrid covering whole width of embankment, with different vertical spacing. The vertical spacing of geogrid is varied from 4.5 m, 3.0 m, 2.3 m, 1.0 and 0.8 m. The effect of providing pond ash mixed with lime layer at the top and side slope on unreinforced pond ash embankment is also investigated in the study. The thickness of this layer at the top of embankment is considered as 0.5 m and at side slope, it is varied from 1 m, 1.5 m and 2 m. The geometry of embankment is represented in Fig. 4.1

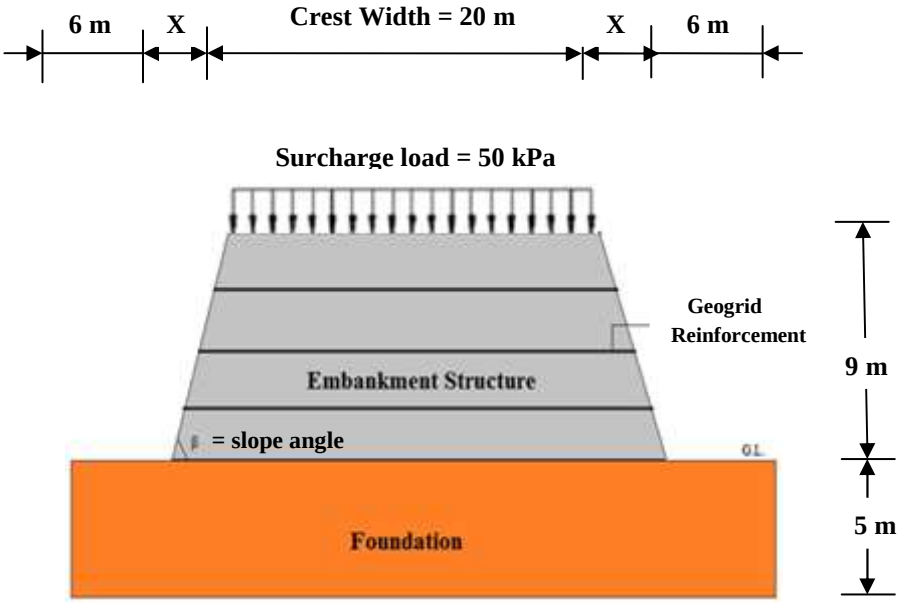

Fig. 4.1: Geometry of Embankment Model

4.2 Properties of Materials:

1) Properties of Pond Ash (Embankment structure) :

In present study the embankment structure is considered to be constructed with Pond ash. The properties of pond ash such as unit weight, cohesion, angle of internal friction, tensile strength and permeability are obtained from laboratory test results. Young's modulus of elasticity is considered to be 3200 kPa (Sinha et al., 2009) and Poisson's ratio is assumed to be 0.3. The properties of pond ash are shown in Table 4.1.

Table 4.1: Properties of Pond Ash

Properties	**Pond Ash**
Unit weight, Υ (kN/m^3)	15.06
Submerged unit weight, Υ_{sub} (kN/m^3)	6.41
Cohesion , c (kPa)	5.15
Angle of internal friction, ϕ (deg.)	33.40
Young's Modulus of Elasticity, E (kPa)	3200
Poisson ratio's (μ)	0.3
Tensile strength (kPa)	0
Permeability (m/s)	7.00×10^{-6}

2) Properties of Soil (Foundation) :

The properties of soil such as unit weight, cohesion, angle of internal friction, tensile strength and permeability are obtained from labora9tory test results. Young's modulus of elasticity is considered to be 7500 kPa (as E = 300 +6, where N is SPT value = 33 as per Soil investigation report of DTU campus) and Poisson's ratio is assumed to be a 0.3. The properties of soil are shown in Table 4.2.

Table 4.2: Properties of Soil

Properties	**Soil**
Unit weight, Υ (kN/m^3)	19.65
Submerged unit weight, Υ_{sub} (kN/m^3)	10.42
Cohesion , c (kPa)	58.32
Angle of internal friction, ϕ (deg.)	33.20
Young's Modulus of Elasticity, E (kPa)	7500
Poisson ratio's (μ)	0.3
Tensile strength (kPa)	5.36
Permeability (m/s)	1.53×10^{-7}

3) Properties of Pond Ash mixed with Lime (Embankment structure) :

In present study the embankment structure is also considered to be constructed with Pond ash + lime (91:09 by weight, Gupta et al, 2013). In present work, pond and mixed with lime layer is also provided at the top and side slope of unreinforced pond ash embankment. The properties of pond ash mixed with lime such as unit weight, cohesion, angle of internal friction, tensile strength and permeability are obtained from laboratory test results. Young's modulus of elasticity is considered to be 30×10^3 kPa and Poisson's ratio is taken as 0.3 (Sahu and Kumar, 2012). The properties of pond ash + lime are shown in Table 4.3.

Table 4.3: Properties of Pond Ash + Lime

Properties	**Pond Ash + Lime**
Unit weight, Υ (kN/m^3)	17.24
Submerged unit weight, Υ_{sub} (kN/m^3)	7.56
Cohesion , c (kPa)	300.35
Angle of internal friction, ϕ (deg.)	46.40
Young's Modulus of Elasticity, E (kPa)	30×10^3
Poisson ratio's (μ)	0.3
Tensile strength (kPa)	137.93
Permeability (m/s)	3.27×10^{-6}

4) Properties of Geogird (Reinforcement in Embankment Structure) :

A Bi–axial Geogrid, considered in the present work for reinforcement in pond ash embankment, has shown in Fig. 4.1. The properties of geogrid, as per specified by the manufacture, are shown in Table 4.4.

Table 4.4: Properties of Geogrid

Properties	**Geogrid**
Typical dimensions (m)	0.4×0.4
Tensile Strength (kN/m)	40
Stiffness (kN/m)	760

Fig. 4.2: Bi-axial Geogrid

CHAPTER- 5

FINITE ELEMENT MODELLING

5.1 Software used for Analysis PHASE^2

In the present work, a parametric study is carried out using a computer software program PHASE^2. PHASE^2 is finite element method (FEM) based, 2-dimensional elasto-plastic program for calculating shear strains and displacements around underground openings or surface excavations in rock or soil. This program can be used for design and analysis in geotechnical and civil engineering problems such as support design, groundwater seepage, finite element slope stability, and probabilistic analysis. In PHASE^2 program, finite element slope stability analysis is carried out using shear strength reduction method. In PHASE^2 program, critical strength reduction factor (SRF) values can be determined with different failure criterions such as:

- Mohr-Coulomb Failure Criterion
- Hook-Brown Failure Criterion
- Generalized Hook-Brown Failure Criterion
- Drucker-Prager Failure Criterion

5.2 Validation of Software

The results obtained for unreinforced fly slope from Bishop's method by Bhardwaj and Mandal (2008) using centrifuge test are compared with the result obtained from finite element analysis using PHASE^2 software. In the work by Bhardwaj and Mandal (2008), slope model is considered with slope geometry shown in Fig. 5.1. The fly ash properties considered by Bhardwaj and Mandal (2008), in the analysis are Cohesion = 9.50 kN/m^2, Friction Angle = 18.32 deg., Unit weight = 11.92 kN/m^3 and Poisson's ration = 0.30.

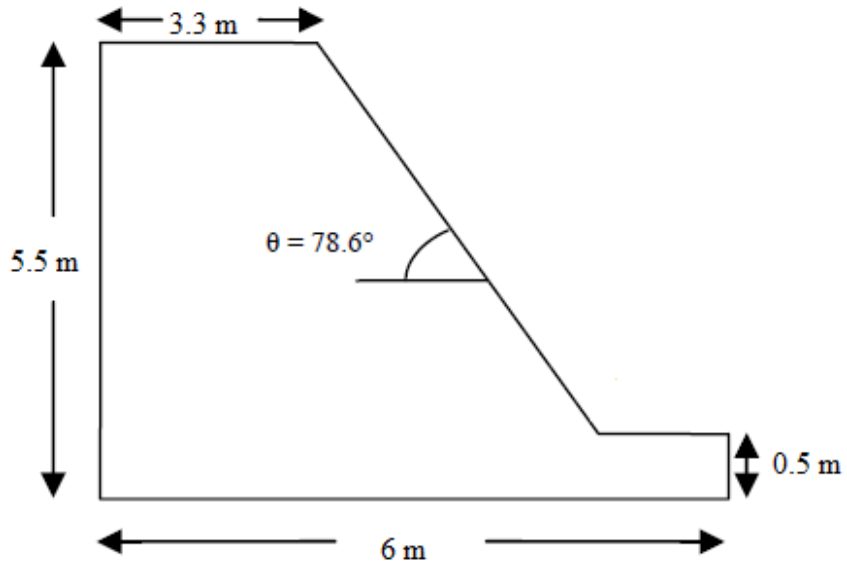

Fig. 5.1: Slope Geometry (Bhardwaj and Mandal, 2008)

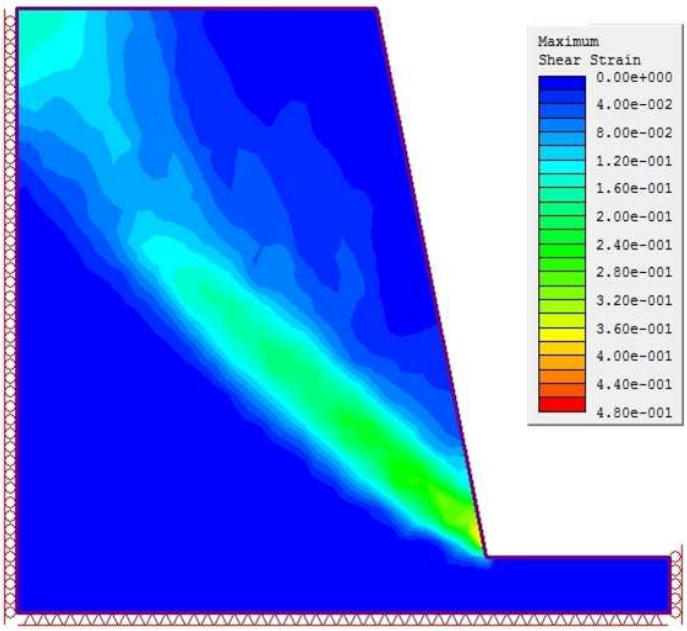

Fig. 5.2: Shear Strain contours obtained from finite element analysis using PHASE^2

Factor of safety is 0.88 as determined by the Bhardwaj and Mandal (2008) using bishop's method and the factor of safety obtained from FEM analysis using PHASE^2 software is 0.85. When compared the results the variation in factor of safety is observed to be about 3.4 %. A fairy good agreement can be seen the results.

5.3 Finite Element Modelling of Embankment Slope

In the present study the finite element modelling has been performed for a Highway embankment model with varying different parameters. Around 115 cases have been considered for the current study. Finite Element-Shear Strength Reduction (SSR) technique has been used to analysis. Then the effect of different parameters on critical SRF, tension in geogrid and strains in slopes has been analyzed. Finite Element Modelling includes:

a) Finite Element Discretization and Meshing

2D, 6-noded plane strain elements has been used to discretize the profiles of embankment slope models. A uniform meshing has been used in the present analysis study.

b) Boundary Conditions

Face: The slope face was kept free.
Lateral sides: Roller boundary conditions are assumed of the model such that displacement is allowed in y-direction and displacement is restrained in the x-direction.
Bottom: The bottom boundary has been kept fixed so that no displacement is allowed either in x-direction or y-direction.

c) Gravity Loading

In Foundation Soil: Both Field stress and a body force (self-weight) are considered
In Embankment Structure: Only body force (self-weight) is considered because embankment soil is manually deposited on the top of foundation soil. Therefore, there is no in-situ stress in the embankment structure.
The body force is calculated using the unit weight defined for the material in the material properties. Weight above an element applied by the material is calculated by the unit weight of the material given as input in Phase2. The horizontal to vertical stress ratio is kept as 1.0.

d) Hydraulic Boundary Conditions

In case of flood analysis, hydraulic boundary conditions need to be specified to the model.
A Total head value = 1 m is considered due to ponded water at the both sides edge of embankment slope (above ground level), when considering Flood level = 1m
A Total head value = 4.5 m is considered at the both sides of embankment slope (above ground level), when considering Flood level = 4.5 m i.e., half submerged case.

The Total head boundary conditions represent the elevation of the phreatic line (ponded water)

e) Factor of Safety (FOS) and Strength Reduction Factor (SRF)

Slope fails because of its material shear strength on the sliding surface is insufficient to resist the actual shear stresses. The value of factor of safety used to examine the stability state of slopes. The value of FOS, greater than 1 means the slope is stable and slope is considered to be instable when FOS value is lower than 1. The factor of safety against slope failure, in accordance to the shear failure, is simply calculated as:

$$FOS = \tau / \tau_f \quad (5.3.1)$$

Where τ is the shear strength of the sloping soil, which can be calculated through Mohr-Coulomb criterion as:

$$\tau = c + \sigma_n \tan\Phi \quad (5.3.2)$$

and τ_f is the shear stress on the sliding surface, which can be calculated as:

$$\tau_f = c_f + \sigma_n \tan\Phi_f \quad (5.3.3)$$

Where, c_f and Φ_f are the factored shear strength parameters. These can be calculated as:

$$c_f = c / SRF \quad (5.3.4)$$

$$\Phi_f = \tan^{-1}(\tan\Phi / SRF) \quad (5.3.5)$$

Where, SRF is strength reduction factor. This method has been named as the 'shear strength reduction method'. In order to determine the factor of safety, PHASE^2 program performs an analysis and provides the information about the value of SRF starting from SRF=1 that will just cause the slope to fail. The final value of FOS or SRF was obtained from the analysis.

f) Failure criterion

The failure criteria used in this study is the non-convergence of the solution (Griffiths and Lane, 1999). When the FEM algorithm cannot converge within a user specified maximum number of iterations, it indicates that no stress distribution can be found that can simultaneously able to satisfy both the Mohr- Coulomb failure criterion and global equilibrium (Griffiths and Lane, 1999). Slope failure and numerical non-convergence occur simultaneously, and are followed by a significant increase in the nodal displacements within the mesh.

g) Stopping Criterion for PHASE^2

PHASE^2 allows choosing one of the stopping criteria: (a) Absolute Energy and (b) Square Root Energy. For the current study absolute energy criteria and energy tolerance of 0.1% is considered.

Some embankment slope models generated by the PHASE^2 program are shown below:

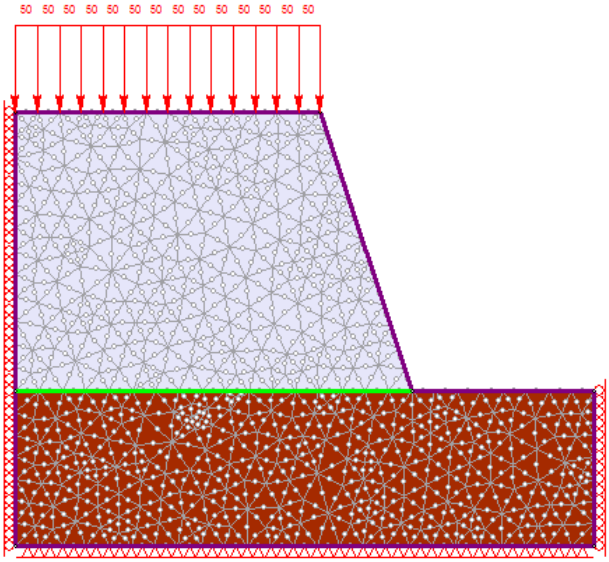

Fig. 5.3: Unreinforced embankment slope model

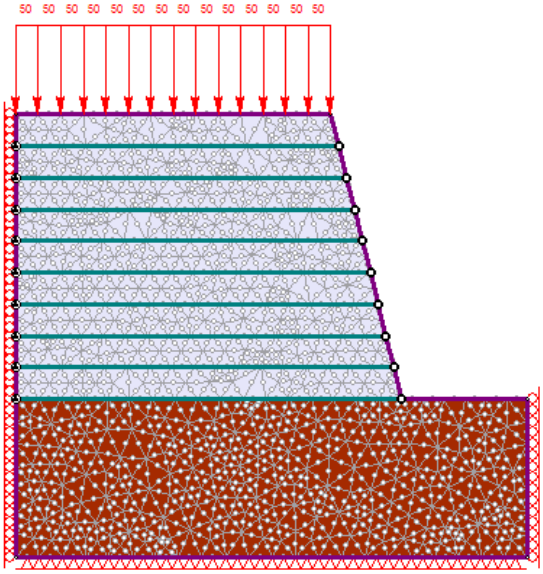

Fig. 5.4: Reinforced embankment slope model

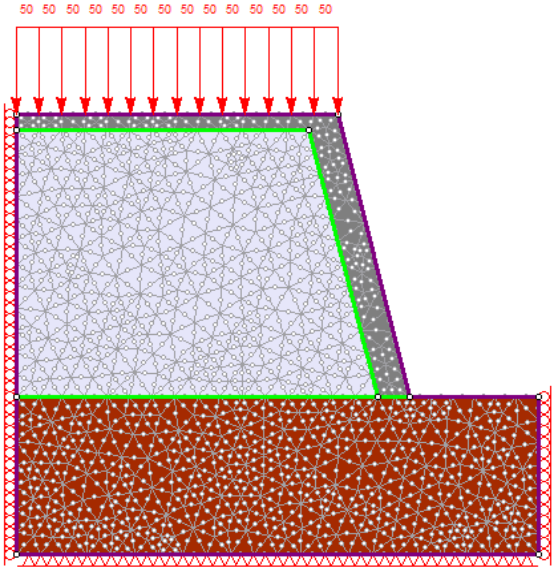

Fig. 5.4: Unreinforced embankment slope model with pond ash and lime layer

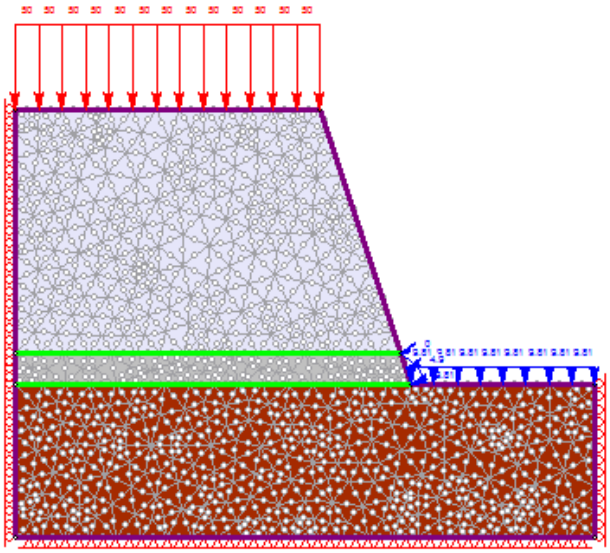

Fig. 5.5: Unreinforced embankment slope model for flood condition

CHAPTER- 6

SETTLEMENT ANALYSIS

6.1 Settlement Calculation for Embankment

As mentioned earlier, a nominal surcharge load of 50 kPa has been considered on the top surface of embankment for modeling the traffic load**.** This surcharge load will lead to settlement of embankment structure and precise prediction of the settlement of embankment structure is very necessary. Therefore, to predict the settlement of embankment structure, the **Schmertmann and Hartman (1978) method** has been used in the present study.

In Schmertmann and Hartman (1978) method an empirical relationship has been utilized to investigate the pattern of vertical strains in the stressed soil zone. The Schmertmann and Hartman (1978) have given an equation to calculate settlement of a structure resulting from the combined effect of soil compression and volume distortion. In this method the following equation is used for settlement calculation (δ):

$$\delta = C_1 C_2 \Delta p \Sigma (I_z / E) \Delta z \quad (6.1)$$

Where,

Δp = Increase in effective overburden pressure at embankment level
Δz = Thickness of layer under consideration
C_1 = Depth embedment factor
C_2 = Correction factor for creep
I_z = Strain influence factor
E = Young's Modulus

1) Calculation of Load (Δp) at Embankment Level :

In present case, a nominal surcharge load of 50 kPa is considered at the top of embankment. Therefore, Δp = 50 kPa

2) Calculation of Depth Embedment Factor (C_1):

Depth embedment Factor, C_1 is applied to consider the effect of embedment. Therefore, in the present case, C_1 = 1.0.

3) Calculation of Correction Factor for Creep (C_2):

The Correction factor for creep is calculated as:

$$C_2 = 1 + 0.2 \log_{10} (t / 0.1) \quad (6.2)$$

Where, t = time at which settlement is to be calculated in years.

In present study, time for settlement calculation is varied from 10, 20, 30 40 and50 years. For these different time intervals, the value correction factor (C_2) has been given in Table 6.1.

Table 6.1: Values of Correction Factor (C_2)

Time (t)	10 years	20 years	30 years	40 years	50 years
Value of C_2	1.4	1.46	1.49	1.52	1.54

4) Calculation of Thickness of Layer under Consideration (Δz) :

In present case, settlement is determined for embankment structure. Therefore, Δz = 9m

5) Calculation of Strain Influence Factor (I_z) :

The Strain influence factor is calculated as:

$$I_z = 0.5 + 0.1\sqrt{\frac{\Delta p}{\sigma_z}} \tag{6.3}$$

Where, σ_z = Vertical Pressure at depth B/2 and B is width of embankment.

σ_z can be given by Approximate Stress distribution Method, as:

$$\sigma_z = \frac{q\,(B \times L)}{(B+Z)(L+Z)} \tag{6.4}$$

Where, q = Surcharge load
B = Width of embankment
L = Height of embankment
Z = B/2

In present case, q = 50 kPa, B = 20 m, Z = 10 m and L = 9 m
Therefore, σ_z = 15.79 kPa
And I_z = 0.6779

6) Calculation of Young's Modulus (E) :

In the present case, as discussed earlier, E = 3200 kPa for pond ash (Sinha et al., 2009)

E = 30×10^3 kPa for pond ash mixed with lime (Sahu and Kumar, 2012)

Hence, Settlement (δ) for embankment structure for various time interval has been given in Table 6.2.

Table 6.2: Settlement for Embankment Structure

Time, t (years)	Settlement, δ (m) For Pond Ash	Settlement, δ (m) For Pond Ash + Lime
10	13.34×10^{-2}	1.42×10^{-2}
20	13.92×10^{-2}	1.48×10^{-2}
30	14.20×10^{-2}	1.52×10^{-2}
40	14.49×10^{-2}	1.55×10^{-2}
50	14.68×10^{-2}	1.57×10^{-2}

`

CHAPTER – 7
RESULTS & DISCUSSIONS

7.1 Laboratory Investigations Results:

7.1.1 SEM Analysis

Scanning electron microscope provides the information about the morphology of the sample particles. SEM results of pond ash shows that the pond ash particles are rounded in shape. This shows the spherules of alumina silicates in pond ash. SEM results of soil indicates that the soil particles are sub angular particles. SEM results of pond ash and lime, cured sample shows the bonded particles of pond ash and lime.

These results were found to be in good agreement with the results obtained by Negi and Sarkar (2013), for pond ash and lime mixture.

7.1.2 EDS Analysis

Energy dispersive spectrum results shows the percentages of different elements, such as silicon (Si), oxygen (O), aluminum (Al), calcium (Ca) and Iron (Fe), etc., in pond ash , soil and lime.
The EDS results evidenced the presence of the following components: silica (SiO_2) and alumina ($A1_20_3$) and low amounts of hematite (Fe_2O_3) in pond ash.

These results were found to be in good agreement with the results obtained by Mishraa and Das (2013), in which it is concluded that coal ash samples are mainly constituted of silica (SiO_2), alumina (Al_2O_3) with little amounts of Fe_2O_3, MgO, MnO, K^2O, and T_iO_2.

7.1.3 Particle Size Distribution and Atterberg Limits Results

Particle size distribution graph shows that pond ash is poorly graded material. Particle size distribution graph of soil indicates that the soil is sandy silt.
Atterberg limits show that pond ash is non-plastic material and plastic limit as well as plasticity index of soil is low. Hence, the soil used in the present study is sandy silt with low plasticity.

7.1.4 Standard Proctor Test Results

Maximum dry density (MDD) of pond ash, soil and pond ash + lime is 12.14, 17.23 and 14.31 kN/m^3 respectively. Optimum moisture content (OMC) of pond ash, soil and pond ash + lime is 24.07%, 14.03% and 20.47% respectively. Compaction curve of pond ash shows that there is a less change in density with variation in water content. Pond ash is also easy to

compact as there are no heavy lumps to break down in comparison to natural soil. This property of pond ash is useful for embankment construction.

7.1.5 Permeability Tests Results

The Hydraulic conductivity of pond ash, soil and pond + lime was found to be 7×10^{-6}, 1.53×10^{-6} and 3.27×10^{-6} m/s respectively, at MDD and OMC. Permeability test results shows that the permeability of pond ash is high as compared to natural soil which ensures the efficient drainage which ensures the better workability.

7.1.6 Strength Tests Results

Unconfined compressive strength at MDD and OMC, for pond ash and soil sample was found to be 78.99 and 143.87 kPa respectively, while for pond ash + lime with 28 days curing it is found to be 826.33 kPa.
Tensile strength at MDD and OMC for pond ash and soil was found to be 0 and 5.36 kPa respectively, while for pond ash + lime with 28 days curing it is found to be 137.93 kPa.
Cohesion and angle of internal friction at MDD and OMC, for pond ash were found to be 5.15kPa and 33.4^{o} respectively. For soil, these were found to be 58.32 kPa and 33.2^{o} respectively, while for pond ash + lime with 28 days curing, these were found to be 300.35 kPa and 46.4^{o} respectively.

The Strength tests of pond ash + lime evidenced that the unconfined compressive strength, tensile strength as well as shear strength are very high as compared to natural soil and pond ash. This occurred due to the formation of cementitious material. The silica (SiO_2), alumina ($A1_20_3$) and ferrous oxide (Fe_2O_3) present in pond ash and lime (CaO), chemically reacted with each other in presence of water and has been formed cementitious material such as (calcium silicate hydrate ($CaO\text{-}SiO_2\text{-}H_2O$), calcium aluminate hydrate ($CaO\text{-}Al_2O_3\text{-}H_2O$) and calcium ferroaluminate hydrate ($CaO\text{-}Al_2O_3\text{-}Fe_2O_3\text{-}H_2O$), which attributed to increase in strength of pond ash and lime mixture.

All these geotechnical properties of pond ash lies in the range recommended by IRC-SP: 58-2001 for use of pond ash in embankment construction.

7.2 Finite Element Modelling Results:

7.2.4 Shape of Failure Surface and Location of Peak Tension

The Potential failure surface of embankment slope was found to be circular in shape as shown in Fig. 7.1, which shows a good agreement with the work done by Kamal et al. (2005), in which, it is concluded that the potential failure surface of embankment is circular. The Peak tension in the particular geogrid layer, is refers to the maximum tension mobilized in that geogrid layer along its length. In the present study, it observed that peak tension in georid reinforcement is found generally within the potential failure surface as shown in Fig. 7.1. The tension developed in georid layers are shown with the help bar graphs along geogrid layer in Fig. 7.1.

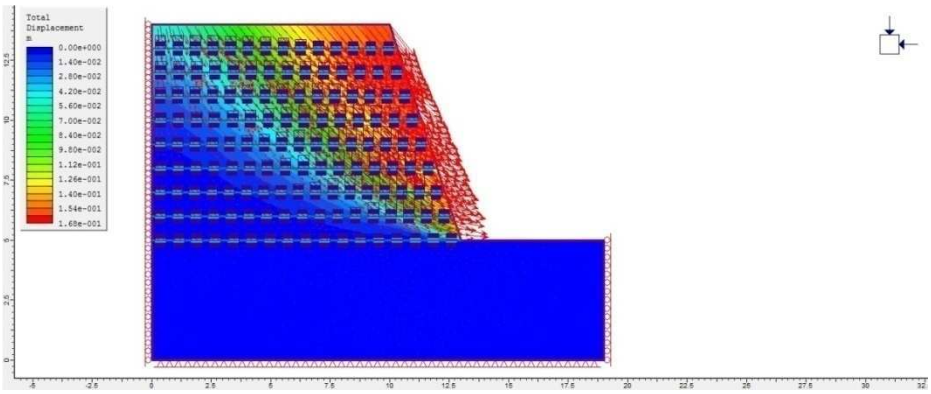

(a)

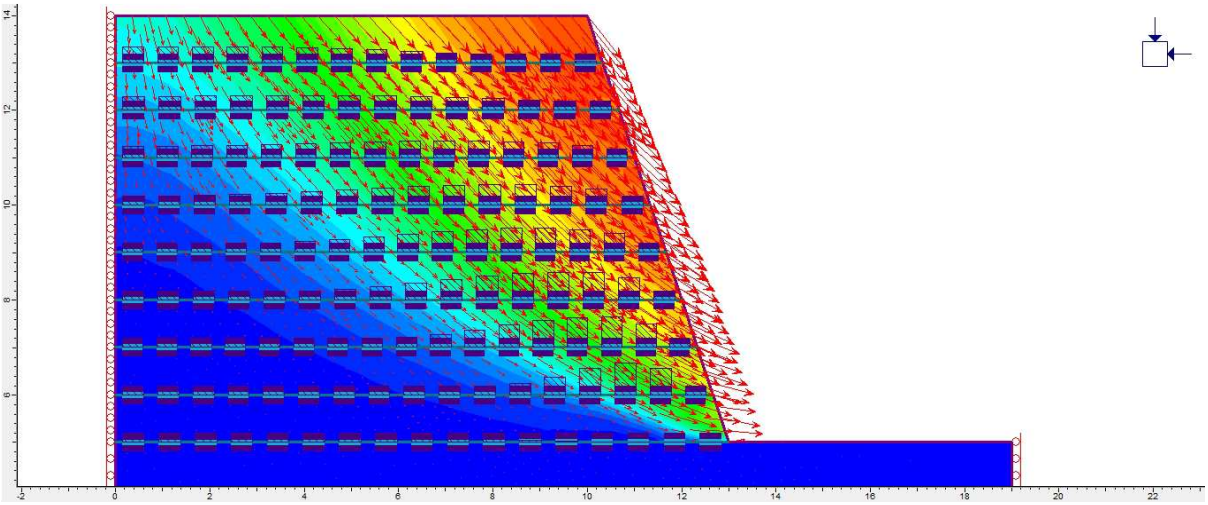

(b)

Fig. 7.1: Shape of Failure Surface and Location of Peak Tension (Slope Angle = 72^{o}, vertical spacing = 1 m. (a) Total Displacement Contours and (b) Total Displacement Contours (Zoom in)

This occurred due to the shear strains generation in the pond ash, present in embankment. The shear strains generated in the pond ash will attributed to the generation of tensile forces in the geogrid reinforcement layers as shown in Fig. 7.2 and 7.3 The tension in the geogrid reinforcement layers are negligible in the absence of shear strains in soils as can be seen from the graph in Fig.7.4 and 7.5

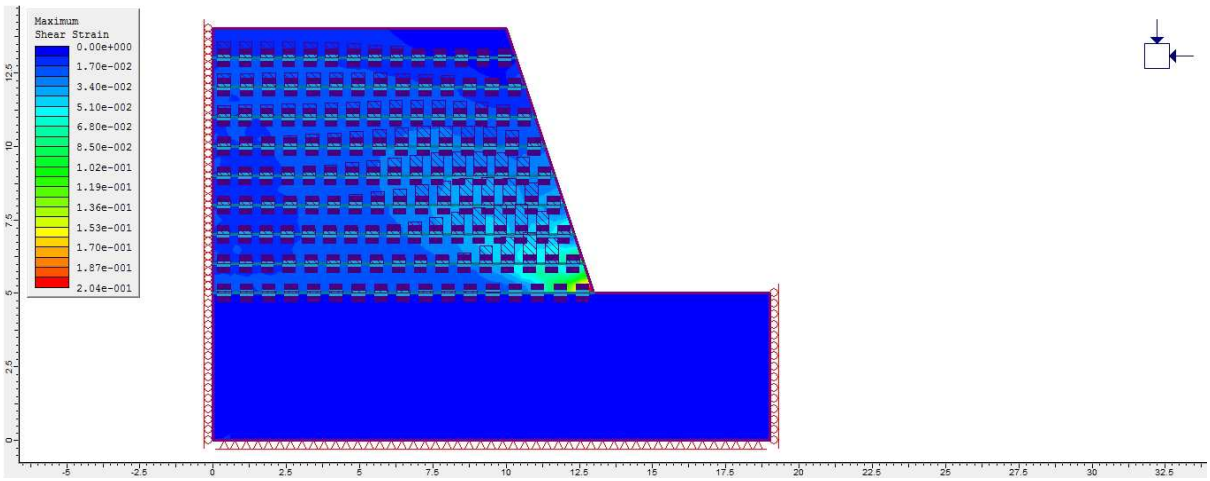

(a)

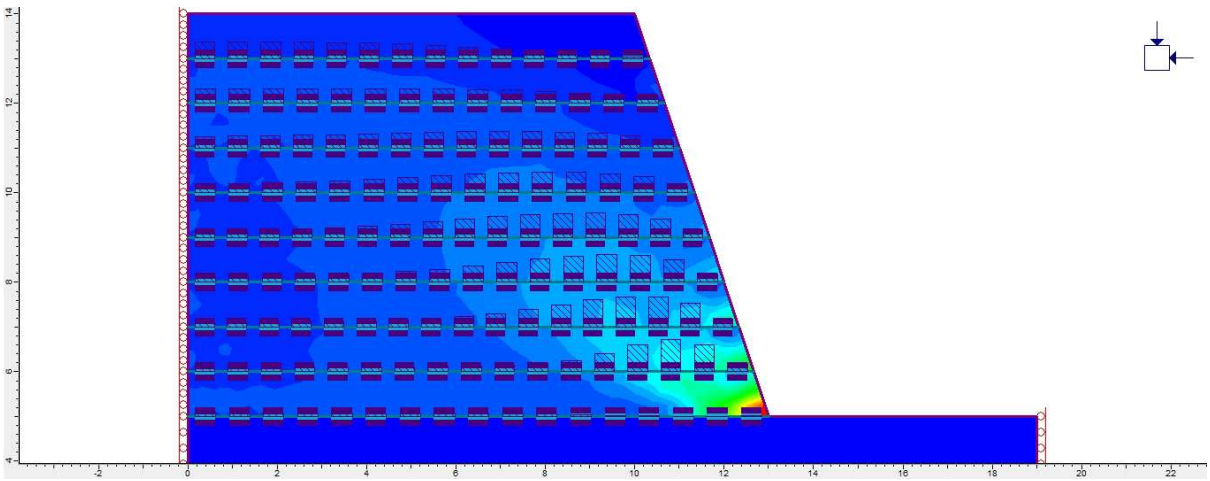

(b)

Fig. 7.2: Shape of Failure Surface and Location of Peak Tension (Slope Angle = 72^{o}, vertical spacing = 1 m. (a) Shear Strain Contours and (b) Shear Strain Contours (Zoom in)

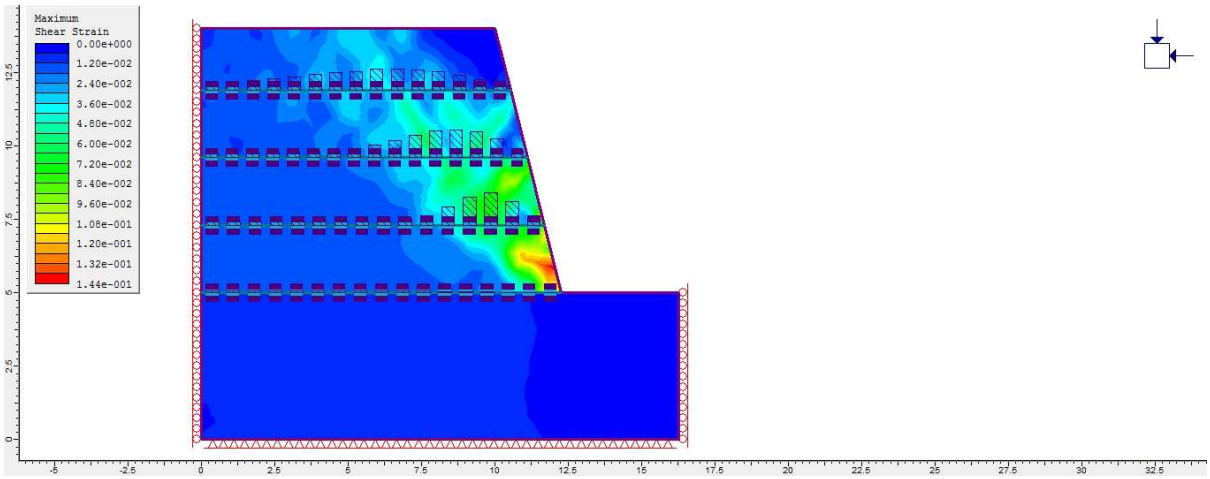

(a)

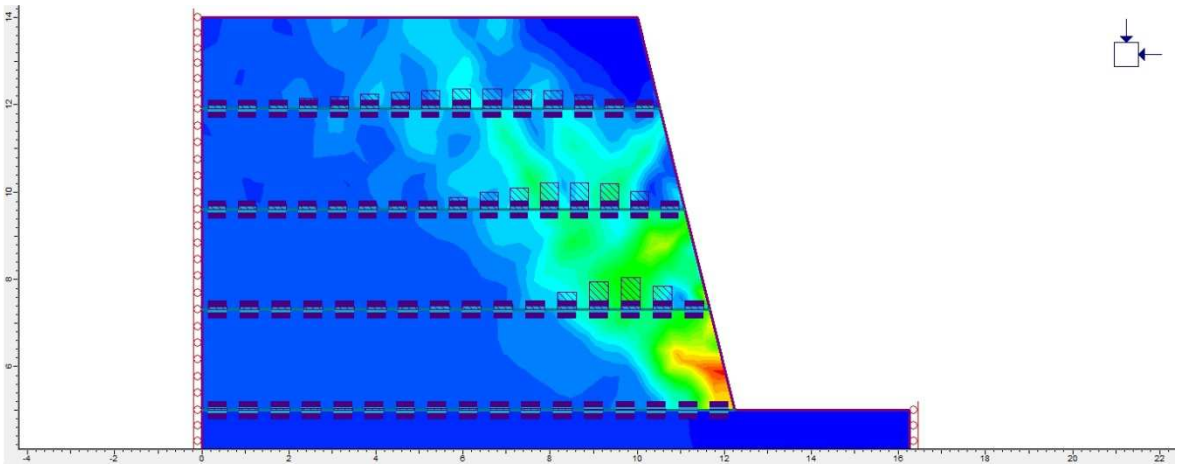

(b)

Fig. 7.3: Shape of Failure Surface and Location of Peak Tension (Slope Angle = 76^{o}, vertical spacing = 2.3 m) (a) Shear Strain Contours and (b) Shear Strain Contours (Zoom in)

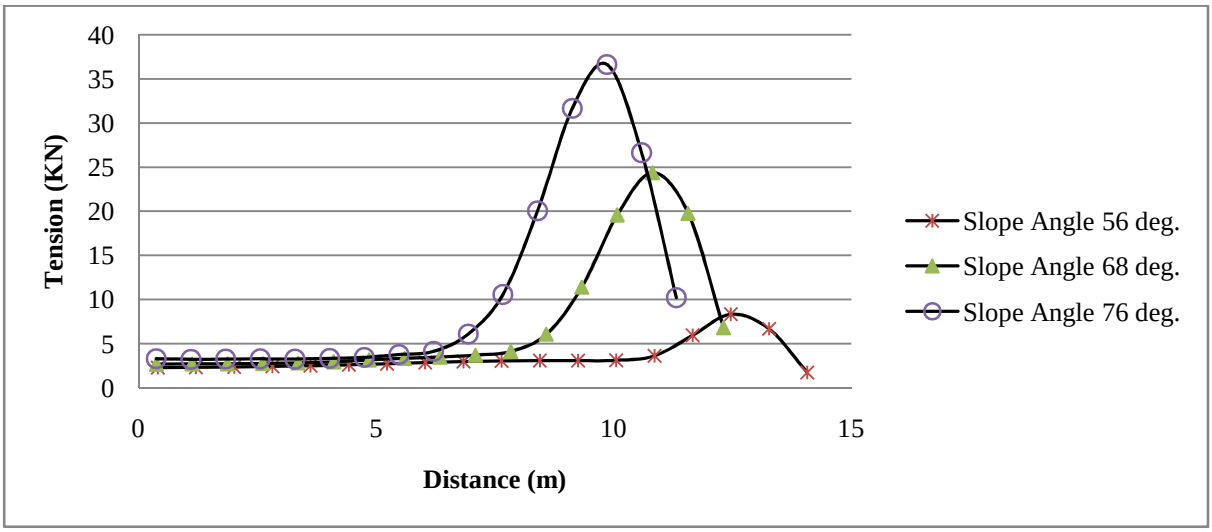

Fig. 7.4: Tension v/s Distance along Geogrid Layer 2 (Slope Angle = 76^{o}, vertical spacing = 2.3 m)

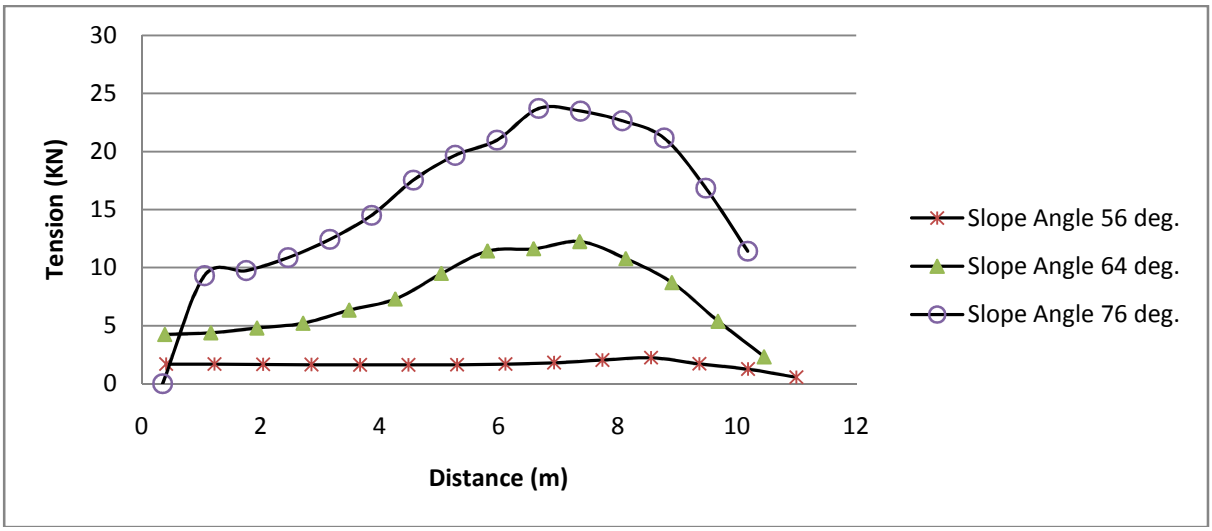

Fig. 7.5: Tension v/s Distance along Geogrid Layer 4 (Slope Angle = 76^{o}, vertical spacing = 2.3 m)

The results show a good agreement with the work done by Zornberg and Arriaga (2003), in which, it is concluded that the location of the reinforcement maximum peak strain does not occur near the toe of the structure as assumed by conventional design methods, but was located approximately at mid-height of the reinforced slopes.

7.2.5 Location of Maximum Peak Tension and Distribution Pattern of Tension along Slope Elevation

The Maximum peak tension in georid reinforcement refers to the maximum of peak tension among all the geogrid layers along the slope elevation as shown with the help of bar graphs in Fig. 7.6. The maximum peak tension in a reinforced slope is always assumed to be at the bottom of the slope in design practice and the distribution pattern of tension along the slope was assumed to be triangular with zero at the crest and maximum at the toe. In the present study this distribution pattern of tension along the slope elevation was found to be different The Distribution pattern of tension along the slope elevation with different slope inclination can be seen in Fig. 7.7 to 7.10.

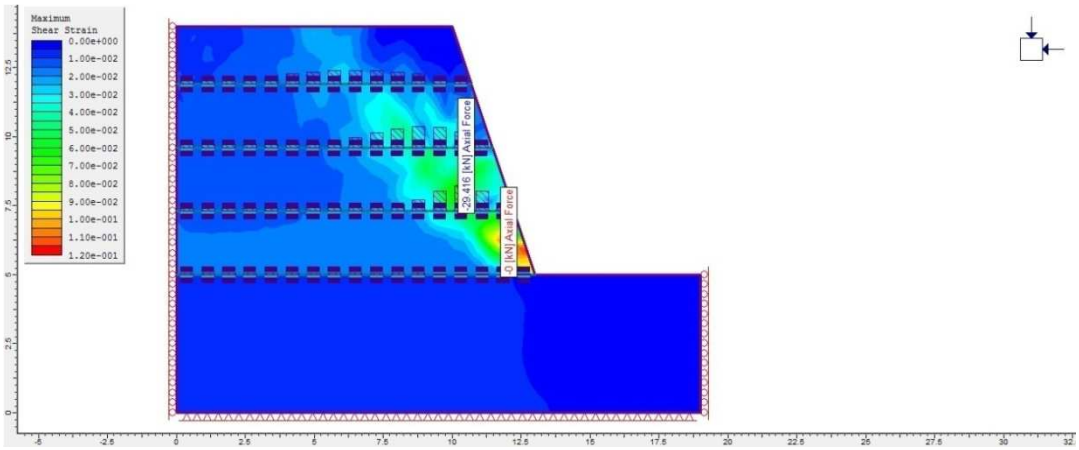

(a)

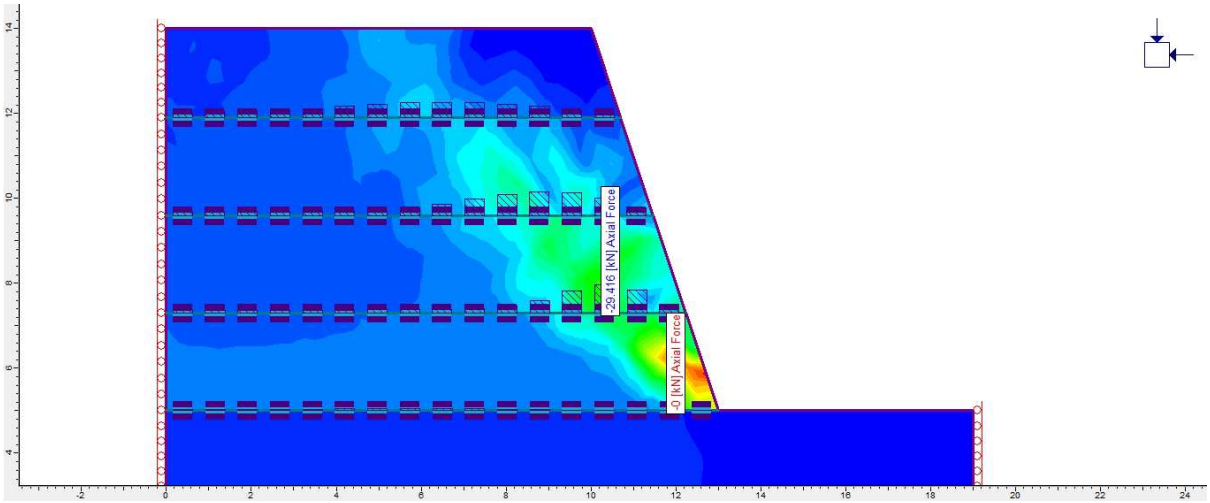

(b)

Fig. 7.6: Location of Maximum Peak Tension (Slope Angle = 72^{o}, vertical spacing = 2.3 m) (a) Shear Strain Contours and (b) Shear Strain Contours (Zoom in)

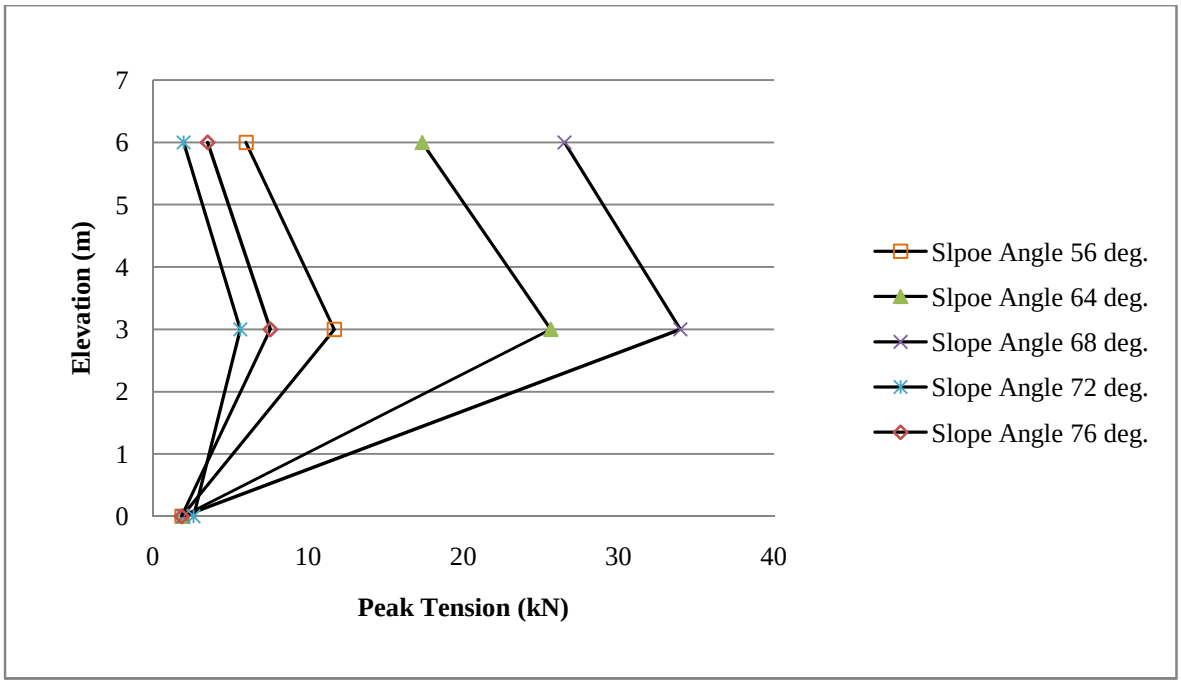

Fig. 7.7: Elevation v/s Peak Tension (vertical spacing = 3.0 m)

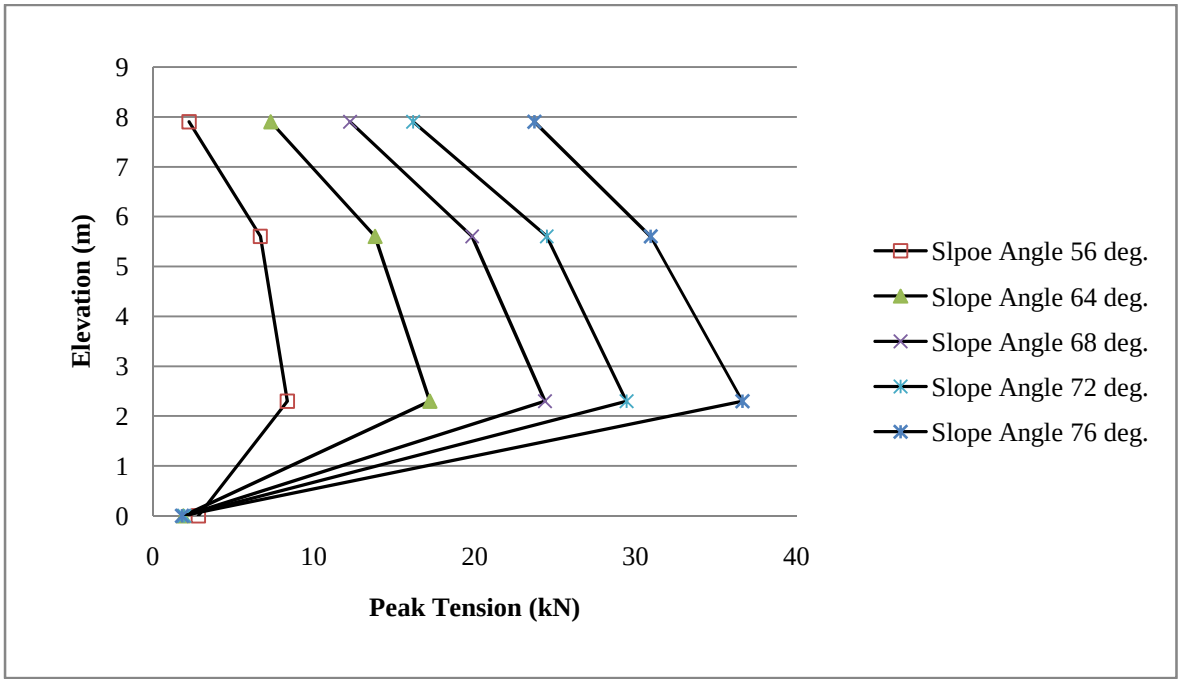

Fig. 7.8: Elevation v/s Peak Tension (vertical spacing = 2.3 m)

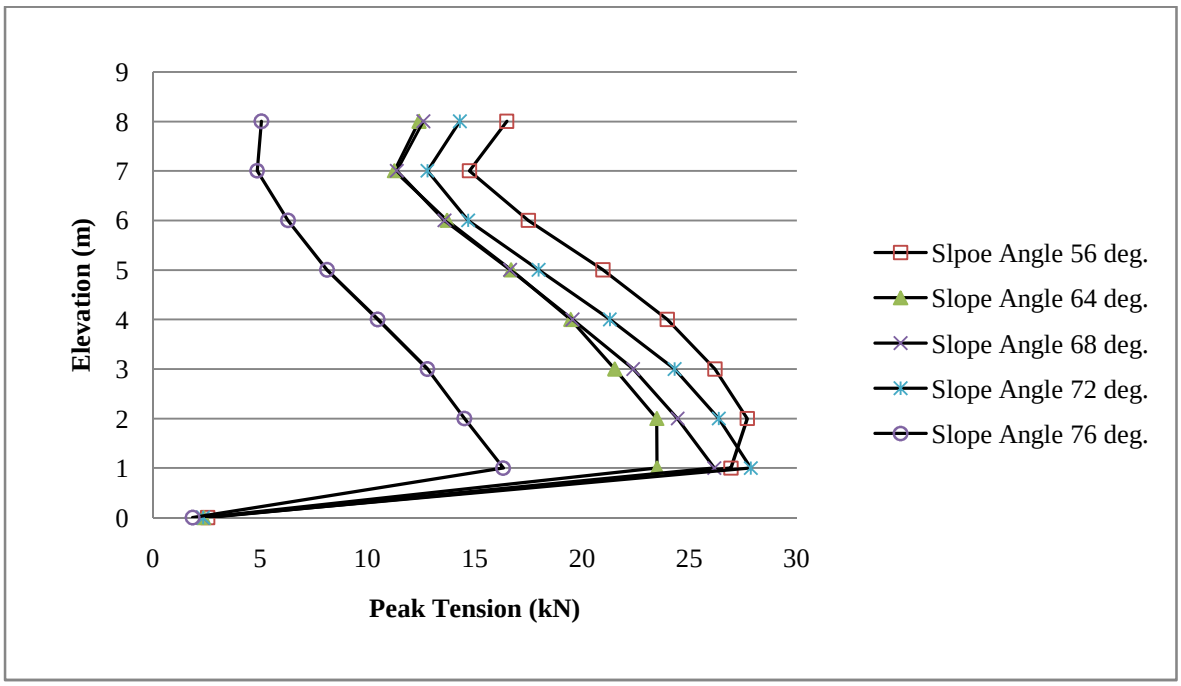

Fig. 7.9: Elevation v/s Peak Tension (vertical spacing = 1.0 m)

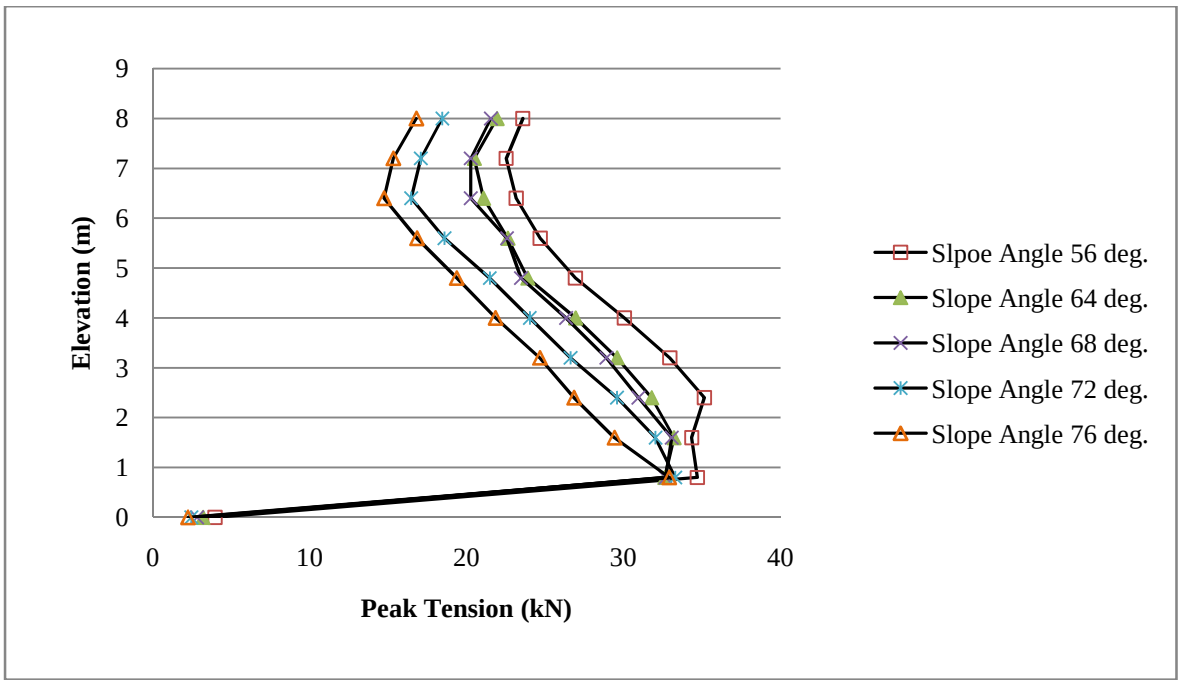

Fig. 7.10: Elevation v/s Peak Tension (vertical spacing = 0.8 m)

This Distribution pattern of tension along the slope may be occurred because tension in geogrid layers along a slope elevation was found to be maximum at that point along the potential failure surface of the slope where the overburden pressure is maximum. Since, at the mid- height along the potential surface of the slope, the overburden pressure is maximum, causing the maximum horizontal stresses at that particular point. The maximum tension will be mobilized at that point along the potential failure surface, to maintain local horizontal equilibrium.

The Distribution patterns as shown in Fig. 7.7 to 7.10 was found to be in good agreement with the distribution pattern obtained by Zornberg et al., 2003, in which the maximum peak tension was shown somewhere in the middle of the slope as explained in Fig. 7.11

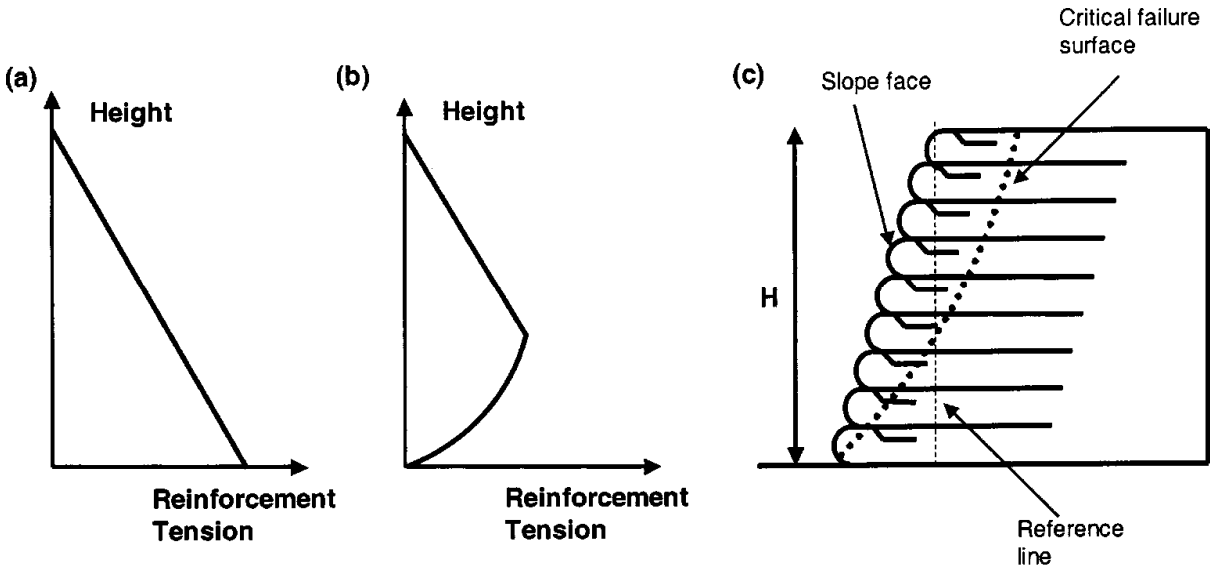

Fig.7.11: Distribution of reinforcement peak tension with height: a) for reinforced walls used in design; b) for reinforced slopes proposed; and c) schematic cross section. (Zornberg et al. 2003)

7.2.6 Parametric study

In the present work, a parametric study is carried out in which following was covered.

- Effect of geogrid reinforcement on shear strain within the soil
- Effect of vertical spacing of geogrid reinforcement
- Effect of providing pond ash + lime layer at the top and side slope of embankment
- Critical SRF values with different embankment slope inclination in normal and flood condition

7.2.6.1 Effect of Geogrid Reinforcement on Shear Strain within the Soil

In the present study it is found that the shear strains developed within the soil mass, get reduced by providing geogrid layers along the slope elevation, which results in the increase in strength of soil mass. Shear strain development within unreinforced and reinforced slope can be seen in Fig. 7.12

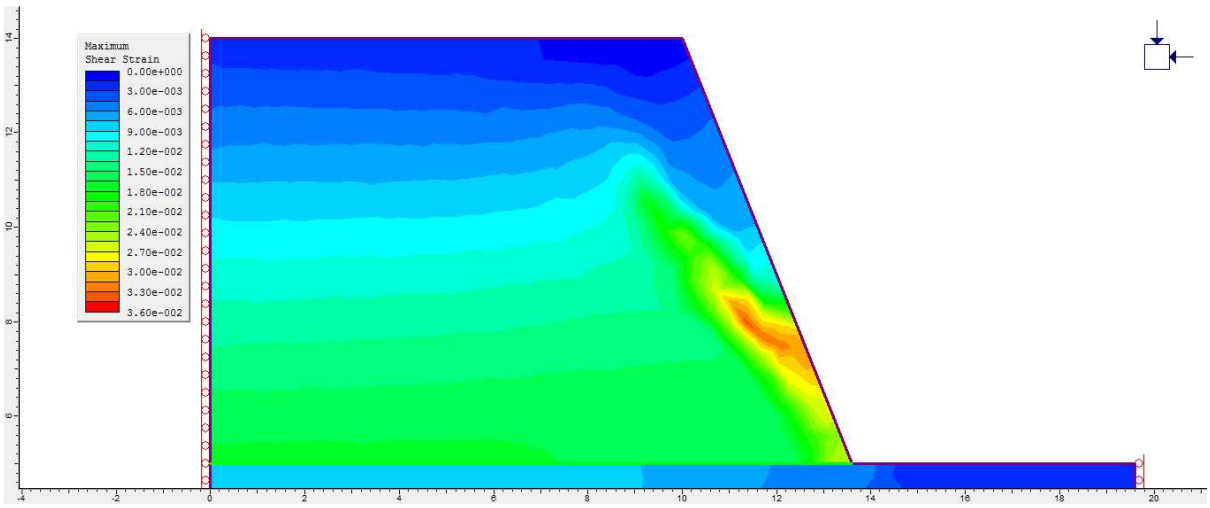

(a)

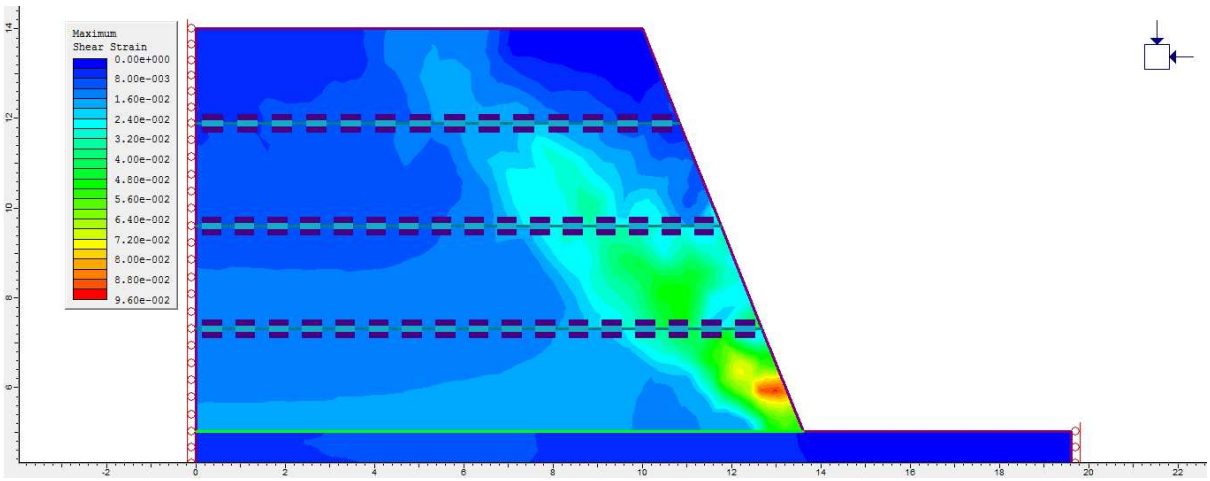

(b)

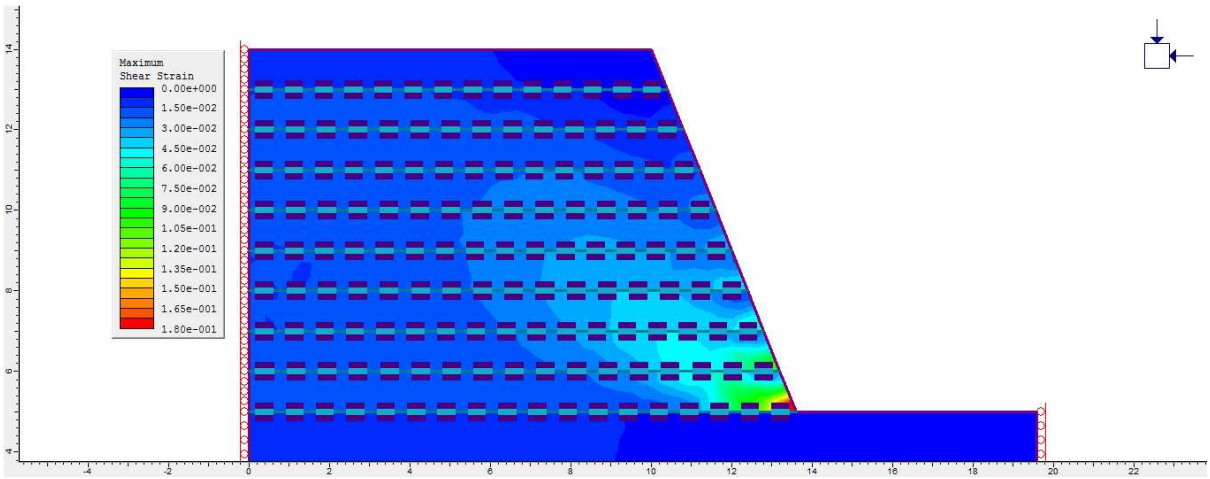

(c)

Fig. 7.12: Shear Strain Contours (Zoom in) with Slope Angle = 68^{o} (a) Unreinforced, (b) Vertical Spacing = 2.3 m and (c) Vertical Spacing = 1.0 m.

It can be seen that as the vertical spacing between geogrid was decreased, the shear strains were reducing rapidly and also shifting towards the toe of the slope as can be seen from Fig. 7.15. When no geogrid layer was installed in the slope, the shear strains were more concentrated in the middle portion of slope rather than the toe. As geogrid layers were installed in the slope, the shear strains get reduced and shifts towards toe of the slope due to increment in confinement in the middle of the slope. Also, due to the restraining effect of reinforcement, shear stress within the embankment slope gets reduced.

7.2.6.2 Effect of Vertical Spacing of Geogrid Reinforcement

The Effect of vertical spacing of geogrid reinforcement layers was studied in present work. The Effect of vertical spacing of geogrid reinforcement layers can be seen in Fig. 7.13 and 7.14.

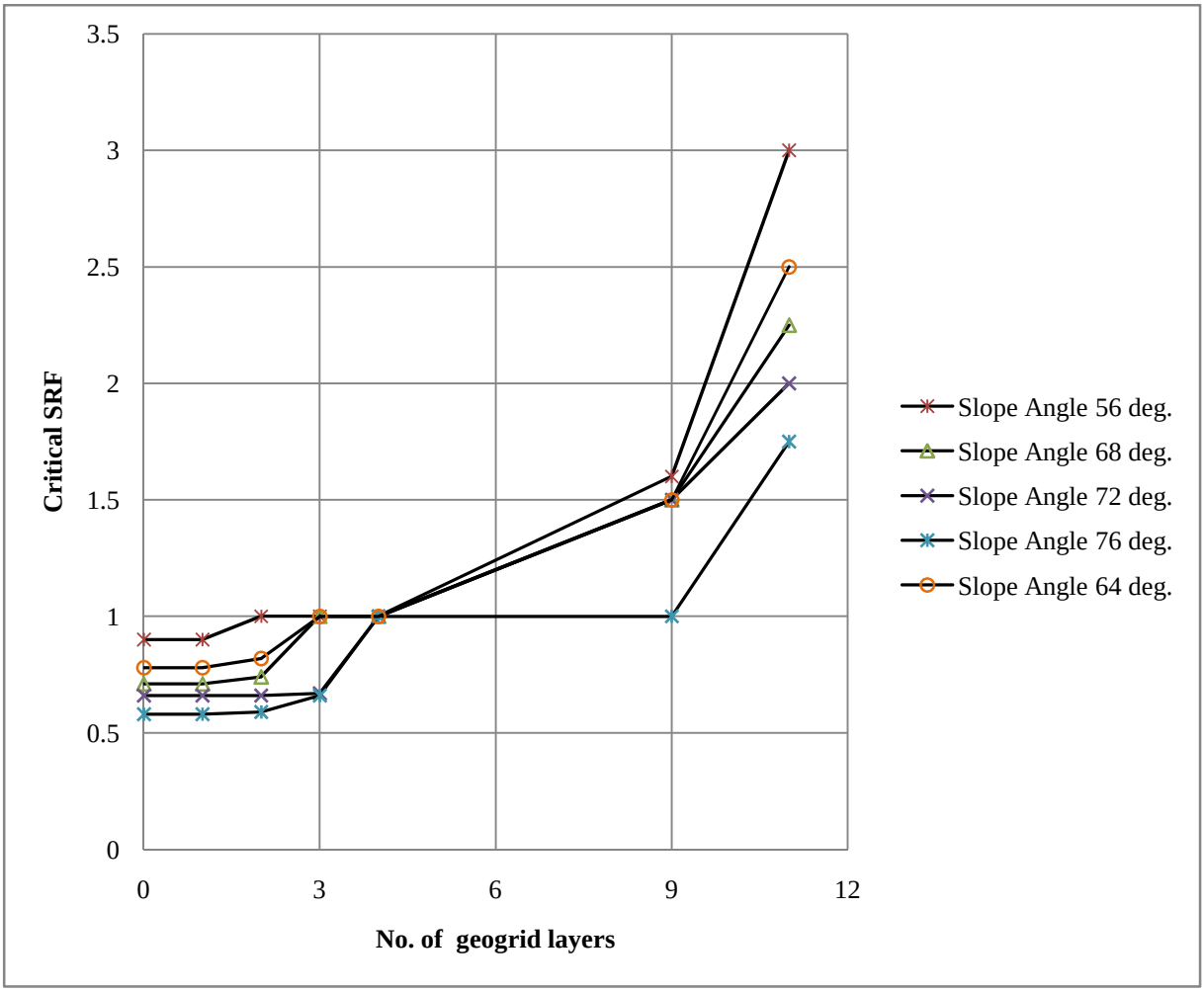

Fig. 7.13: Critical SRF v/s No. of Geogrid Layers (with different Slope Angles) in Normal Condition

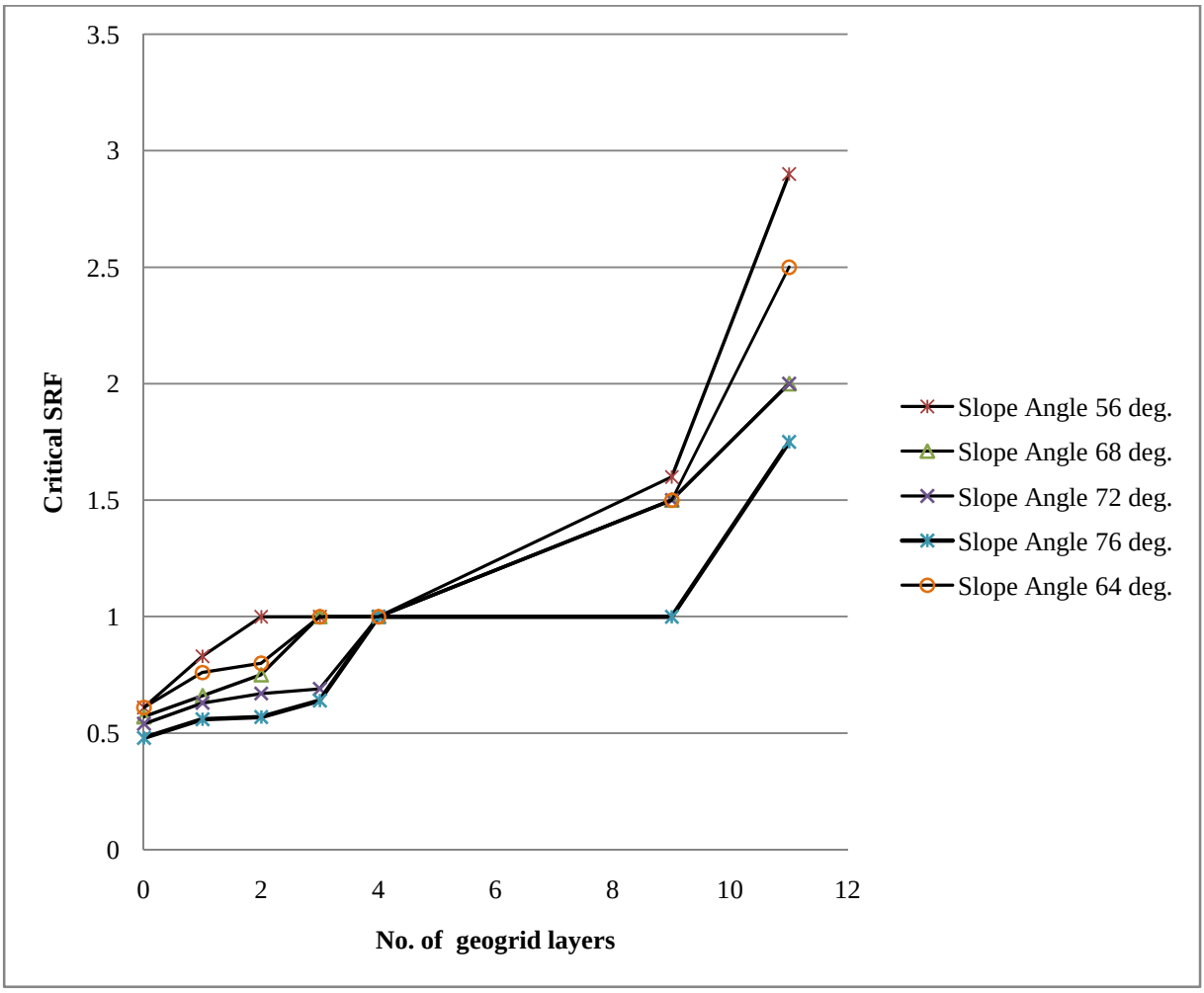

Fig. 7.14: Critical SRF v/s No. of Geogrid Layers (with different Slope Angles) in Flood Condition (F.L = 1m)

It can be seen that as the vertical spacing of geogrid layers get reduced, the critical SRF value increased. This can be due to generation of more tensile forces in geogrid layers which acts as a resisting force against the driving forces in slopes which is attributed to the increase in critical SRF.

7.2.6.3 Effect of providing Pond Ash + Lime layer at the Top and Side Slope of Embankment

In the present study, a pond ash mixed with lime layer is provided at the top and side slope of embankment. In this, a layer of thickness 0.5 m is provided at the top and a layer with varying thickness is provided at the side slope. The variation of thickness is kept as 1.0, 1.5 and 2.0 m. The influence of providing pond ash mixed with lime layer was studied as it is that seen shear strain get reduced within the soil as it can be seen in Fig. 7.15.

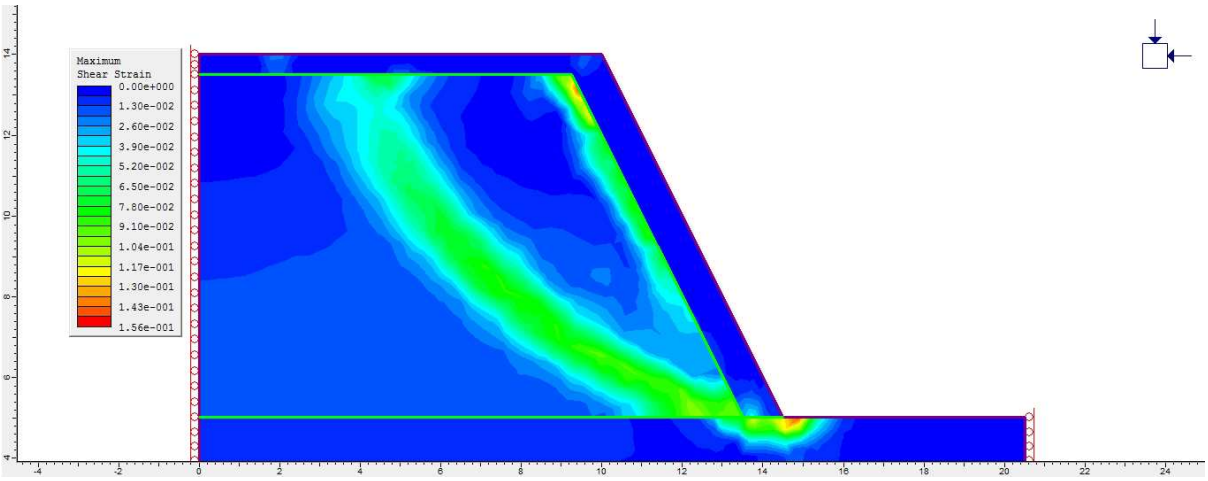

(a)

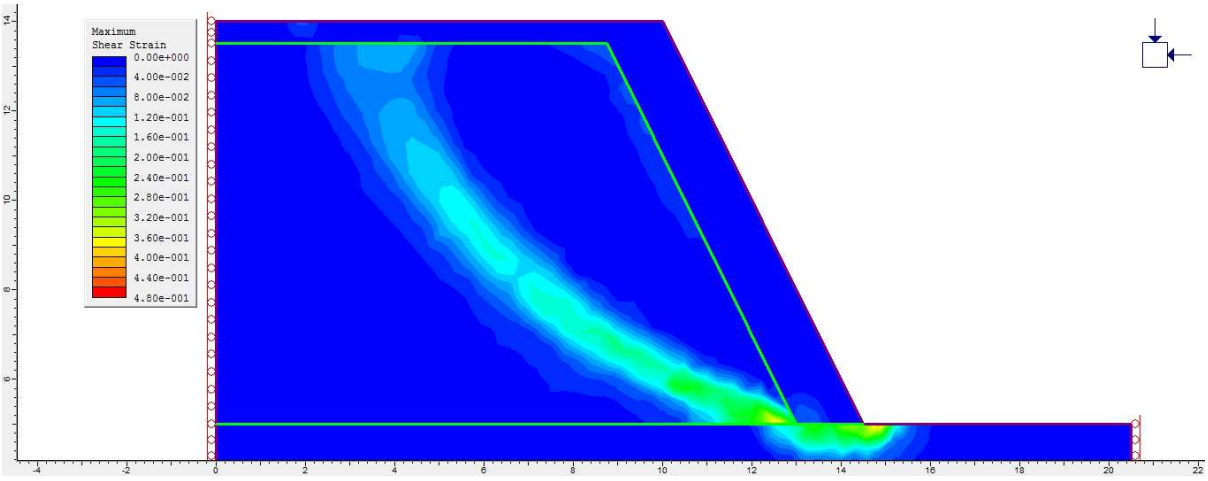

(b)

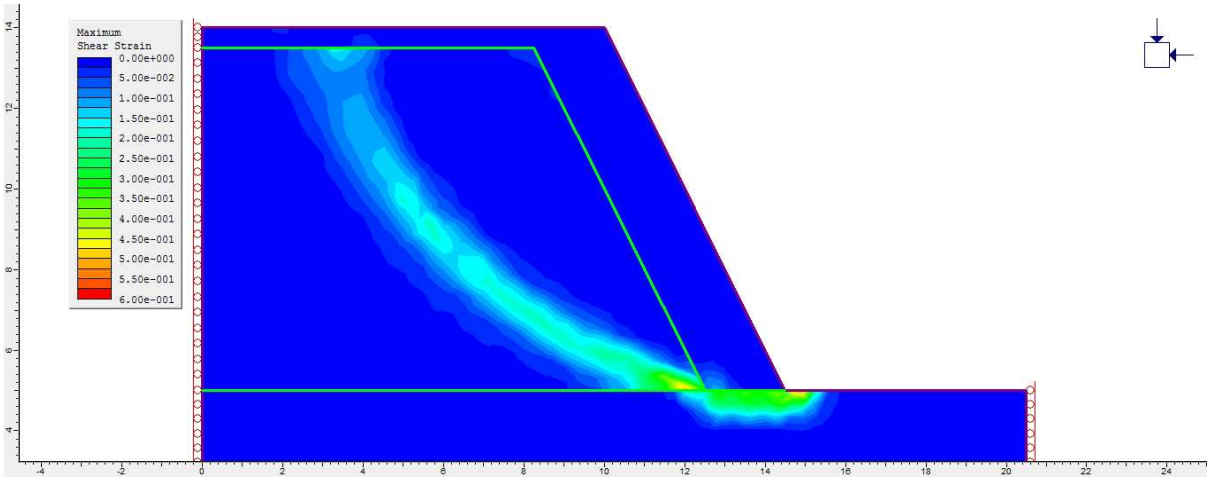

(c)

Fig. 7.15: Shear Strain Contours (Zoom in) with Slope Angle = 64^{o}, (a) With 1.0 m thick Layer at Side Slope and 0.5 m layer at Top, (b) With 1.5 m thick Layer at Side Slope and 0.5 m layer at Top and (c) With 2.0 m thick Layer at Side Slope and 0.5 m layer at Top.

It can be seen that the shear strains in the embankment slope is reducing with the increase in pond ash + lime layer thickness at the side slope. This can be occurred due to the reduction in shear stress developed within the pond ash, present in embankment structure, as this layer provides strength to the structure. The effect of providing these layers on Critical SRF values of slope can also be seen in Fig. 7.16 and 7.17

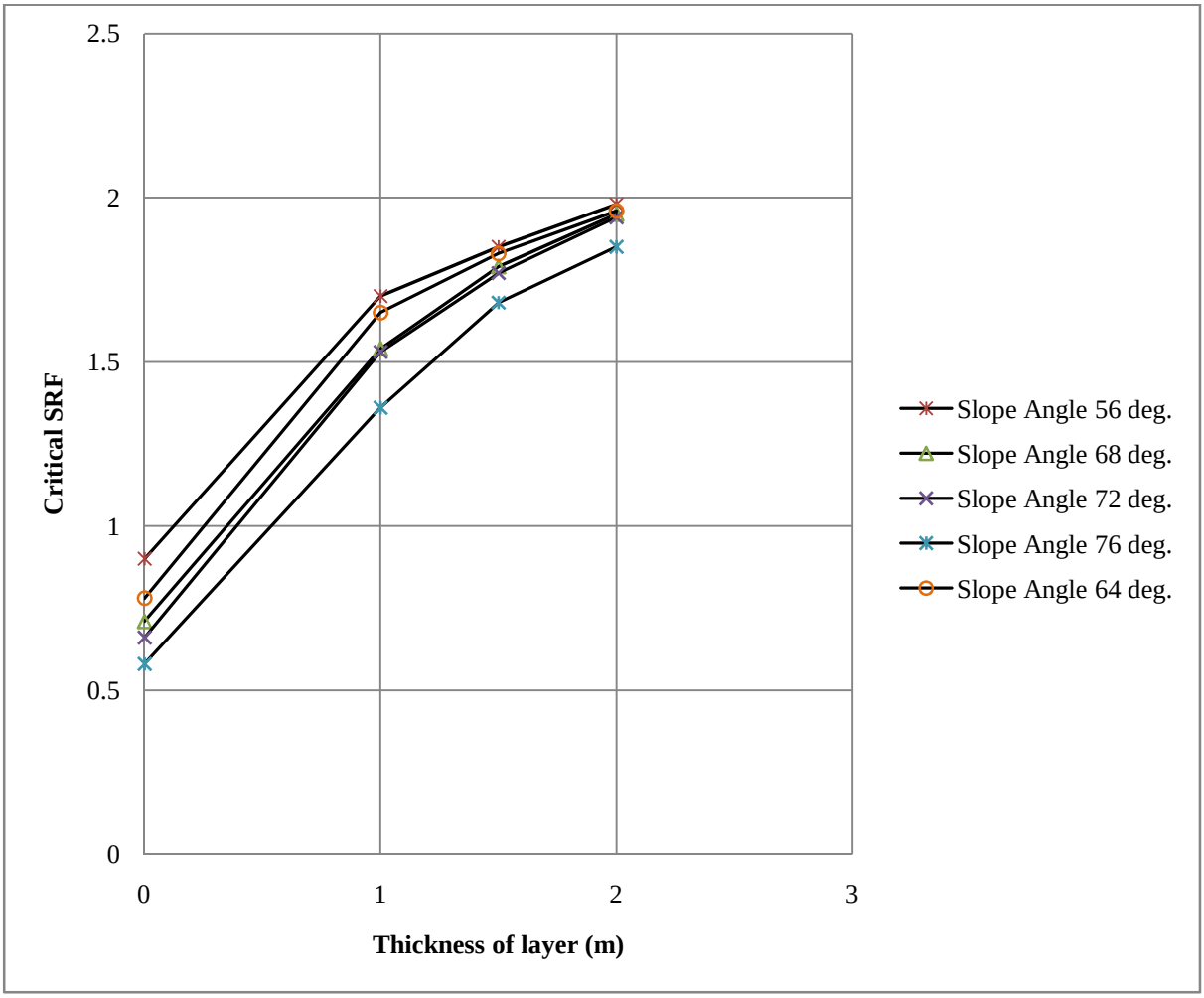

Fig. 7.16: Critical SRF v/s Thickness of Layers (with different Slope Angles) in Normal Condition

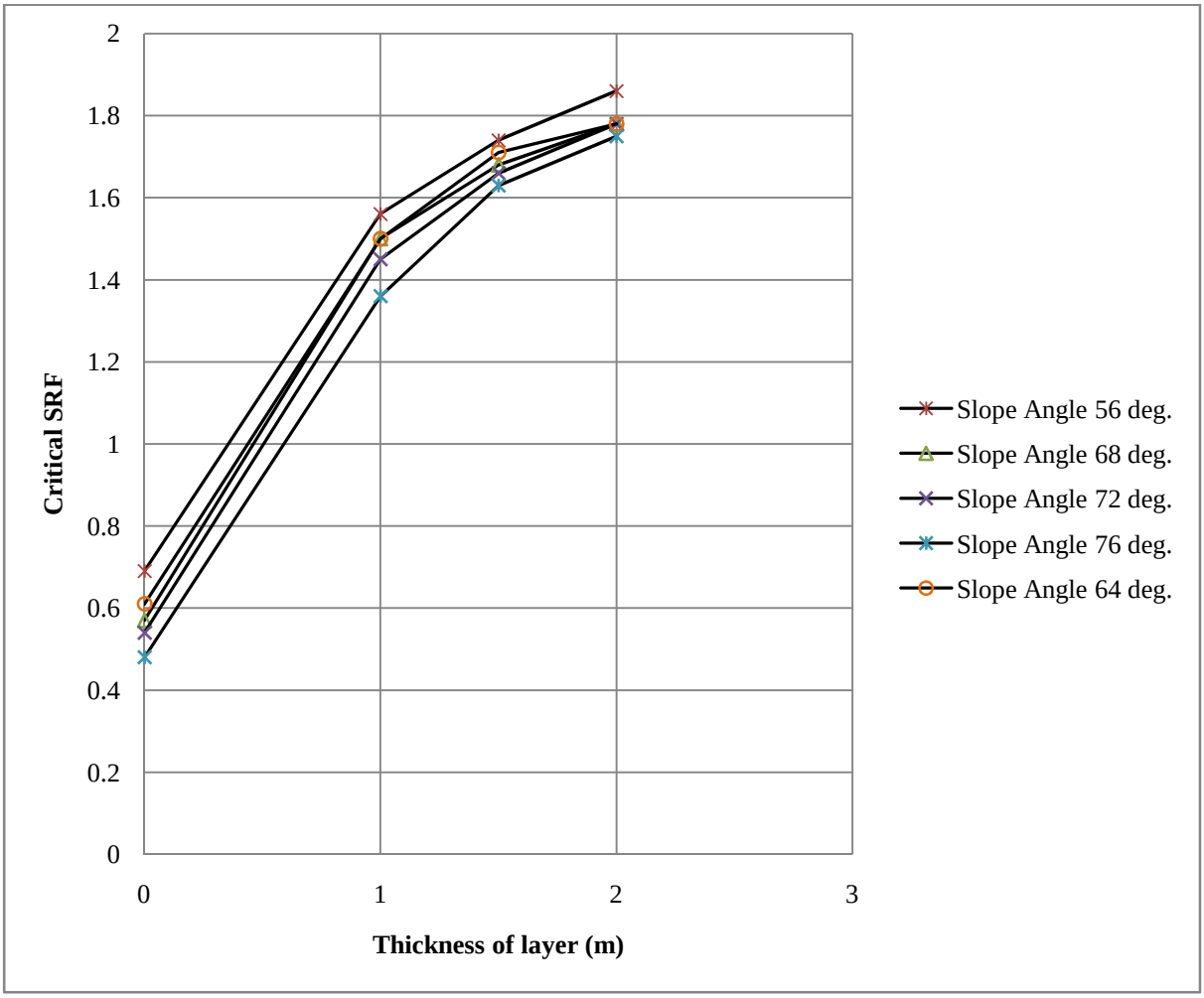

Fig. 7.17: Critical SRF v/s Thickness of Layers (with different Slope Angles) in Flood Condition (F.L = 1m)

It can be seen that the critical SRF values get increased with the increase in thickness of pond ash +lime layer. It may be occurred due to the additional shear strength provided by this layer. As discussed earlier in laboratory investigations that the shear strength of pond ash + lime is very high as compared to the pond ash alone due to the formation of cementitious material.

7.2.6.4 Critical SRF Values with different Embankment Slope inclination in Normal and Flood condition

The Critical SRF values of unreinforced slope, reinforced slope with different spacing, unreinforced slope provided with pond ash mixed with lime layer, and unreinforced embankment with pond ash + lime material, with various slope angles is studied and are shown in Fig. 7.18 to 7.22

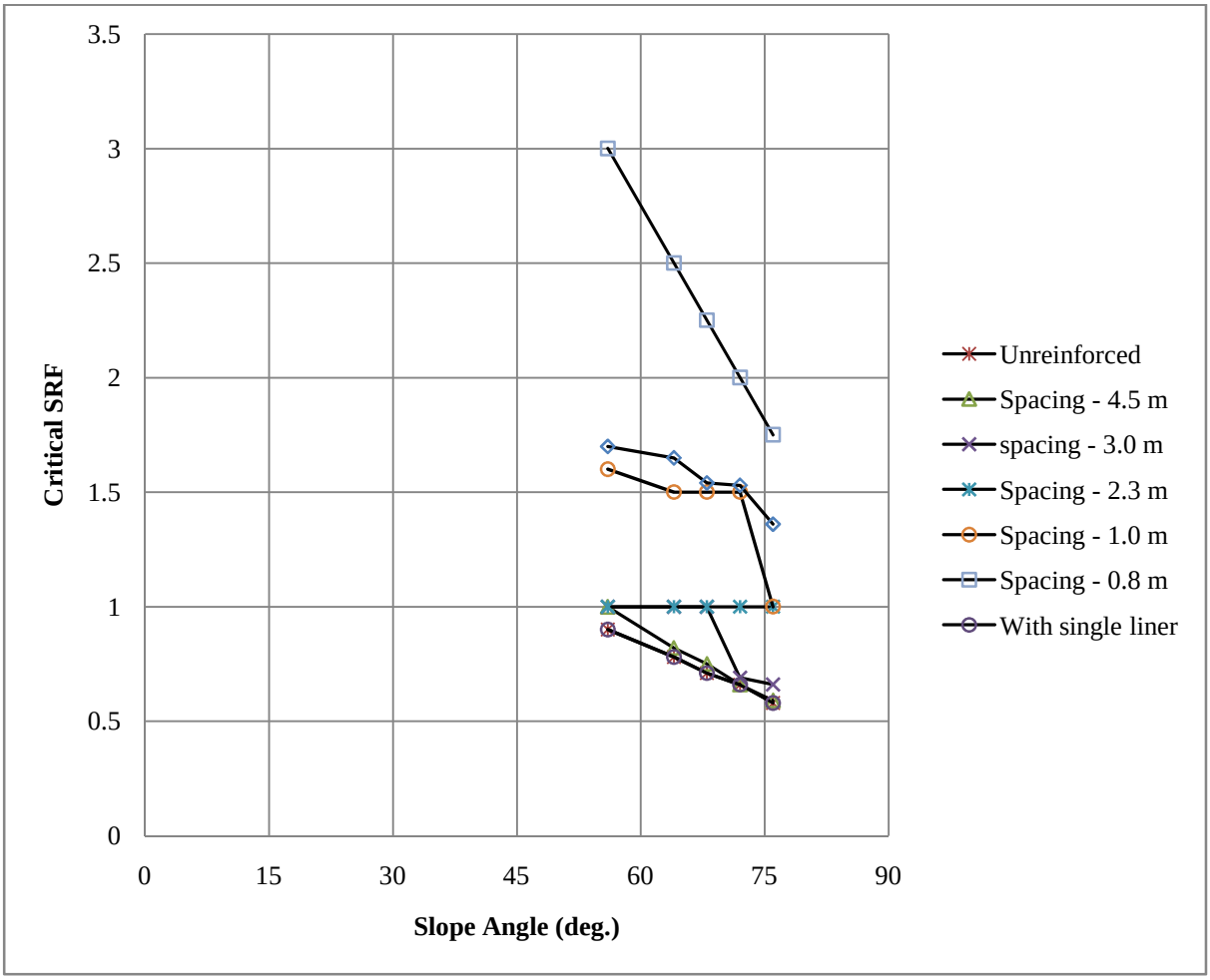

Fig. 7.18: Critical SRF v/s Slope Angle (with different reinforcement condition) in Normal Condition

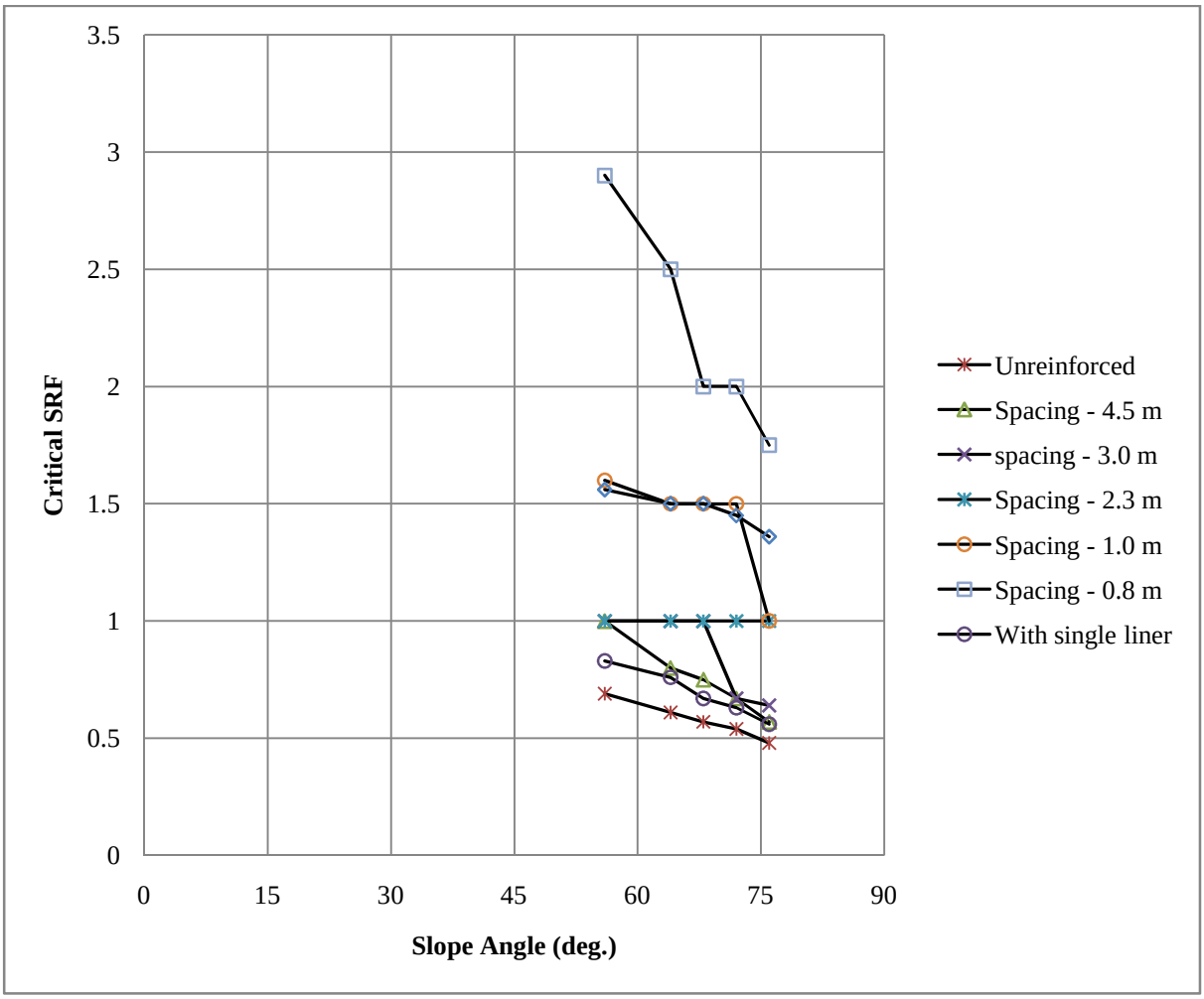

Fig. 7.19: Critical SRF v/s Slope Angle (with different reinforcement condition) in Flood Condition (F.L = 1m)

It can be seen that the Critical SRF values increased with the increase in geogrid reinforced layers or as vertical spacing of georid layers get reduced in normal condition as well as in flood condition. Critical SRF values are maximum with 0.8m spacing of geogrid liner for different slope angles.

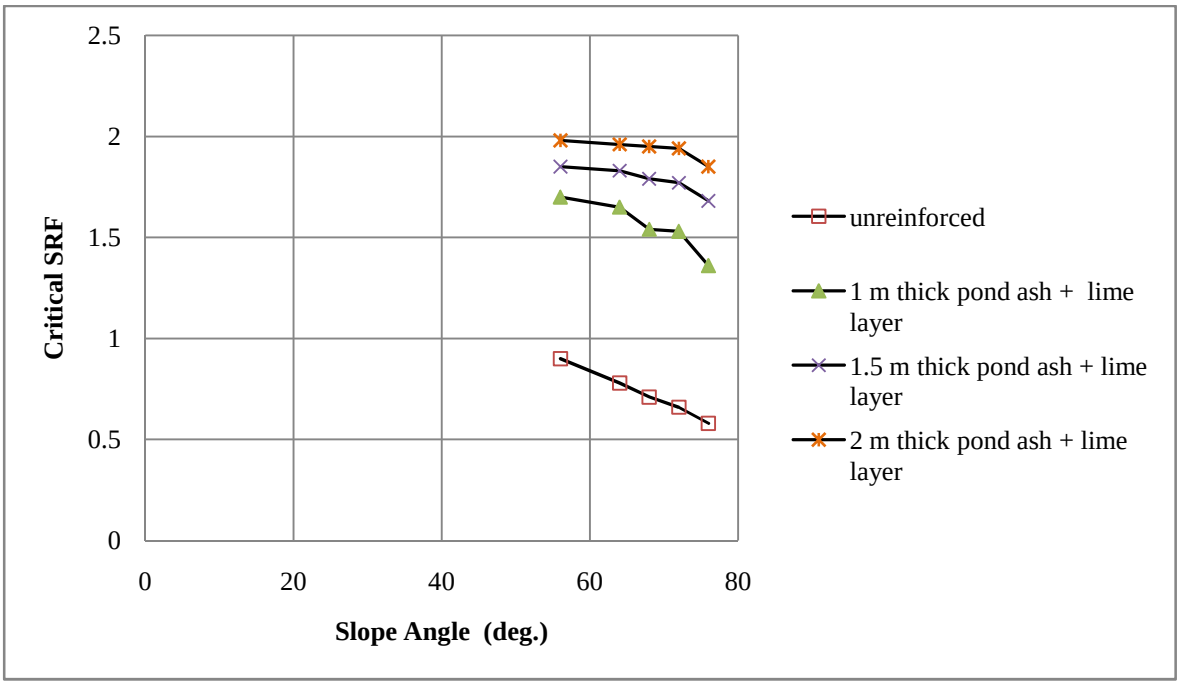

Fig. 7.20: Critical SRF v/s Slope Angle (with various thickness of Pond ash-lime mix layer) in Normal Condition

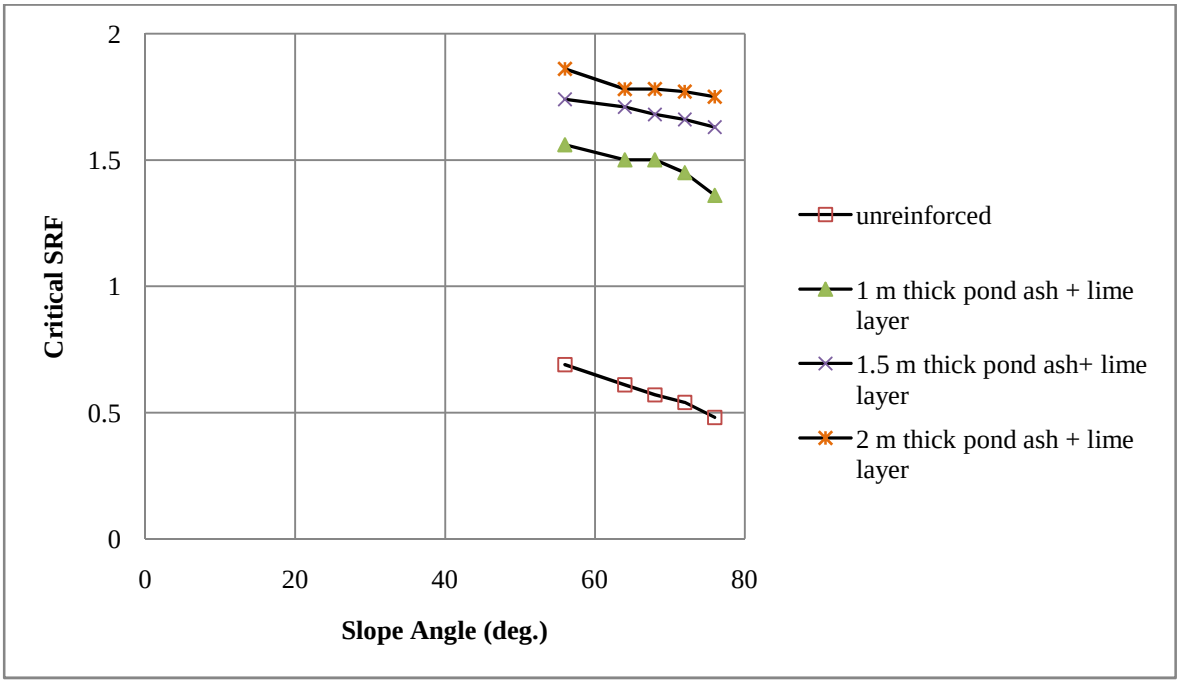

Fig. 7.21: Critical SRF v/s Slope Angle (with various thickness of Pond ash-lime mix layer) in Flood Condition (F.L = 1 m)

It can be seen that the Critical SRF values increased with the increase in thickness of pond ash-lime mix layer at the side slope of embankment, in normal condition as well as in flood condition. Critical SRF values are maximum with thickness of pond ash- lime mix layer is 0.5 m at the top of embankment and 2.0 m thickness at side slope of embankment.

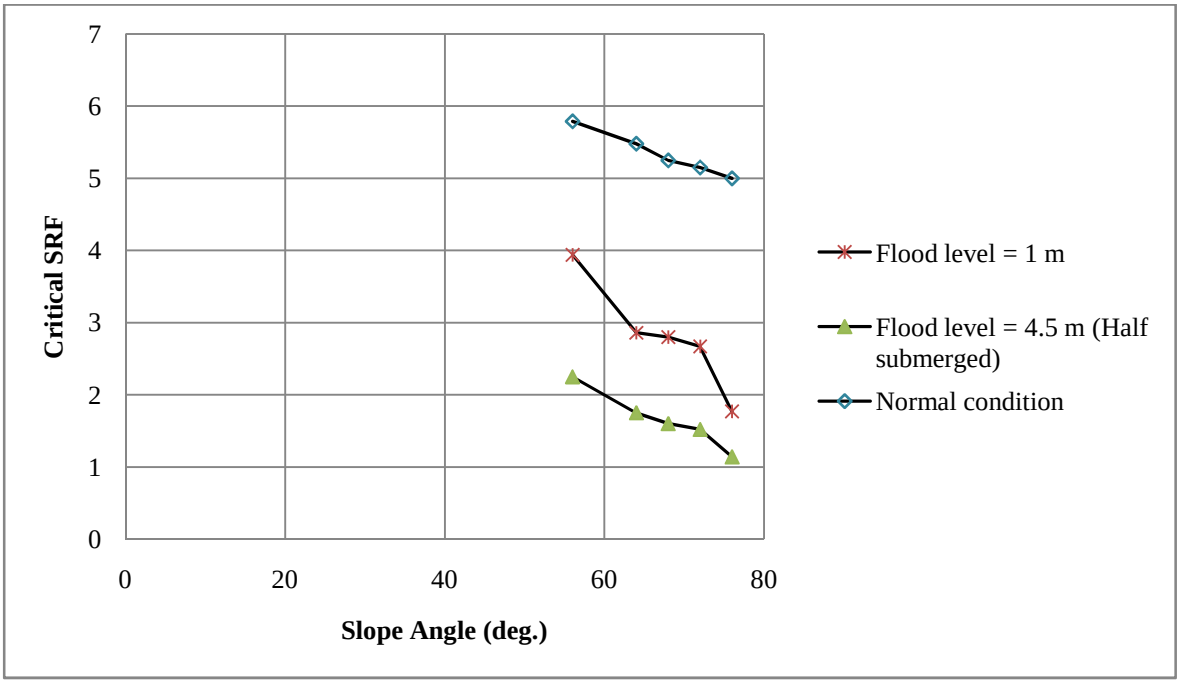

Fig. 7.22: Critical SRF v/s Slope Angle, when Pond-Lime mix material used in Embankment Structure

In the present study it is observed that the Critical SRF values are maximum when pond ash-lime mix material is used for embankment construction. Also, it can be seen that this embankment will also be safe in half submerged case.

CHAPTER – 8

CONCLUSIONS AND FUTURE SCOPE

8.1 Conclusions

1. SEM results of pond ash shows that the pond ash particles are rounded in shape. This shows the spherules of alumina silicates in pond ash. Dark matter presence shows magnetite. SEM results of soil indicates that the soil particles are sub angular particles. SEM results of pond ash and lime, cured sample shows the bonded particles of pond ash and lime.

2. The EDS results evidenced the presence of the following components: silica (SiO_2), alumina ($A1_20_3$) and hematite (Fe_2O_3) in pond ash.

3. The Compaction curve of pond ash shows that there is a less change in density with variation in water content. Pond ash is also easy to compact as compared to natural soil, as there are no heavy lumps to break down. This property of pond ash is useful for embankment construction.

4. The Hydraulic conductivity of pond ash was found to be high which ensures the effective drainage for better workability.
.
5. The Unconfined compressive strength at MDD and OMC, for pond ash + lime with 28 days curing, was found to be 826.33 kPa which very higher than for pond ash.

6. Tensile strength at MDD and OMC, of pond ash + lime with 28 days curing, was found to be 137.93 kPa, which very higher than of pond ash.

7. Cohesion and angle of internal friction for pond ash + lime with 28 days curing it is found to be 300.35 kPa and 46.4^o respectively, which very higher than of pond ash.

8. The Strength tests of pond ash and lime mixture evidenced that the unconfined compressive strength, tensile strength as well as shear strength are very high. This is due to the formation of cementitious material. The silica (SiO_2), alumina ($A1_20_3$) and ferrous oxide (Fe_2O_3) present in pond ash and calcium oxide (CaO) present in lime, chemically reacted with each other in presence of water and has been formed cementitious material such as (calcium silicate hydrate ($CaO\text{-}SiO_2\text{-}H_2O$), calcium aluminate hydrate ($CaO\text{-}Al_2O_3\text{-}H_2O$) and calcium ferroaluminate hydrate ($CaO\text{-}Al_2O_3\text{-}Fe_2O_3\text{-}H_2O$), which attributed to increase in strength of pond ash and lime mixture. The formation of cementitious material was also evidenced by SEM test, which shows a bonded particle of pond ash and lime.

9. The Potential failure surface of embankment slope was found to be circular in shape.

10. The peak tension in georid reinforcement was found to be within the potential failure surface, due to the generation of tensile forces in the geogrid reinforcement layers as a result of shear strains generated in the pond ash.

11. The distribution pattern of tension along the slope was assumed to be triangular with zero at the crest and maximum at the toe. In the present study, the distribution pattern of tension along the slope elevation was found to be different for reinforced embankment. The maximum peak tension in a reinforced slope is always assumed to be at the bottom of the slope in design practice. In present study, it is found somewhere at the mid- height along the potential surface of the slope due to the presence of maximum overburden pressure at that point, which is in good agreement with the results obtained by Zornberg and Arriaga (2003).

12. Shear strains within the embankment get reduced by providing geogrid reinforcement along the embankment slope. Shear strains within the embankment get rapidly reduced as the vertical spacing between geogrid layers was decreased, due to the restraining effect of reinforcement which attributed to the reduction in shear stress within the embankment.

13. When no geogrid layer was installed in the slope, the shear strains were more concentrated in the middle portion of slope rather than the toe. As geogrid layers were installed in the slope, the shear strains get reduced and shifts towards toe of the slope, due to increment in confinement in the middle of the slope.

14. Critical SRF values were increased with the decrease in vertical spacing of geogrid layers. This can be due to generation of more tensile forces in geogrid layers which acts as a resisting force against the driving forces in slopes which is attributed to the increase in critical SRF.

15. Shear strains within the embankment slope were reduced with the increase in pond ash + lime layer thickness at the side slope.

16. Critical SRF values were increased with the increase in thickness of pond ash +lime layer. It may be occurred due to the additional shear strength provided by this layer, as the shear strength of pond ash + lime is very high as compared to the pond ash alone due to the formation of cementitious material.

17. Critical SRF values increased with the increase in thickness of pond ash-lime mix layer at the side slope of embankment, in normal condition as well as in flood condition. Critical SRF values are maximum with thickness of pond ash- lime mix layer is 0.5 m at the top of embankment and 2.0 m thickness at side slope of embankment.

18. Critical SRF values are maximum when pond ash + lime (91:09, by weight), is used for embankment construction. And this embankment will also safe in half submerged case.

19. Settlement in pond + lime (91:09, by weight), is also very less.

20. With the help of geogrid reinforcement, an embankment can be provided a slope inclination of 1H: 4V, which is very steeper than 1H:1V as used in common practice. Therefore, considering the length and height of the embankment 2000 m and 9m respectively, 13500 m^2 land can be saved, by using 1H: 4V slope inclination.

21. The utilization of pond ash for embankment construction with the crest width 20 m and height 9m, approx. 2.88×10^3 to 2.21×10^3 m^3 to pond ash can be utilized which will attributed to reduction in land, which is wasted due to the disposal of pond ash which will also attributed to the reduction in environment pollution.

22. By providing pond ash- lime mix layer at the top and side slope of embankment, cost of geogrid reinforcement can be reduced.

8.2 Future Scope

.

- In SEM samples can be first separated by gravity metric method and then analyzed so as to study the morphology more clearly.
- Strength of pond ash mixed with lime can be calculated with more curing time.
- Another geosynthetic material can be used. Stiffness of reinforcement can be varied and its effect on critical SRF value, tension in reinforcement and shear strains can be analyzed.
- Displacement of slopes under various conditions can be analyzed.
- Strains in the geogrid layers along slope elevation can be calculated using FEM based software PLAXIS 2D.
- Various water tables can be considered in the analysis and its effect on critical SRF value, shear strains and displacement in slope can be analyzed.
- Effect of dynamic forces on all the parameters can be analyzed.

REFERENCES:

1. Beeghly, J. H. and Schrock, M. (2009): "Dredge Material Stabilization using the Pozzolanic or Sulfo-Pozzolanic Reaction of Lime by-Products to make an Engineering Structure Fill", Proceedings of the World of Coal Ash (WOCA) Conference, Lexington, USA, May 4-7.
2. Bhardwaj, D.K. and .Mandal, J.N. (2008): "Study on Polypropylene Fiber Reinforced Fly Ash Slopes", Proceeding of the 12th International Conference of International Association for Computer Methods and Advances in Geomechanics (IACMAG), Goa, India, October 1-6.
3. Chai, J.C., Miura, N. and Shen, S.L (2002): "Performance of embankments with and without reinforcement on soft subsoil", Can. Geotech. J., Vol. 39, No. 7, pp. 838–848.
4. Griffiths, D. V. and Lane, P. A. (1997): "Finite element slope stability analysis - Why are engineers still drawing circles?", Proceedings of the 6th International Symposium Numerical Models in Geomechanics**,** Balkem, Rotterdam, pp. 589-593.
5. Griffiths, D. V. and Lane, P. A. (1999): "Slope stability analysis by finite elements", Geotechnique, Vol. 49, No. 3, pp. 387-403.
6. Gupta, S., Negi, P., and Gupta, A. (2013): "Geotechnical Behaviour of Fine Sand Mixed with Pond Ash and Lime", International Journal of Scientific & Engineering Research, Volume 4, no. 4, ISSN 2229‐5518.
7. Hammah, R.E., Curran, J.H., Yacoub, T.E. and Corkum, B. (2004): "Stability analysis of rock slopes using the finite element method", Proceedings of the ISRM Regional Symposium EUROCK and the 53rd Geomechanics Colloquy, Salzburg, Austria, pp. 783-788.
8. IRC: 6-2000, "Standard Specification and Code of Practice for Road Bridges." Section –II (Load & Stresses), Fourth Revision
9. IRC: 36-1970, "Recommended Practice for the Construction of Earth Embankments for Road Works.
10. IRC-SP: 58-2001, Guidelines for use of Fly Ash in Road Embankments.
11. IS: 2720, Part 3 (1973), "Methods of test for soils- Determination of Specific Gravity".
12. IS: 2720, Part 4 (1985), "Methods of test for soils- Grain size analysis''.
13. IS: 2720, Part 5 (1985), "Methods of test for soils- Determination of Liquid and Plastic Limit".
14. IS: 2720, Part 7 (1980), "Methods of test for soils- Determination of Water Content-Dry Density relation using Light Compaction".
15. IS: 2720, Part 8(1980), "Methods of test for soils- Determination of water content-dry density relation using heavy compaction".
16. IS: 2720, Part 10 (1973), "Methods of test for soils- Determination of Unconfined Compressive Strength''.

17. IS: 2720, Part 11 (1993), “Methods of test for soils- Determination of the Shear Strength Parameters of a specimen tested in Unconsolidated Undrained Triaxial Compression without the measurement of Pore Water Pressure
18. IS: 2720, Part 17 (1986), “Methods of test for soils- Laboratory Determination of Permeability’’.
19. IS: 10082 (1981), “Methods of test for soils- Determination of Tensile Strength by Indirect tests on Rock Specimen".
20. Kamal, A. A., Pauleen, A. L., and Heshmati , A. R. (2005): “Parametric Study of Reinforced and Unreinforced Embankment on Soft Soil”, Proceedings of the 13th ACME Conference, University of Sheffield, March 21-22.
21. Liu, F., Wu, J., Chen, K. and Xue, D. (2010): “Morphology Study by Using Scanning Electron Microscopy”, Microscopy: Science, Technology, Applications and Education, pp. 1781-1792.
22. Mishraa, D.P., Das, S.K, (2010): “A Study of Physico-Chemical and Mineralogical Properties of Talcher Coal Fly Ash for Stowing in Underground Coal Mines”, Materials Characterization, Vol. 61, No. 8, pp. 1252 – 1259.
23. Mohanty, M. (2012): “Geotechnical Properties of Lightly Cemented Fly Ash” M. tech thesis, National Institute of technology, Rourkela-769008, India.
24. Negi, P. and Sarkar, R. (2013): “Effect of Curing on Compaction Behavior of Pond Ash mixed with Marble Dust and Lime”, International Journal of Earth Sciences and Engineering, Vol. 6, No. 1, pp. 211-216.
25. Pandian, N.S. (2004): “Fly ash characterization with reference to geotechnical applications”. J. Indian Inst. Sci., Vol.84, No. 8, pp. 189–216.
26. Sahu, S.K. and Kumar, G. (2012): “Design of Fly Ash Dyke for Seepage and Stability Analysis”, B.tech thesis, Department of Civil Engineering National Institute of Technology Rourkela – 769008, India
27. Schmertmann, J.H. and Hartman, J.P. (1978): “Improved strain influence factor diagram,”Journal of geotechnical engineering division, ASCE, Vol. 104, No.8, pp. 1131-1135.
28. Sinha, A.K., Havanagi, V. G, Mathur, S. and Guruvittal, U. K (2009): “Investigation and design of a fly ash road embankment in India by CPT’, report published by Central Road Research Institute, New Delhi, India.
29. Shiwakoti, D.R., Pradhan, T.B.S. and Leshchinsky, D. (1998): “Performance of Geosynthetic-Reinforced Soil Structures at Limit Equilibrium State”, Geosynthetics International, Vol. 5, No. 6, pp. 555-587.
30. Siavoshnia, M. Kalantari, F. and Shakiba, A. (2010): “Assessment of Geotextile Reinforced Embankment on Soft Clay Soil”, Proceedings of the 1st International Applied Geological Congress, Department of Geology, Islamic Azad University, Iran, April 26-28, pp. 1779-1784.
31. Vashi, J.M., Desai, A.K. and Solanki, C.H. (2012): “Assessment of reinforced embankment on soft soil with PET and PP Geotextile”, International Journal of Civil and Structural Engineering, Vol. 2, No. 3, pp. 828-837.

32. Zornberg, J.G. and Arriaga, F. (2003): “Strain Distribution within Geosynthetic-Reinforced Slopes”, Journal of Geotechnical and Geoenviromental Engineering, ASCE, Vol. 129, No. 1, pp. 32-45.

33. Zornberg, J.G., Sitar, N. and Mitchell, J.K. (1998): “Limit Equilibrium as basis for Design of Geosynthetic Reinforced Slopes”, Journal of Geotechnical and Geoenvironmental Engineering, Vol.124, No. 8, pp. 684-698.